EXAMINATION OF FATIGUE BEHAVIOUR OF CARBON FIBER REINFORCED POLYMER COMPOSITES

A Thesis Submitted to
the Graduate School of Engineering and Sciences of
İzmir Institute of Technology
in Partial Fulfillment of the Requirements for the Degree of

DOCTOR OF PHILOSOPHY

in Mechanical Engineering

by
Mehmet Deniz GÜNEŞ

July 2021
İZMİR

ACKNOWLEDGMENTS

I would like to give my sincere thanks to my advisor Prof. Dr. Metin Tanoğlu for his useful comments, guidance, support, encouragement and motivation.

I would like to thank the rest of my PhD thesis commitee members Assoc. Prof. Dr. Sinan Kandemir and Assist. Prof. Dr. Selçuk Saatçı for their encouragement and helpful comments

I would like to thank to my labmates and friends Bertan Beylergil, Zeynep Ay Solak, Serkan Kangal, Osman Kartav, Yusuf Can Uz, Ceren Türkdoğan, Seçkin Martin, Mustafa Aydın, Hikmet Sinan Üstün, Hatice Sandallı, Gözde Esenoğlu, H. Arda Deveci and Mehmet Ziya Okur for their help and unconditional support.

I would like to thank to my father Nejat Güneş and my sister Seda Gürpınar and her family members Hulisi Gürpınar, Göktuğ Gürpınar and Doruk Gürpınar for their love and support.

Lastly, I offer my sincere thanks to my wife Dr. Oylum Çolpankan Güneş for her love, motivation and unlimited support and patience during my PhD study.

ABSTRACT

EXAMINATION OF FATIGUE BEHAVIOUR OF CARBON FIBER REINFORCED POLYMER COMPOSITES

This PhD thesis aims to examine the fatigue behavior of sandwich panels fabricated from adhesively bonded aluminum honeycomb core and carbon fiber reinforced polymer composite face sheets.

Initially, sandwich panels were manufactured with three different amounts of adhesive in their interface. Static flexural behavior was characterized with three-point bending tests. Load-displacement curves and static flexural failure modes were obtained and utilized to compare the static flexural behavior of fabricated sandwich. Fatigue behavior of sandwich panels were characterized with the three-point bending fatigue tests. Stiffness degradation curves were used to identify the failure cycles of sandwich panels. Fatigue failure modes and S-N curves were obtained to find out the effect of amount of adhesive on fatigue behavior of sandwich panels.

The other study within this thesis was made to investigate the effect of core thickness on the fatigue behavior of the sandwich panels based on aluminum honeycomb core and carbon fiber reinforced polymer composite face sheets. Sandwich panels were fabricated by using three different aluminum honeycomb core thickness. Static flexural tests were carried out to determine the static flexural behavior of developed sandwich panels. Load-displacement curves and failure modes were obtained from flexural tests. In addition to this, core shear tests were performed to investigate the core shear strength of the honeycomb cores with different core thickness. Effect of core thickness on fatigue behavior of sandwich panels were characterized with fatigue failure modes and S-N curves. Stiffness degradation method was used to determine the fatigue failure cycles of the sandwich panels.

ÖZET

KARBON FİBER TAKVİYELİ POLİMER KOMPOZİTLERİN YORULMA DAVRANIŞININ İNCELENMESİ

Bu doktora tezi, yapıştırıcıyla birleştirilmiş alüminyum balpeteği ara tabaka ve karbon fiber takviyeli polimer kompozit yüzey levhalarından imal edilen sandviç panellerin yorulma davranışını incelemeyi amaçlamaktadır.

Başlangıçta, sandviç paneller, ara yüzeylerinde üç farklı miktarda yapıştırıcı ile üretilmiştir. Statik eğme davranışı, üç nokta eğme testleri ile karakterize edilmiştir. Farklı miktarda yapıştırıcı ile üretilmiş sandviç panellerin statik eğme davranışını karşılaştırmak için yük-deplasman eğrileri ve statik eğme kırılma modları elde edilmiş ve kullanılmıştır. Sandviç panellerin yorulma davranışı, statik eğme testleri ile aynı test fikstüründe yorulma testleri ile karakterize edilmiştir. Sandviç panellerin hasar çevrimlerini belirlemek için direngenlik düşüş eğrileri kullanılmıştır. Yapıştırıcı miktarının geliştirilen sandviç panellerin yorulma davranışı üzerindeki etkisini bulmak için yorulma hasar modları ve S-N eğrileri elde edilmiştir.

Bu doktora tezi kapsamındaki diğer çalışma, alüminyum bal peteği ara tabakalı ve karbon fiber takviyeli polimer kompozit yüzey levhalarından yapılan sandviç panellerin yorulma davranışına ara tabaka kalınlığının etkisini araştırmak için yapılmıştır. Sandviç paneller üç farklı kalınlıkta alüminyum bal peteği ara tabaka kullanılarak üretilmiştir. Geliştirilen sandviç panellerin statik eğme davranışını belirlemek için statik eğme testleri yapılmıştır. Eğme testlerinden yük-deplasman eğrileri ve hasar modları, elde edilmiştir. Buna ek olarak, farklı ara tabaka kalınlıklarına sahip ara tabakaların ara tabaka kayma mukavemetini araştırmak için ara tabaka kayma testleri yapılmıştır. Çekirdek kalınlığının sandviç panellerin yorulma davranışı üzerindeki etkisi, yorulma hasar modları ve S-N eğrileri ile karakterize edilmiştir. Sandviç panellerin yorulma hasar çevrimlerini belirlemek için direngenlik düşüş yöntemi kullanılmıştır.

TABLE OF CONTENTS

LIST OF FIGURES

Figure **Page**

Figure **Page**

Figure **Page**

Figure **Page**

Figure **Page**

LIST OF TABLES

CHAPTER 1

INTRODUCTION

1.1. Introduction

Because of their high specific strength, specific stiffness, and tailor ability, usage of fiber-reinforced polymer (FRP) composite materials is increasing in structural applications such as aerospace, wind turbine blades, marine industries, automation, and so on. They are rapidly replacing conventional metallic materials due to these superior properties. Fiber reinforced composites are generally anisotropic and inhomogeneous. The mechanical properties of fiber reinforced polymer materials mainly depend on the properties of its ingredients. The mechanical properties of FRP structures are combined with matrix strength, fiber strength and stiffness, chemical stability, and the strength of the interface between fiber and matrix. FRP structures are exposed to the fluctuating loads in their wide range application areas which causes the fatigue failure on the structures. Therefore, Fatigue is primary failure cause for fiber reinforced polymeric composite materials (Wang et al. 1998, Curtis 1991, Ansari, Singh, and Azam 2018).

Fiber reinforced polymer composites are made of a polymeric matrix and a reinforcement fiber phases. Reinforcement fibers could be derived from different materials such as glass, aramid, or carbon (Ansari, Singh, and Azam 2018). Carbon fiber reinforced polymer (CFRP) composite materials are commonly used in the application areas which requires highly amount of weight saving such as aerospace, automotive, marine and defense industries (Curtis 1991, Cheon and Kim 2021, Maurya et al. 2021). It can be easily stated that fatigue characteristic of CFRP composites is highly significant regarding their requirements of application areas.

CFRP composites can be utilized as a low weight reinforcing material in a structural element or a face sheet on a sandwich panel in the applications. Sandwich panels are a type of laminated composite structures formed by two thin face sheets and a thicker but lightweight core. Face sheets are generally made from composite laminates and metals and core material could be made by metallic or non-metallic honeycombs, porous foams, balsa woods or trusses. The face sheets are typically adhesively bonded to

the core and bear most of the bending and in-plane loads. Flexural stiffness, out-of-plane shear, and compressive strength are all provided by the core. Sandwich panel structural performance is influenced not only by the properties of the face sheets, but also by the properties of the core, the adhesive bonding of the core and face sheet, and the geometrical dimensions of those components (Daniel and Abot 2000). Sandwich structures provides high specific strength and stiffness with their high moment inertia to the structures. Those superior features enabled to be used in aerospace, automotive, yacht and even bridge applications. Usage in those application areas requires to investigate the fatigue behavior of sandwich structures (Shi, Liu, and Fang 2018, Li, Li, and Wang 2012, Anwar et al. 2017, Sun et al. 2017, Blok et al. 2017, Davalos et al. 2001).

Lots of studies are existing in the literature about fatigue behavior of sandwich structures. Some of those structures emphasized on development of analytical and numerical models to predict the fatigue life of sandwich panels (Upreti et al. 2020, Cecchini and Yusif 2019, Rajaneesh et al. 2018). Otherwise, experimental studies were carried out by researchers on previous studies (Mathieson and Fam 2014, Pehlivan and Baykasoğlu 2019, Chemami et al. 2012). Fatigue response of sandwich panels were characterized by stiffness degradation and S-N (Wöhler curves) in the experimental studies. Experimental studies will be explained in literature review section in Chapter 2.

Although lots of paper exists in the literature about the fatigue behavior of sandwich panels, only limited number of those are consisting of the fatigue behavior of sandwich panels made by CFRP face sheets and aluminum honeycomb cores. In this thesis, fatigue behavior of the aluminum honeycomb cored with CFRP face sheets sandwich panels are characterized with the effect of amount on adhesive on the core-face interface and the thickness of honeycomb core experimentally.

1.2. Aim of the Study

The main objective of this thesis is to characterize the flexural fatigue behavior of the aluminum honeycomb cored CFRP based sandwich panels experimentally. Also, static flexural behavior of developed sandwich panels was determined within this thesis. Besides, core shear properties of aluminum honeycomb cores with different thickness were evaluated. The significant objectives of the thesis are listed below;

- Fabrication of adhesively bonded aluminum honeycomb core and CFRP face sheet-based sandwich panels with three different amounts of adhesive on the core-sheet interface.
- Characterizing the effect of amount of adhesive on static flexural properties of the developed sandwich panels.
- Obtaining load displacement curves and static flexural failure modes of sandwich panels with different amount of adhesive.
- Characterizing the effect of amount of adhesive on the fatigue behavior of sandwich panels.
- Obtaining stiffness reduction curves and S-N curves of the sandwich panels have different amount on adhesive on core-face interface.
- Fabrication of adhesively bonded aluminum honeycomb core and CFRP face sheet-based sandwich panels with three different aluminum honeycomb core thickness.
- Characterizing the effect of core thickness on static flexural properties of the developed sandwich panels.
- Obtaining load displacement curves and static flexural failure modes of sandwich panels with different core thickness.
- Characterizing the effect of core thickness on the fatigue behavior of sandwich panels.
- Obtaining stiffness reduction curves and S-N curves of the sandwich panels have different core thickness.

1.3. Thesis Outline

A brief information and importance about fatigue behavior of CFRP reinforced and CFRP face sheet-based sandwich panels were given at the beginning of the Chapter 1. After that, aim of the study and thesis outline were explained. At the end of the Chapter 1, novelty of the thesis was emphasized.

In Chapter 2, fundamental concepts and literature review were given. Chapter 2 begins with a brief overview of composite materials to explain some significant terminologies that should be known for the reader. Definition, classification, types, and

manufacturing methods of composite materials were summarized in that section. It follows with a brief information about the sandwich structures. Definition classification and components of sandwich structures were explained to identify the important terminologies to the reader. After that, important definitions, and terminologies about fatigue concept of the polymeric composites were identified. At the end of the Chapter 2, a detailed literature review was given to explain the history of the fatigue of sandwich composites history and commonly utilized methods.

In Chapter 3, Effect of amount of adhesive on the composite face sheets and aluminum honeycomb interface on static and fatigue flexural behavior of adhesively bonded of sandwich panels were investigated. Fabrication method of face sheets and sandwich panels were explained. Static and fatigue flexural tests and test set-ups were defined in that section. Static flexural test results were given and evaluated with load-displacement curves and failure modes. Effect of amount of adhesive on the fatigue behavior of sandwich panels were characterized with flexural fatigue failure modes and S-N curves at the end of the Chapter 3.

In Chapter 4, Effect of core thickness on static and fatigue flexural behavior of adhesively bonded of sandwich panels were investigated. Static and fatigue flexural tests and core shear strength of honeycomb core tests and set-ups were defined in that section. Static flexural and core shear strength tests results were given and evaluated with load-displacement curves and failure modes. Effect of aluminum honeycomb core thickness on the fatigue behavior of sandwich panels were characterized with flexural fatigue failure modes and S-N curves at the end of the Chapter 4.

In Chapter 5, concluding remarks and potential future works for this thesis were given.

1.4. Novelty of Thesis

In this thesis, fatigue behavior aluminum honeycomb cored with carbon fiber reinforced polymer face sheets sandwich panels were examined. To our knowledge, there limited number of studies published in the literature on the fatigue behavior of investigation of the aluminum honeycomb cored carbon fiber reinforced polymer

composite face sheet-based sandwich structures. Besides, static flexural behavior of the developed sandwich panels was characterized.

Effect of amount of adhesive on the static and fatigue flexural behavior of the sandwich panels with aluminum honeycomb core and GFRP face sheets were investigated. A different load-displacement curve characteristic and failure modes were observed from literature. In flexural fatigue tests, failure mode was shifted from interfacial debonding to core crushing by optimized the amount of adhesive. S-N curve of the sandwich panels regarding to amount of adhesive also obtained. To best of out knowledge, there is no publication about investigation of the effect of amount of adhesive on static and fatigue behavior of sandwich structures with CFRP face sheets and aluminum honeycomb core.

Another study within this thesis was about examination of effect of core thickness of the sandwich panels made from adhesively bonded aluminum honeycomb core and CFRP face sheets. In that study, both static and fatigue flexural behavior of sandwich panels were determined. A different load-displacement curves from the literature were obtained from static three-point bending tests as well. Fatigue failure modes and S-N curves with respect to core thickness of the sandwich panels were determined. An optimum core thickness for a better fatigue strength were found. A different failure mode for the sandwich panels that have high thickness were found. Also, core shear strength of the aluminum honeycomb cores with different core thickness was characterized. Besides, to best of our knowledge, this is the first study about the investigation on the effect of core thickness on static and fatigue behavior of the sandwich structures with CFRP face sheets and aluminum honeycomb core.

CHAPTER 2

FUNDAMENTAL CONCEPT AND RELEVANT LITERATURE

2.1. Introduction to Composite Materials

2.1.1. Definition of Composite Materials

Composite materials have been the most promising material and one of the hotspot research topics in the field of engineering and material sciences from the middle of 20th century. The reason of this rapid growth and popularity of composite materials is their remarkable structural and mechanical properties, resistance to chemicals, fire, corrosion and wear and combination of these properties (Rajak, Pagar, Kumar, et al. 2019, Rajak, Pagar, Menezes, et al. 2019). Composite materials have been extensively utilized over a wide range of applications such as aerospace, automotive, marine, wind and thermal power generators, marine, civil construction, telecom appliances etc. due to their important features (Ravishankar, Nayak, and Kader 2019, Singh et al. 2017).

Composite materials which are the formation of two or more constituent materials having different physical or chemical properties make up a very broad and important class of engineering materials. For a material to be considered as a composite, there are some points that should be included in the definition: It should consist of two or more physically distinct and mechanically separable materials. It produces a different material with unique and optimum properties when combined. It can be made by mixing the separate materials in such a way that the dispersion of one material in the other can be done to achieve optimum properties. It possesses superior characteristics different from the individual components (Clyne and Hull 2019). Many composite materials are composed of just two phases: matrix and reinforcement. Matrix is the continuous phase and surrounds the other phase, reinforcement. Reinforcement can be in the form of particles, fibers and whiskers of natural or synthetic material. Matrix is generally seen as a relatively soft phase, whereas reinforcement phase in composites is stronger and stiffer than the matrix as it carries the applied load to the material (Callister and Rethwisch 2018).

2.1.2. Classification of Composite Materials

Properties of each of the component effect the overall properties of composites, therefore, there is need of studying their classification and distinct properties thoroughly. There are several different types of composites; however, the classification based on matrix and reinforcement material is generally and extensively used.

2.1.2.1. Composite Materials Based on Matrix Material

Examples of typical microstructures for the three main classes, grouped according to the nature of the matrix, are shown in Figure 2.1.

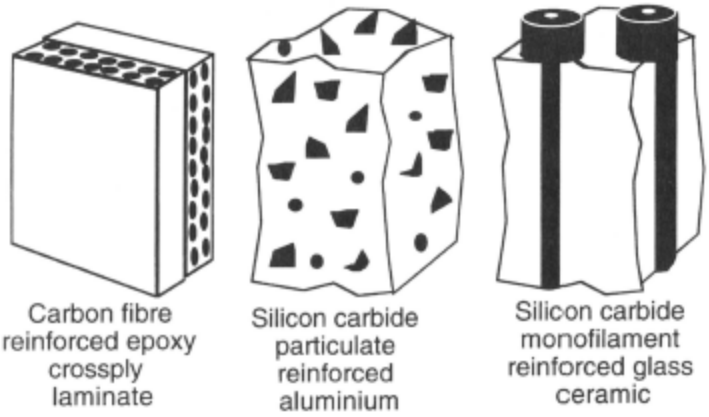

Figure 2.1. Classsification of composite materials (Source: Clyne and Hull 2019)

Ceramic matrix composites (CMCs) are composed of ceramic reinforcements and ceramic matrix. Ceramic materials are inherently resilient to oxidation and deterioration at elevated temperatures, and therefore they can be ideal candidates for use in high-temperature applications, specifically for components in automobile and aircraft gas turbine engines. However, their fracture toughness values are very low and in the presence of flaws they are undergo catastrophic failures. In addition, they are extremely susceptible to thermal shock and are easily damaged during fabrication and/or service. CMCs are

designed to overcome the limitations of monolithic ceramics by ceramic reinforcement in particulates, fibers, or whiskers shapes that have embedded into a ceramic matrix and thus exploit the attractive high temperature strength and environmental resistance of ceramic materials without rifaceg a catastrophic failure (Chawla 2012, Rajak, Pagar, Kumar, et al. 2019).

Metal matrix composites (MMCs) is a type of composite which consist of metallic matrix and dispersed ceramics like oxides and carbides, or metallic reinforcement. Materials such as directionally solidified eutectic alloys, oxide dispersion strengthened alloys, Al–Si eutectic casting alloys, pearlitic steel and two-phase lamellar alloys such as gamma Ti-Al are the common examples of this type of composites. MMCs have a balance of physical and mechanical properties. They provide high thermal and electrical conductivity, good resistance to aggressive environments, good impact and erosion resistance and good fatigue and fracture properties. In addition, MMCs add higher strength and stiffness than the matrix alloy, excellent wear resistance and lower coefficient of thermal expansion. They have been widely used in different applications such as transportation, thermal management, and aerospace (Miracle 2005).

Polymer matrix composites (PMCs) are composed of thermoplastic or thermoset polymer matrix and reinforcement, generally carbon, glass, aramid and metal fibers. Thermosets are more popular in use than thermoplastics due to their higher strength and resistance to elevated temperatures. PMCs are used in the greatest diversity of composite applications, as well as in the largest quantities due to their ease of fabrication and low cost. They have established as engineering structural materials because of the introduction of high-performance fibers (carbon, boron, and aramid), some new and improved matrix materials. Nevertheless, glass fiber reinforced polymers represent the largest class of PMCs. Carbon fiber reinforced PMCs are considered as the most important structural composites, especially in the aerospace application (Callister and Rethwisch 2018, Chawla 2012, Rajak, Pagar, Kumar, et al. 2019).

2.1.2.2. Composite Materials Based on Reinforcement Geometry

Particle reinforced composites with large-particle and dispersion strengthened subclasses are one the type of composites based on reinforcement geometry. There is a

difference in terms of strengthening mechanism between these two composites. In large-particle reinforced composites, the large term is used to indicate that the interaction between particle and matrix are on the atomic or molecular level. The stiff and hard reinforcing particles tend to restrain the movement of the matrix phase. The matrix transfers some of the applied stress to the particles and they bear a fraction of the load. In this type of composite, it is important to have a strong bonding at the matrix-particle interface for the effective reinforcement or improvement of the mechanical behavior of the composites. In dispersion-strengthened composites, particles diameters are in the nanometer range (between 10 and 100 nm). The interactions between particle and matrix lead to strengthening occur on the atomic or molecular level. In this type of composites, matrix bears the major portion of an applied load and the small, dispersed particles impede the motion of dislocations. Therefore, plastic deformation is restricted and mechanical behavior of the composites improve (Callister and Rethwisch 2018).

Fiber reinforced composites are considered as the most important type of composites. In this type of composites, dispersed phase of synthetic fibers such as glass, carbon, basalt and aramid or natural fiber in a composite structure revealed enhanced material properties such as high strength, stiffness and resistance to chemical, temperature and wear. In essence, the aim of designing the fiber reinforced composites is having a high specific strength and moduli. The fibers can be continuous or discontinuous according to the length of fiber or aligned or randomly oriented according to the array in the composites (Callister and Rethwisch 2018). Considering the overall composite production, glass fiber reinforced polymer composites have an enormous volume. The density of glass fiber is quite low, and the strength is quite high. It has quite high strength-to-weight ratio and moderate modulus-to-weight ratio. They continue to be used for reinforcement of polyester, epoxy, and phenolic resins. It has low cost and it is available in a variety of forms (Chawla 2012). Carbon is a high-performance fiber material, and therefore it is the most used reinforcement in advanced polymer matrix composites. They have the highest specific modulus and specific strength of all reinforcing fiber materials, and they maintain their high tensile modulus and high strength at elevated temperatures. They are not susceptible to moisture or a wide variety of solvents, acids, and bases. The manufacturing processes of fiber and composites are relatively inexpensive and cost effective. Most importantly, they exhibit a diversity of physical and mechanical characteristics which allow composites incorporating these fibers to have specific engineered properties (Callister and Rethwisch 2018).

2.1.3. Manufacturing Techniques for Fiber Reinforced Composite (FRP) Composites

2.1.3.1. Hand layup Method

Hand layup method is applied for natural as well as synthetic fiber to fabricate the composite. It is the most common and widely used open mold composite manufacturing method. Figure 2.2 represents the schematic illustration of hand layup method. In this method, initially, after applying a thin layer of antiadhesive coat to the surface of the mold to avoid adhesion after the process, fiber preforms are placed in an open mold. Then, polymer resin is poured or applied using a brush on a reinforcement material. Uniform load is applied by roller which helps to enhance the interaction between the successive layers of the reinforcement and the matrix materials. In addition, it removes the air present in the interface of matrix and reinforcement. Finally, the mold is left so that the resin will cure, usually at room temperature, though heat is sometimes used to ensure a proper curing process (Masuelli 2013, Rajak, Pagar, Menezes, et al. 2019).

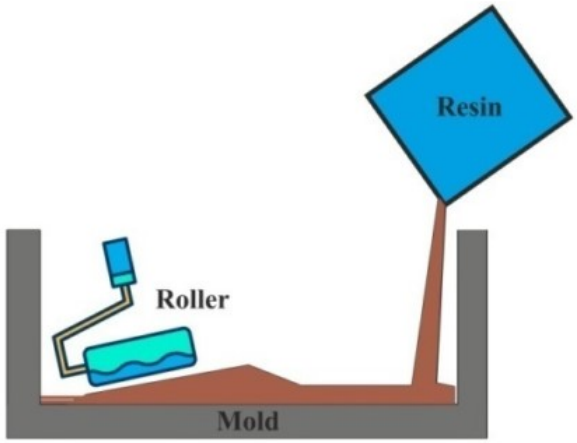

Figure 2.2. Schematic illustration of hand layup method (Source: Rajak, Pagar, Menezes, et al. 2019)

2.1.3.2. Vacuum Bag Molding

The schematic illustration of vacuum bag molding is seen in Figure 2.3. This method uses a flexible nylon, polyethylene, or polyvinyl alcohol film PVA to enclose and seal the mold, and generally this method is performed with the assistance of the hand layup method. Initially, laminate is first made by hand layup method, and then after it is placed between the vacuum bag and the mold to ensure infusion of fibers into the matrix material. The air between the mold and the vacuum bag is then drawn out by a vacuum pump (Rajak, Pagar, Menezes, et al. 2019).

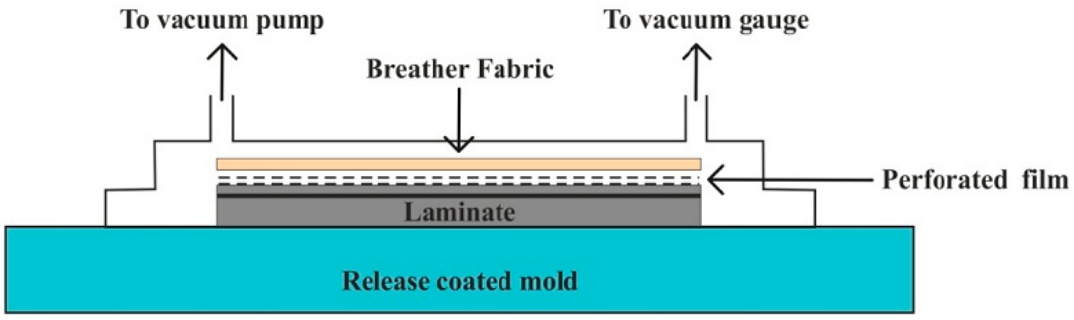

Figure 2.3. Schematic illustration of vacuum bag molding method (Source: Rajak, Pagar, Menezes, et al. 2019)

2.1.3.3. Compression Molding

The preheated molds mounted on a hydraulic or mechanical press is used in this method. Figure 2.4 represents the stepwise processing of compression molding. Initially, a prepared reinforcement from prepreg is placed into mold cavity. Prepreg is the composite industry's term for continuous-fiber reinforcement pre-impregnated with a polymer resin that is only partially cured. Then, the mold is closed, and they are pressed against each other to get a desired shape. The material is compacted & cured inside by pressure and heat. Compression molding offers many advantages such as excellent detailing for geometric shapes, short cycle time, a high degree of productivity, and

automation with dimensional stability (Callister and Rethwisch 2018, Masuelli 2013, Rajak, Pagar, Menezes, et al. 2019).

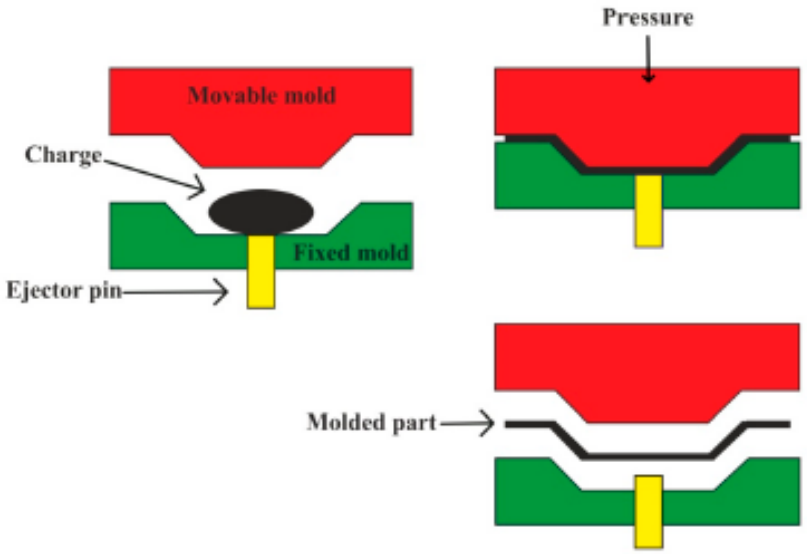

Figure 2.4. Compression molding process (Source: Rajak, Pagar, Menezes, et al. 2019)

2.1.3.4. Pultrusion

Pultrusion method is used to fabricate the components having continuous lengths and a constant cross-sectional shape such as rods, tubes, beams, etc. Figure 2.5 represents the schematic illustration of pultrusion process. In this method, initially, continuous fiber bundles are impregnated with a resin, and then they pulled through a die which preforms to desired shape. Saturated material then extruded from the heated closed die, and it keeps pulling continuously through the die. The curing of the resin matrix is initiated in this heated die. Tubes and hollow sections are made possible by using center mandrels or inserted hollow cores. This method is a continuous process and is easily automated, a wide variety of shapes are possible. However, production rates are relatively high (Callister and Rethwisch 2018, Masuelli 2013).

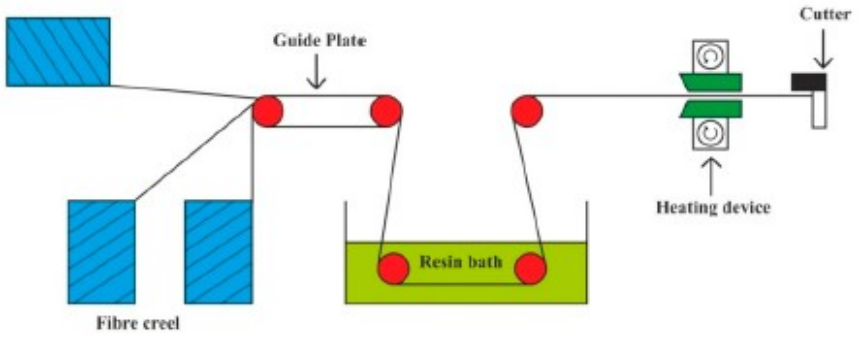

Figure 2.5. Schematic illustration of pultrusion process (Source: Rajak, Pagar, Menezes, et al. 2019)

2.1.3.5. Filament Winding

Filament winding is continuous and self-automated process which leads to reduce cost. In this method, continuous fibers are accurately positioned in a predetermined pattern to form a hollow shape. Therefore, it is useful to create axisymmetric, as well as some non-axisymmetric, composite parts, such as pipe bends. In this method, initially, continuous prepreg sheets, roving, or monofilament are fed through a resin bath and then, they are wounded onto a rotating mandrel in specific orientations, as displayed in Figure 2.6. After the appropriate number of layers have been applied, mandrel is removed leaving a final geometric shape, and curing is carried out (Callister and Rethwisch 2018, Masuelli 2013, Rajak, Pagar, Menezes, et al. 2019).

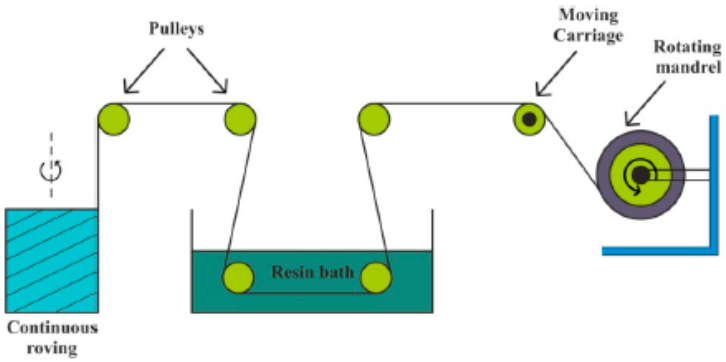

Figure 2.6. Schematic illustration of filament winding (Source: Rajak, Pagar, Menezes, et al. 2019)

2.1.3.6. Resin Transfer Molding (RTM)

In RTM method, preform fiber reinforcement mats are placed into a bottom of the mold and preheated resin is injected under pressure through an injector. The schematic illustration of RTM is given in Figure 2.7. A variety of combinations of fiber material with its orientation, including 3D reinforcements, can be achieved by RTM. In addition, composite structural parts with high-quality, high-strength and surface quality are produced in this method (Rajak, Pagar, Menezes, et al. 2019).

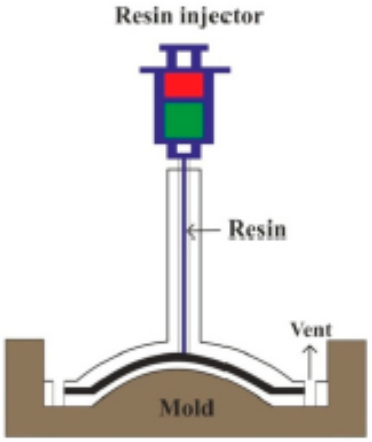

Figure 2.7. Schematic illustration of resin transfer molding process (Source: Rajak, Pagar, Menezes, et al. 2019)

2.1.3.7. Vacuum Assisted Resin Transfer Molding (VARTM)

VARTM is another composite manufacturing method using resin transfer as RTM. However, in this method, vacuum is used for injection. Preform fibers are placed on a mold and a perforated tube is positioned between vacuum bag and resin container. Vacuum is applied and it causes the resin to be sucked through the perforated tubes over the fibers to consolidate the laminate structure, as displayed in Figure 2.8. It is possible to obtain composite structures without any excess air because resin is entirely pulled into cavity under vacuum. In addition, it allows precise tolerances and detailed shaping.

Therefore, it is popular manufacturing method for large objects like boat hulls and wind turbine blades (Masuelli 2013, Rajak, Pagar, Menezes, et al. 2019).

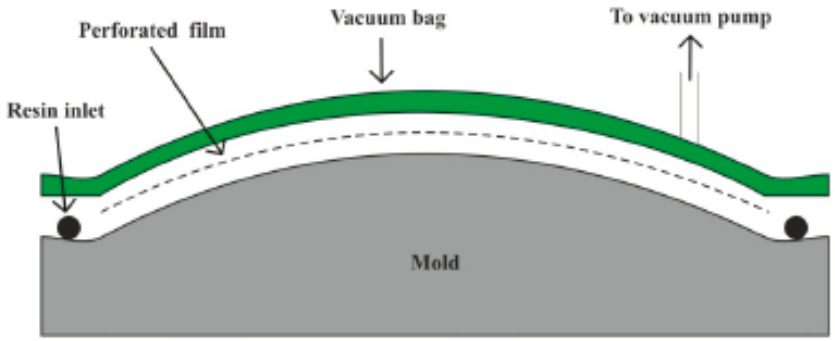

Figure 2.8. Schematic illustration of vacuum assisted resin transfer molding process (Source: Rajak, Pagar, Menezes, et al. 2019)

2.2. Sandwich Structures

2.2.1. Definition and Features of Sandwich Structures

Sandwich structures and laminar composites are the most common structural composites which are the combinations of composites and homogeneous materials. In addition, the properties depend on both the constituent materials and the geometrical design. A laminar composite consists of two-dimensional sheets or panels which have a preferred high-strength direction. In this type of composite, these sheets or panels are stacked and subsequently cemented together, and therefore the orientation of the high-strength direction varies with each layer as shown in Figure 2.9 (Callister and Rethwisch 2018, Sayyad and Ghugal 2017).

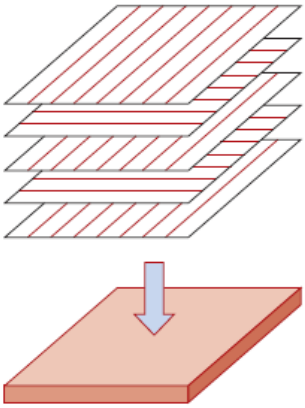

Figure 2.9. The stacking of fiber–reinforced layers for a laminar composite (Source: (Callister and Rethwisch 2018)

Sandwich structure is a three-layer structure composed of an upper and lower face sheets and a core in between them as shown in Figure 2.10. Faces are separated by and adhesively bonded core. The core is attached to the faces and distributes the load from one face to another. The face carries in plane loads, while the core maintains a distance between the faces. Accordingly, they are similar to an I-beam where the faces carry the main share of bending and in-plane loads, while the core sustains transverse shear, redistributes concentrated normal to the surface forces and maintains the integrity of the structure. The faces of sandwich structures are relatively thinner than core (several millimeters), whereas core is the thick one, the thickness may be over 50 mm. The face is characterized as stiff and strong features; while core should be light and thick in order to obtain good mechanical performance sandwich structure. The interface between the face and core is the weakest part of the sandwich structure. Adhesives are used in this interface to bond up and bottom facings with inner core. In order to improve the interface strength, good adhesion should be performed for sandwich structures. The thickness of the adhesive layer is generally negligible because it is much smaller than the thickness of faces or the core (Alsubari et al. 2021, Bari and Bajaj 2014, Birman and Kardomateas 2018, Njuguna 2016).

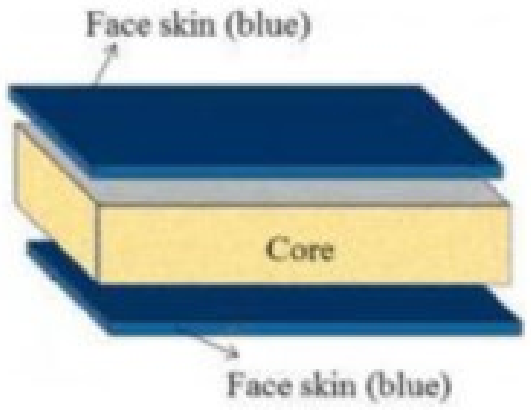

Figure 2.10. Schematic illustration of sandwich structure (Source: (Feng et al. 2020)

Sandwich structures are designed to be lightweight beams or panels having relatively high stiffnesses and strengths. They have been widely used in many application areas such as aircraft structures, ship hulls, wind turbine blades, bridge decks due to their superior bending stiffness, low weight, and excellent thermal insulation and acoustic damping (Atas and Potoğlu 2016). These structures are mostly popular in high performance applications where weight reduction has an extreme importance such as aeronautical structures, high speed marine craft and racing cars. Using lightweight vehicles has advantage on the consuming of the fuel. Composite sandwich structures have gain importance in aerospace and automotive industries because of their extremely low weight, high flexural and transverse shear stiffness and corrosion resistance properties. In addition, they are also a promising candidate in crashworthiness applications as they exhibit high energy absorption capacity when it suddenly subjected to impact loads (Donga 2011).

2.2.2. Classification of Sandwich Structures

Sandwich structures are classified into four types according to the geometry and shape of the core: (a) foam or solid core, (b) honeycomb core, (c) web core, and (d) a corrugated or truss core, as seen in Figure 2.11 (Catapano and Montemurro 2014).

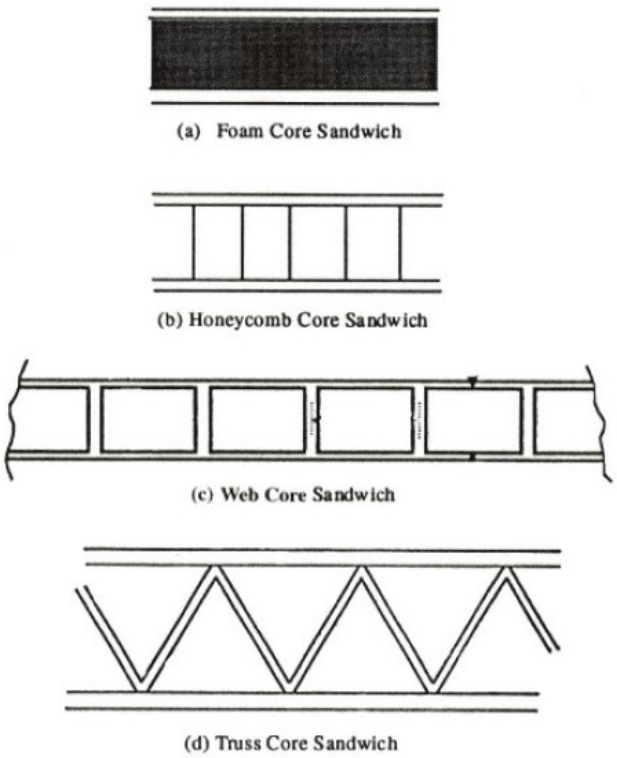

Figure 2.11. Types of sandwich structures (Source: Vinson 2018)

Foam core sandwich structures are a major class of lightweight structure materials and widely used in engineering applications. However, the low compressive strength of foam core limits its use in structural applications. Brocca et al. (Brocca, Bažant, and Daniel 2001) found that composite sandwich structure with lightweight foam core usually fails due to core indentation and crushing. In addition, the absorbing and retaining moisture by foam core reduce the mechanical properties of the structures as well as increase its weight (Manalo, Aravinthan, and Karunasena 2013). Web core construction is similar to to a group of I- beams with their flanges welded together, and the space in the core could be used for liquid storage or as a heat exchanger (Vinson 2018). Truss core sandwich structures are one of the oldest and most used sandwich structures. There are different geometries for truss core such as pyramidal, tetrahedral, Kagome, and X-type configurations (Feng et al. 2020). Honeycomb core structures have gained increasing attention in recent years as they meet the necessary compressive strength of the structures. They are the most used closed-cell prismatic lattice structures. The typical geometries for honeycomb cores include square, triangle, chiral, circular, hexagonal, and auxetic.

Honeycomb core sandwich panel is formed by adhering two thin, rigid faces with a low-density honeycomb core which possess less strength and stiffness. The honeycomb core increases the compressive strength in the through thickness direction of composite sandwich structure. These core materials can perform better in compression and shear at equivalent weight. However, the closed cell of the honeycomb core has disadvantage in entrapping moisture results in potential delamination of the core and faces (Feng et al. 2020, Manalo, Aravinthan, and Karunasena 2013).

2.2.3. Components of Composite Sandwich Structures

Composite sandwich structures are preferred due to their high bending stiffness, high strength to weight ratios, and high corrosion resistance over conventional materials in several applications such as automotive, aerospace, marine and other industrial applications. The strength of composite sandwich structure results from the combination of properties of face, core and interface. The components and materials should be selected by considering the intended application area (Manalo, Aravinthan, and Karunasena 2013).

2.2.3.1. Face Sheet Material

There are various types of materials used as face sheets for composite sandwich structures. Generally, they are prepared from either metals or fiber-reinforced composites due to providing superior strength and stiffness to the structure. Among the metals, aluminum and steel sheets are generally preferred as face materials. In addition, wood-based face sheets are also being used in sandwich structures due to their good thermal and acoustic insulation properties (Khan et al. 2020).

In composite sandwich structures, fiber-reinforced composites faces provide strength, stiffness, thermal stability and other structural properties. Here, fibers carry the applied load on the composite structure Therefore, it is important to select the fibers depending on the desired properties in composite structures. As a reinforcement, generally, three type fiber -carbon, glass and aramid- are commonly used in most

engineering applications (Donga 2011). The matrix in the composites has an important role in the protection of the reinforcement from adverse environment and providing uniform load distribution to the fiber. Therefore, it should be very careful in the selection of matrix material (Strong 2008). As a matrix material, generally, thermosetting and thermoplastic resins are used in fiber-reinforced polymeric composites. Among the common thermosetting matrix materials used with continuous fibers are epoxy and unsaturated polyester resins. Epoxy is one of the major thermoset matrix materials which contains an epoxide group in its chemical structure. Epoxy resins are more expensive than unsaturated polyesters, but they have better moisture resistance, lower shrinkage on curing, a higher maximum use temperature, and good adhesion with glass fibers. An unsaturated polyester resin contains a number of C=C double bonds. The term unsaturated means that there are reactive sites in the molecule (Chawla 2012). Thermoplastics are characterized by linear chain molecules and can be repeatedly melted or reprocessed unlike thermosetting resins. Although repeated melting and processing are possible with thermoplastics, too high a temperature or too long a dwell time at a given temperature can degrade the properties. Common thermoplastic resins are polypropylene, polyamide, thermoplastic polyesters, and polycarbonates (Grünewald, Parlevliet, and Altstädt 2017).

2.2.3.2. Core Material

The availability of various types of core materials is one of the main advantages related with sandwich structures. It is crucial to choose the core material on the type of application and the distinct target parameters since all the core materials has its characteristic chemical, physical and mechanical features. Along with weight and cost, strength, stiffness, and energy absorption are usually the most demanding properties in the design of a sandwich structure. The core materials are generally categorized according to the type of material as polymeric foams, wood, metallic, and ceramic cores (Khan et al. 2020). Balsa is one of the most popular woods preferred in many industrial, commercial and marine applications because of its good strength, low density, and low cost (Lee 1992). As polymeric foams, polystyrene, polyvinyl chloride, polyurethane and polymethacrylimide foams are the most commonly preferred ones for structural applications thanks to their lightweight, low cost, high strength to weight ratio properties

(Campbell 2010). Ceramic cores are getting a great deal of attention, mainly in high temperature applications. Cork agglomerates have very impressive properties like high-impact resistance and good damping qualities when exposed to vibrations. Metallic core based sandwich composites, especially aluminum core composites, are commonly being used and are continuously under research in the aeronautics, marine and automotive industries (Khan et al. 2020).

2.3. Fatigue Concept of Polymer Matrix Composites

The response of a material to cyclic loading, which occurs often in many applications, is represented by its fatigue characteristics. When a material is subjected to cyclic stress, it is widely understood that its strength is dramatically reduced. Metallic materials that are ductile in nature under normal working conditions have been observed to fracture brittlely when subjected to repetitive cyclic stress. The failure cycle varies with some parameters such as stress level, stress state, cyclic mode etc. (Mallick 2007)

Polymer matrix composites have been utilized in many application areas requires long-term durability such as airplanes, ships, spacecraft etc. recent years. Thus, it is significant to estimate the long-term reliability of the composite structures (Guedes 2019). Lifetime of composite materials under long-term cyclic loading forms a complicate process. Initiation and growing of lots of failure mechanism change the strength and identify the lifetime of the composite material (Reifsnider 2012).

2.3.1. Fatigue Failure Principles of Composites

Composite materials are inhomogeneous and anisotropic structures unlike the metals. Composite materials accumulate the failure over time rather than locally, and failure does not always result from the propagation of single macroscopic crack. Failure accumulation micro-structural mechanisms such as fiber breakage and matrix cracking, debonding, transverse-ply cracking, and delamination occur both independently and interactively, and the predominance of one or the other can be strongly influenced by both materials variables and testing conditions (Harris 2003)

Most types of composite materials have failure at low levels of stress in monotonic loading or early in life during cyclic loading. That failure is dispersed across the stressed region and while it does not lower the composite's strength, it generally affects the stiffness. Later in life, the amount of damage accumulated in some regions of the composite may be so significant that the composite's residual load-bearing capability in that region falls below the level of the fatigue cycle's maximum stress, resulting in failure, as shown schematically in Figure 2.12 (Harris 2003).

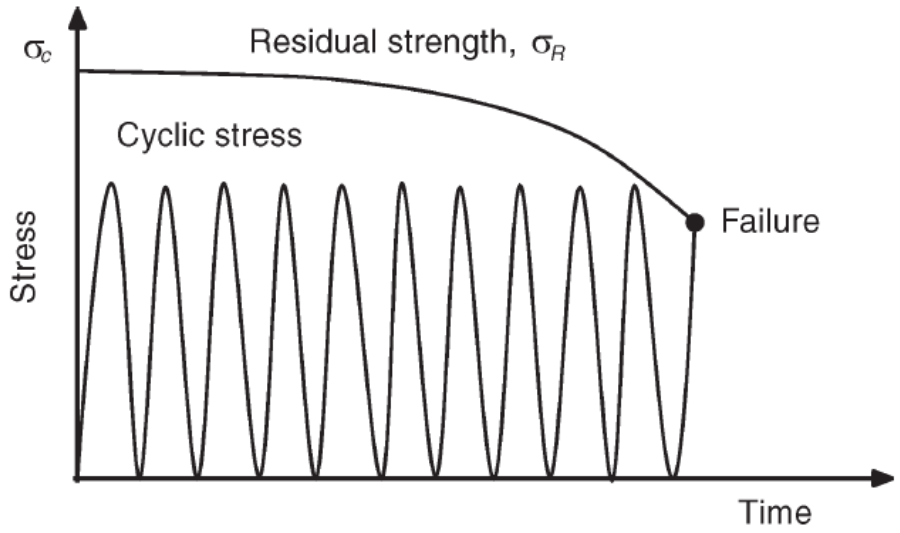

Figure 2.12. Degradation of composite strength by residual strength (σ_R) falls from the composite strength (σ_c) to the level of the fatigue stress until failure occurs (Source: Harris 2003)

In composite laminates, the failure process comprises of the initiation and growth of multiple different damage modes, as well as intricate interactions between them. The failure process as a function of percentage of life of composite laminates containing 0° plies and off (loading) axis (Θ) plies subjected to cyclic loading can be seen in Figure 2.13. Other loading histories, such as those with compressive components and those with mixed tensile and compressive components, can be generated using similar circumstances (Reifsnider 2012).

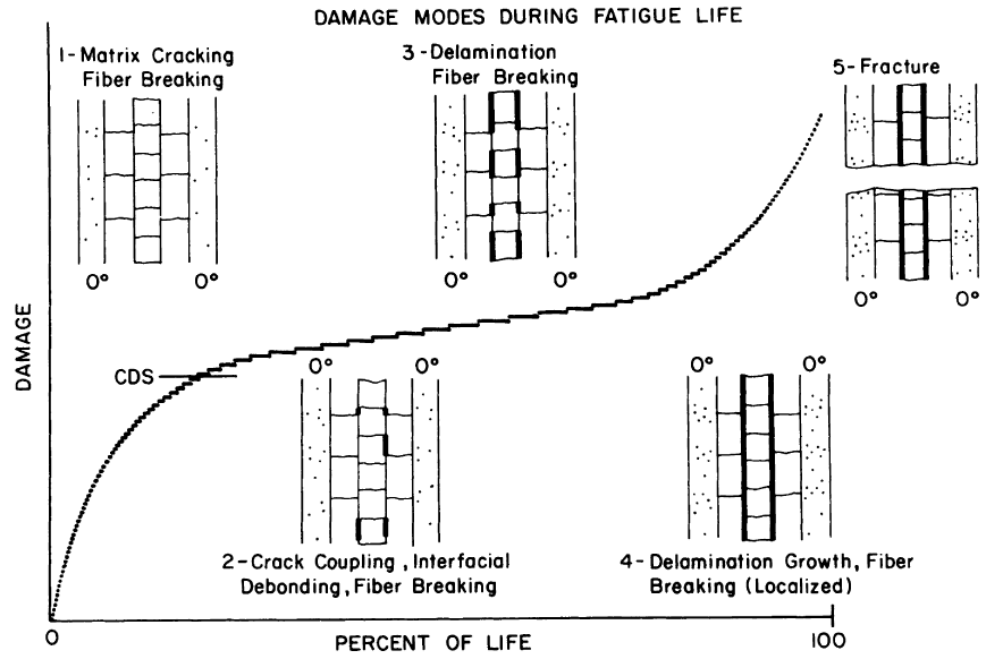

Figure 2.13.Representative matrix and fiber failure modes during the fatigue lifetime of composite laminates (Source: Reifsnider 2012)

2.3.2. Fatigue Testing of Composite Materials

Uniaxial tension–tension cycling has been used to perform most fatigue studies on fiber-reinforced composite materials. Because failure by compressive buckling can occur in thin laminates, tension–compression and compression–compression cycles are not widely used.

Flexural fatigue tests produce completely reversed tension–compression cycling. Interlaminar shear fatigue and in-plane shear fatigue tests were also done in a limited number of cases (Mallick 2007). A representative stress vs. time diagram in a tension-tension fatigue test are shown in Figure 2.14. Some fatigue test parameters such as stress ratio “R”, stress amplitude, defining od 1 cycle, stress range, maximum stress “σ_{max}” and minimum stress “σ_{max}” are also defined on Figure 2.14.

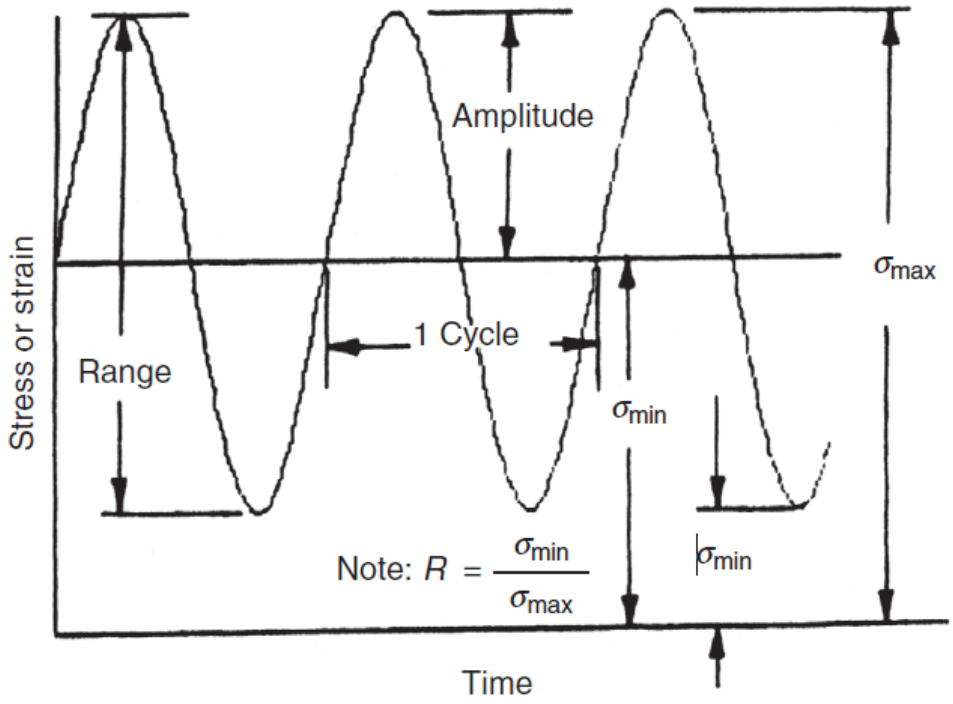

Figure 2.14. A representative stress vs. time diagram in fatigue testing (Source: Mallick 2007)

Internal damping in polymer matrix composites can generate significant heat at high cyclic frequencies, which raises the specimen temperature. Thus, low cyclic frequencies are generally preferred due to the avoiding the temperature rising affects the fatigue behavior of polymeric composites. Fatigue tests can be carried out stress or strain controlled. The specimen is cycled between prescribed maximum and lowest stresses in a stress-controlled test to maintain a constant stress amplitude. The specimen is cycled between defined maximum and lowest stresses in a strain-controlled test to maintain a constant strain amplitude (Mallick 2007).

A fiber-reinforced composite material is distinguished by the gradual softening or loss of stiffness caused by the appearance of microscopic damages long before any visible damage occurs. As a result, in load-controlled tests, the strain in the specimen increases, whereas in strain-controlled tests, the stress in the specimen decreases as shown in Figure 2.15. Microscopic damage also reduces the material's residual strength. Many fatigue tests are performed until the specimen stiffness or residual strength reaches a predetermined

level rather than specimen separation. As a result, cycles to failure may not always accurately represent specimen life at complete fracture (Mallick 2007).

The data collected should provide an accurate representation of the performance over the specified lifetimes. It could be done by generating a full S-N diagram (applied stress versus the number of failure cycle). That typically covers the lifetime range of 100 or 1000 cycles to one million cycles (Harris 2003)

Most of the researchers generates the S-N curves in logarithmic scale and obtain S-$logN$ curves identified by a straight line (Mallick 2007):

$$S = \sigma_U(mlogN + b)$$

Where, S is maximum fatigue stress, N is number of cycles to failure, σ_U is average static strength and m and b are constants (Mallick 2007).

A power-law of S-N curves can be also utilized:

$$\frac{S}{\sigma_U}N^d = c$$

Where c and d are constants (Mallick 2007).

A representative S-N diagram can be seen in Figure 2.15.

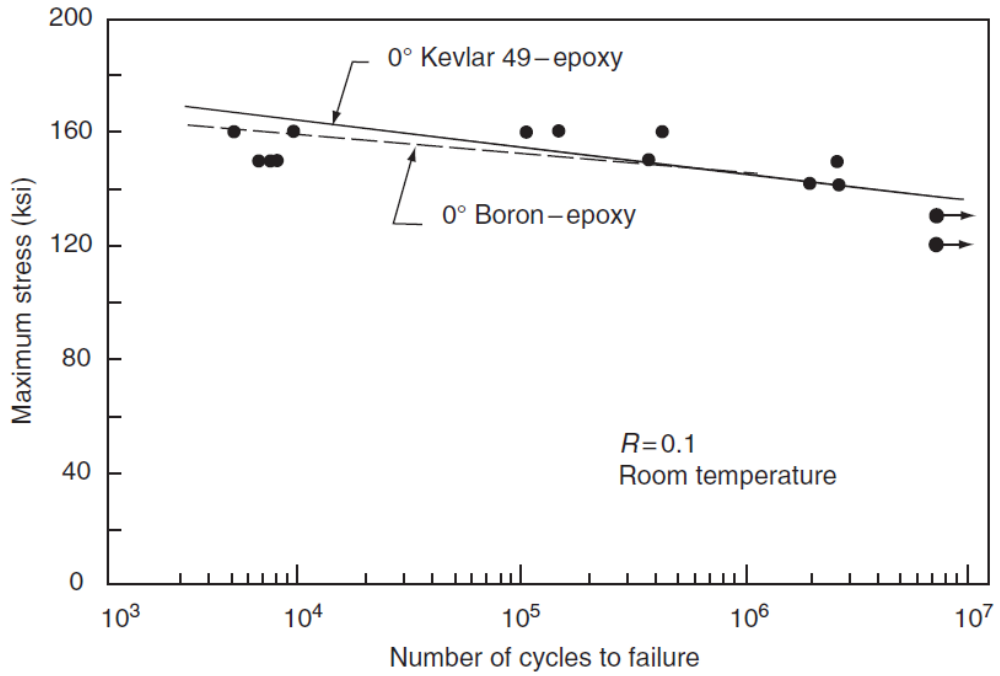

Figure 2.15. A representative S-N diagram for a 0° boron and Kevlar 49 fiber-epoxy composites (Source: Mallick 2007)

2.4. Fatigue Behavior of Sandwich Composites

Sandwich composites are using in many application areas such as wind turbines, automotive industry, bridge structures, spacecraft, and aircraft industry due to their high strength and stiffness to weight ratio, high fatigue resistance and corrosion resistance (Coskun and Türkmen 2012, Manca et al. 2012, Upreti et al. 2020, Manalo, Aravinthan, and Karunasena 2010, Palomba, Crupi, and Epasto 2019). Thus, sandwich structures are exposed to the cyclic loads in their long-term lifetime in those wide-range application areas. That caused an essential attention on investigation of fatigue behavior of sandwich panels.

Investigations on fatigue of sandwich panels began with the foam cored sandwich beams. Burman and Zenkert published a paper about fatigue behavior of foam core sandwich beams in 1997. They used PVC (polyvinylchloride) and PMI (polymethacrylimide) based foam cores and glass fiber reinforced epoxy face sheets. Load controlled fatigue tests were carried-out to developed sandwich structures with different stress ratios. They generated stress-life curves and Haigh diagram. Besides, they investigate the fatigue crack formation and growth at their fatigue tests.

They used four-point bending test fixture and measure the core shear stress per unit width. They performed both static and fatigue tests to their samples. PVC based foam cored samples were tested at stress ratio of R=-1, -0.5, 0.25 and 0.5 while PMI based foam cored samples were tested at stress ratio of R=0.1 and R=-1. Tests were performed at load level of 70, 60, 50, 40, 30 and 25% of static failure load. S/N curves were obtained according to test results and curve fitting were implemented based on the equation (2.1).

$$\tau_{UD} = \tau_{th} + (\hat{\tau} - \tau_{th})e^{-\log\left(\frac{N}{a}\right)^b} \tag{2.1}$$

where τ_{th} is the fatigue threshold, $\hat{\tau}$ is the static failure load and a and b are fitting parameters. The τ_{th} fatigue threshold is the stress that any failure initiate or growth below it.

S/N diagrams of PVC based cored sandwich structures and PMI based cored sandwich structures with different stress ratio is shown in Figure 2.16 and 17 respectively.

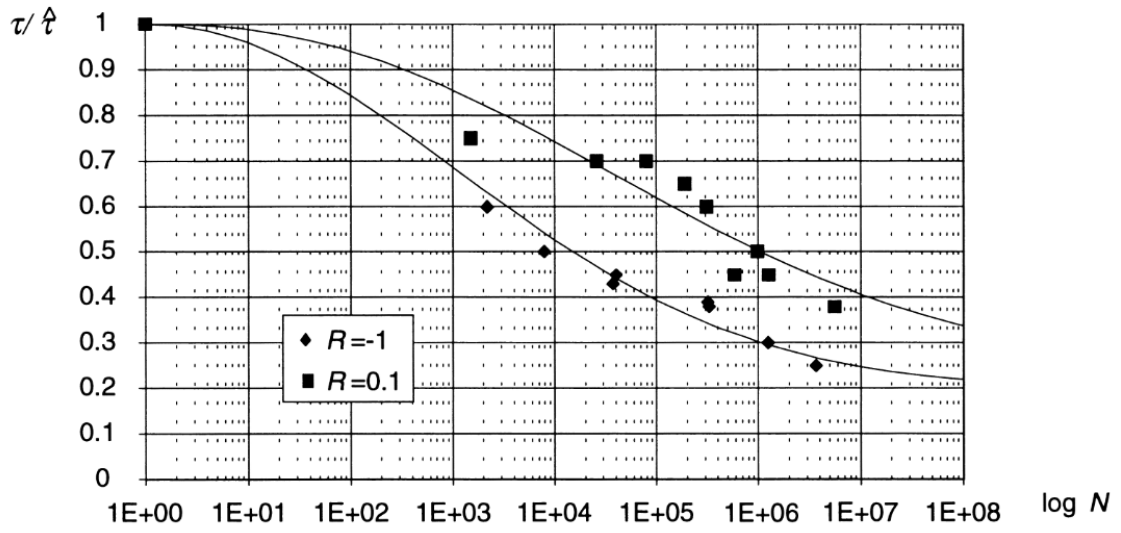

Figure 2.16. S/N curve of PVC based sandwich structures with curve fitting (Source: Burman and Zenkert 1997)

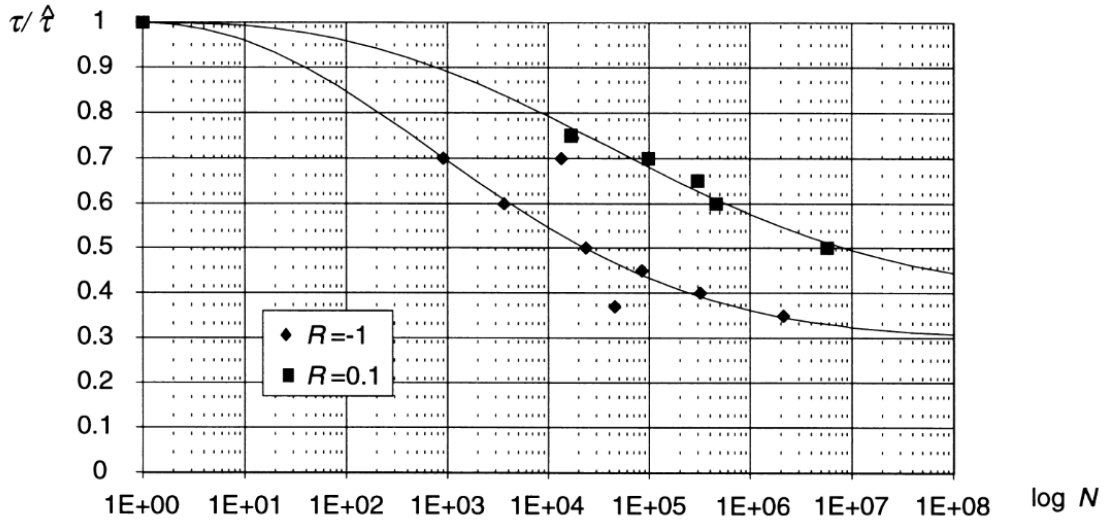

Figure 2.17. S/N curve of PMI based sandwich structures with curve fitting (Source: Burman and Zenkert 1997)

They also investigate the damage formation on foam cored sandwich structures. Figure 2.18 shows the crack formation on foam core of the sandwich with different stress ratios.

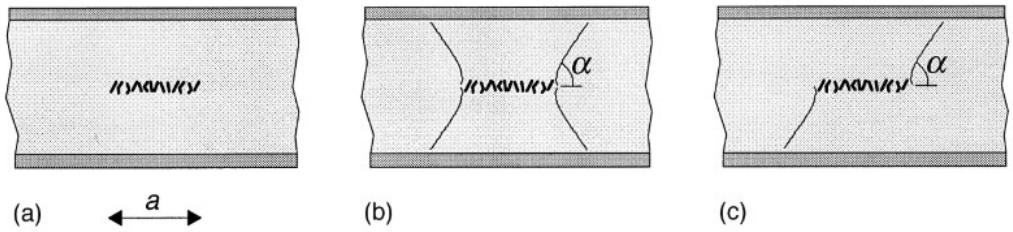

Figure 2.18. (a) initial microcrack forming a macrocrack a, crack propagation angles at (b) R= -1 and (c) R ≠ -1 (Source: Burman and Zenkert 1997)

To sum up, they tested two types of foam cored sandwich structures with different stress ratios and generated S/N curves and investigated the crack formation on foam cores. They found that a significant fatigue life decreasing was seen if the stress ratio $R < 0$. They also found that a linear curve fitting on logarithmic S/N curve validates the test results. Besides, stress amplitude on fatigue tests influenced the fatigue lifetime than mean stress. Furthermore, they found from their experiments that failure formation occurs in the foam core at foam cored structures. Microcracks initially formed on the foam core, and they grew until failure (Burman and Zenkert 1997).

Dai and Hahn experimentally investigated static and fatigue behavior of vacuum-assisted resin transfer molded sandwich panels. They utilized two different core materials which were balsa wood and PVC foam cores and nonwoven E-glass reinforced epoxy face sheets. 3 point and 4 point bending tests were performed to determine the static and fatigue behavior of developed sandwich panels. Static flexural tests were performed both balsa and PVC cored samples yet fatigue tests were performed only balsa cored samples. Fatigue test were carried out to balsa cored sandwich panel with long (965 mm span) and short span (152 mm span) length. Figure 2.19 shows the S/N curves of balsa cored sandwich structures with long and short span length.

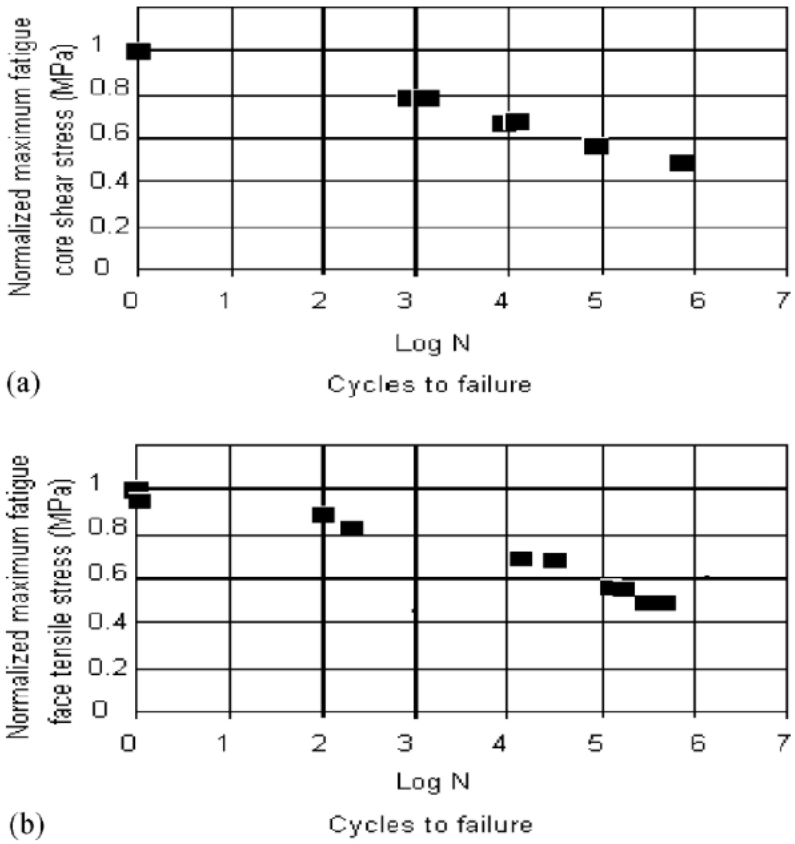

Figure 2.19. S/N curves of balsa cored sandwich panel with (a) short span length, (b) long span length (Source: Dai and Hahn 2003)

At the end of the study, they found that failure occurred at the results of core shear at the short span length fatigue tests and bottom laminate failure for long span length fatigue tests. Core and laminate showed the same fatigue degradation rate according to fatigue test results (Dai and Hahn 2003).

In another study, El Mahi et al. studied the flexural fatigue behavior of sandwich panels. They developed an analytical model based on stiffness reduction approach. An experimental study was also done and characterized with the Wöhler curves. They developed two various analytical models for displacement-controlled tests and load controlled tests. They used PVC foam cores and glass fiber reinforced epoxy face sheets like previous studies. Figure 2.20 shows the stiffness reduction curves of the displacement and load controlled fatigue tests of developed sandwich panel in different loading conditions.

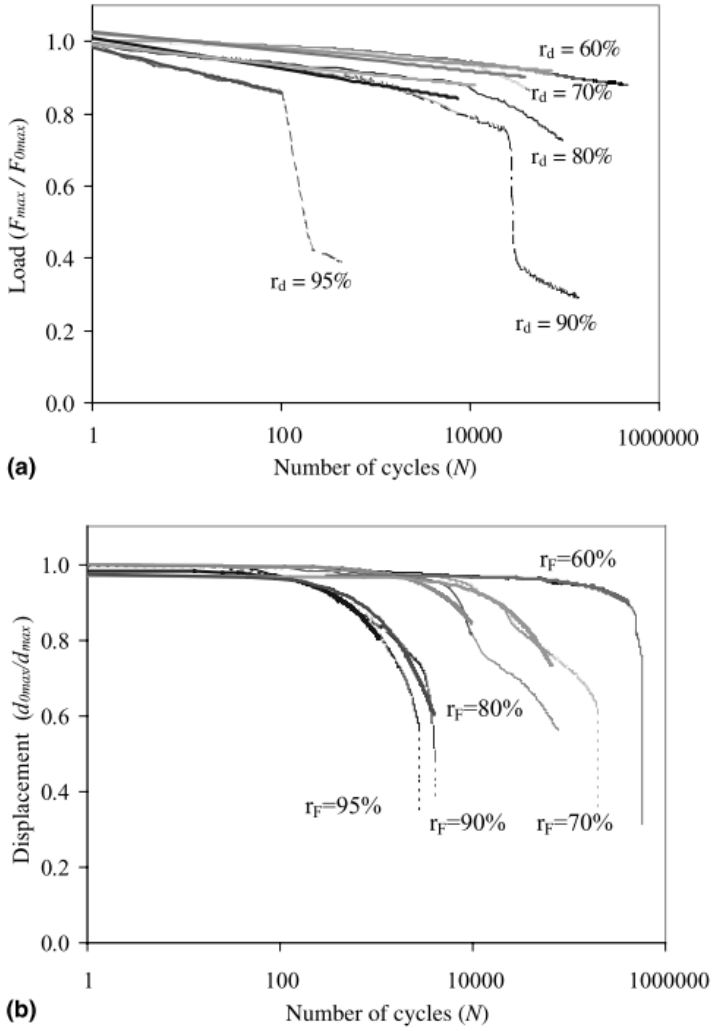

Figure 2.20. Stiffness reduction curves of sandwich panels for (a) displacement-controlled tests (b) load-controlled tests (Source: El Mahi et al. 2004)

Stiffness reduction curves shows the evolution of load and displacement with respect to number of cycles. These models include only damage initiation and propagation according to paper.

Fatigue test results were also characterized with S/N curves (Wöhler curves) and results were compared with analytical model. They used the N_{10} failure criteria which means that the sample were assumed to be failed when the 10% amount of the stiffness of the sample decreased. Wöhler curves of the sandwich panels in displacement and load controlled fatigue tests are illustrated in Figure 2.21.

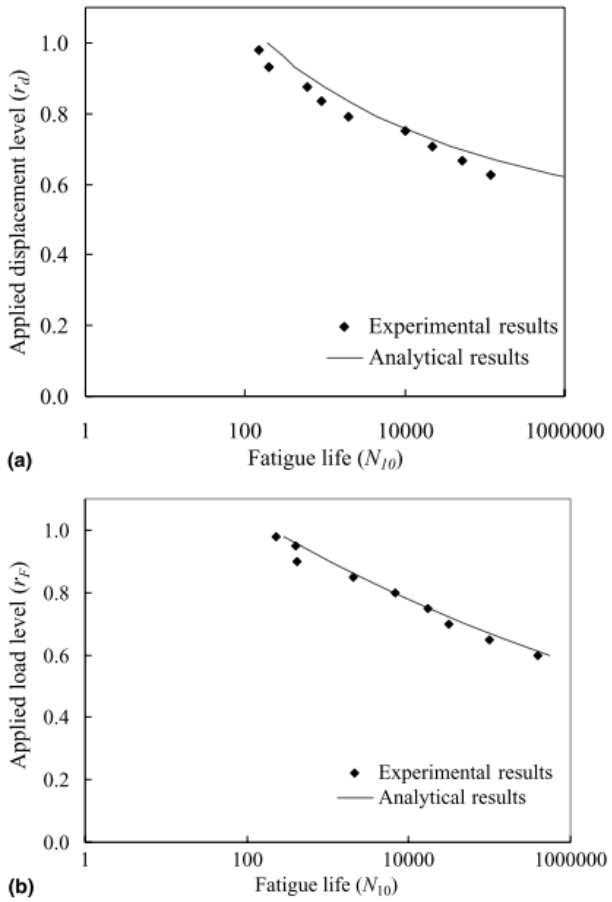

Figure 2.21. Wöhler curves of the sandwich panels with experimental and analytical model results in (a) displacement controlled (b) load-controlled fatigue tests (Source: El Mahi et al. 2004)

Experimental results on the Wöhler curves were represented by the linear curve fitting with the relation of the equation 2.2.

$$r = d - klogN \tag{2.2}$$

Where r is the loading level, N is the fatigue life and d and k are the fitting parameters.

To conclude, they developed an analytical approach based on stiffness reduction method to predict the fatigue life of foam cored sandwich structures and made the model validation with the experimental study. They found that their analytical model and tests results have good correlation (El Mahi et al. 2004).

Kulkarni et al. investigated the fatigue crack growth of PVC foam core sandwich beams under flexural load. They used S2-glass fiber with epoxy resins as face sheets and sandwich panels were manufactured by co-injection resin transfer molding technique.

Fatigue test was performed in a three-point flexure mode at room temperature under load control at a stress ratio of 0.1, using a sinusoidal waveform. A frequency of 3 Hz was used to prevent increase in temperature due to hysteretic heating. The specimens with a 228.6 mm support span, 63.5 mm width were cycled to failure or fatigued to 10^6 cycles. Data was generated at stress levels of 90%, 85%, 80%, 75%, 70%, 65%, and 60% of the ultimate flexural strength. They observed that three different failure mode took place before the specimen failure.

The first type of failure that was observed about 85% of fatigue life was the crack initiation and propagation on the compression side just the 1–1.5 mm below the interface which was the depth of resin penetration into the core material. It was observed that the crack always initiated at the sub-interface created by the resin-soaked, and the dry cells below the actual core–skin interface. Figure 2.22a shows the parallel goes of crack to the beam axis from the point of initiation towards the end support.

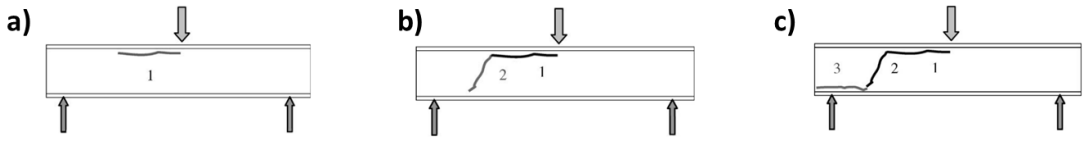

Figure 2.22. a) The first, b) the second, and c) the third type of failure (Source: Kulkarni et al. 2003)

The second damage comes after first failure was core shear. As shown in Figure 2.22b, the propagated crack kinks at a certain distance, and shears through the core thickness. At the end of this event, the crack reaches the bottom face sheet/core interface.

The third failure as shown in Figure 2.22c consists of delamination at bottom face/core interface. While propagating the core shear at a faster rate, the energy at the crack tip is sufficiently high, and crack reaches face sheet where it gets deflected along the core–skin interface. This is the reason the delamination occurs along the core-skin interface rather than sub-interface. After this rapid damage, the specimen ultimately fails.

Figure 2.23 shows the photograph of a failed specimen. It can be observed from the photograph, the crack in the first initiates at the sub- interface whereas for the third damage, the delamination separates the core from the face sheet.

Figure 2.23. The photograph of a failed specimen after cyclic loading (Source: Kulkarni et al. 2003)

Figure 2.24 shows the normalized S–N response of the specimens. The fatigue limit was found to be about 60% of the ultimate strength which was higher than the value of the low- density foam and polymeric composites (45–50%) (Kulkarni et al. 2003)

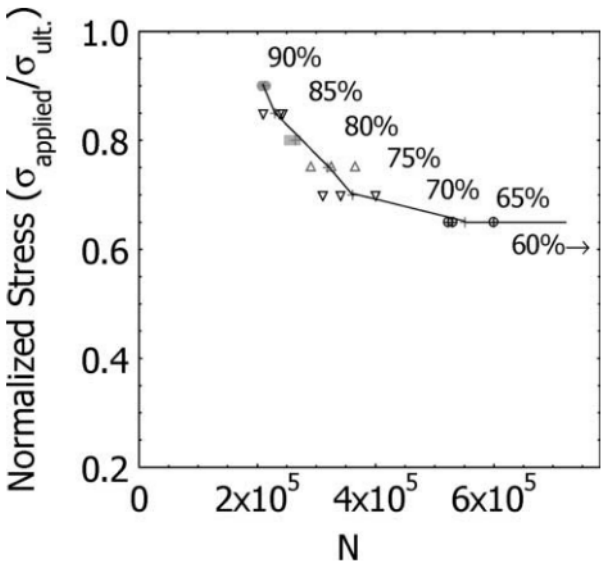

Figure 2.24. Normalized S–N curve (Source: Kulkarni et al. 2003)

Freeman et al. is another research group that studied the fatigue life of foam cored sandwich panels. They investigated the effect of low velocity impact on fatigue life of foam cored sandwich panels. They used carbon fiber epoxy face sheet laminated polyurethane foam cores. They performed the fatigue test in four point bending fixture with stress ratio of R = 0.165 and frequency of 1 Hz. They utilized two types of polyurethane foam cores which are low density and high density. Samples were exposed an impact damage before fatigue tests and effect of that impact on fatigue characteristic of the sandwich samples were determined. They found that the failure mode of the low-density samples is shear failure while bending failure for high density sandwich panels as shown in Figure 2.25 (Freeman et al. 2005).

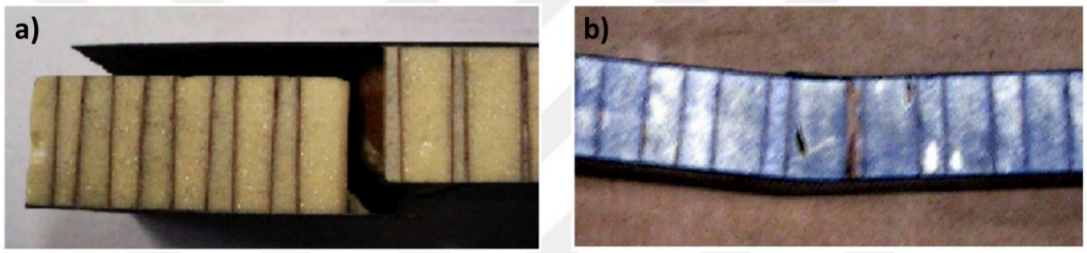

Figure 2.25. a) Shear failure in two layer low density samples b) Bending failure in two layer high density samples (Source: Freeman et al. 2005)

Bezazi et al. derived a model based on Bayesian trained artificial neural network to predict the fatigue life of sandwich panels. Validation of the model was made by experimental studies. They used glass fiber reinforced polymer as face sheet material while PVC foam as core material. Test was carried out in displacement controlled. Stiffness reduction curves of the sandwich panels were investigated to generate the fatigue prediction model. Figure 2.26 shows the stiffness reduction curves of sandwich panels for three different loading conditions.

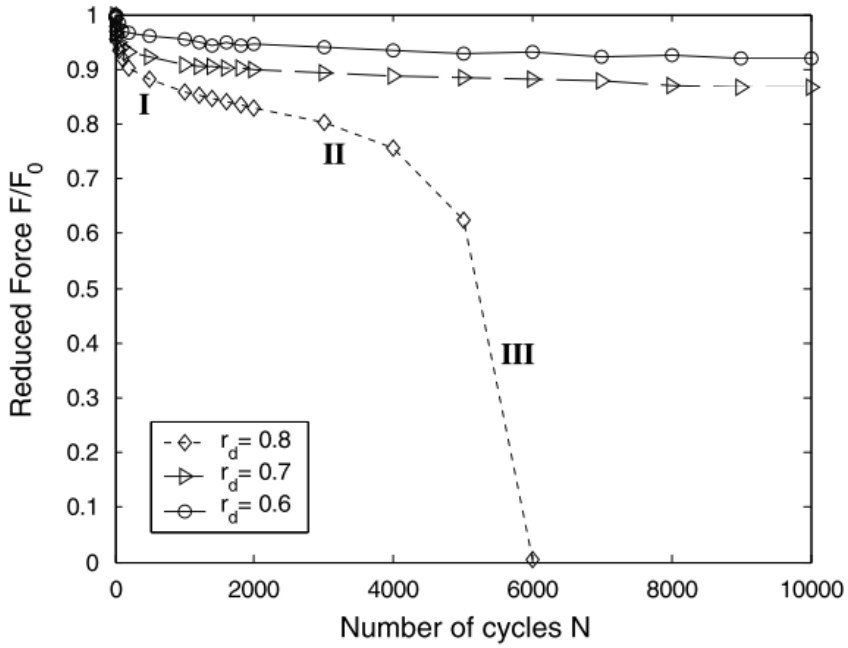

Figure 2.26. Stiffness reduction curves of sandwich panels in three different loading levels (Source: Bezazi, Pierce, and Worden 2007)

Stiffness reduction curves were divided into three phases. In phase I, a sharp reduction of the stiffness of the sandwich panels were seen. In phase II, reduction rate of the stiffness decreased and in phase III, rapid reduction of the stiffness loss rate was observed until the failure. They utilized that to derive their fatigue prediction model (Bezazi, Pierce, and Worden 2007).

In addition to the studies on foam core sandwich structures, attention of researchers in fatigue behavior of honeycomb cored sandwich structures has increased.

Belingardi et al. investigated the fatigue behavior of sandwiches beams consisting of aluminum honeycomb core and carbon fiber composite faces by four-point bending tests. Fatigue tests were performed at a room temperature under direct load control. The test load was sinusoidal with a frequency f= 10 Hz and a load ratio R = 0.1. The bending stiffness values of the specimens were monitored during the tests to obtain information about the possible reduction of the sandwich structural properties with fatigue cycling.

Figure 2.27 illustrated the failed specimen after fatigue test. They observed that there was not any damage in the honeycomb core, whereas a debonding of the composite face from the honeycomb area around the face fracture was seen.

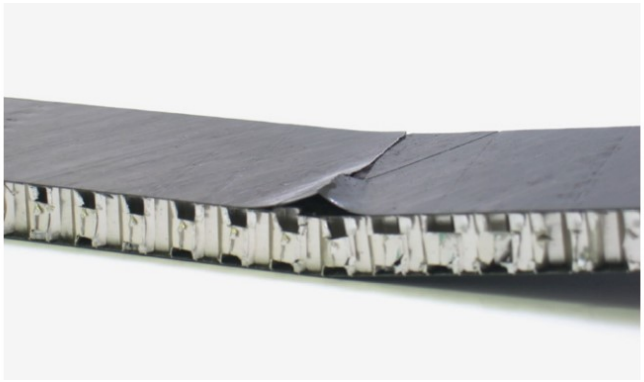

Figure 2.27. The failed sandwich sample after fatigue test (Source: (Belingardi, Martella, and Peroni 2007)

Stiffness reduction method was used in that study to identify the fatigue failure cycle as well. The bending stiffness per unit specimen width values as a function of fatigue cycle number are shown in Figure 2.28. During the test, the bending stiffness remained at the same value in both cases. For the test with a failure, a sudden reduction of the stiffness was seen before the failure due to local buckling failure of the compressed face. As a result, the fatigue damage nucleated and grew without causing the specimen stiffness to decrease until it failed.

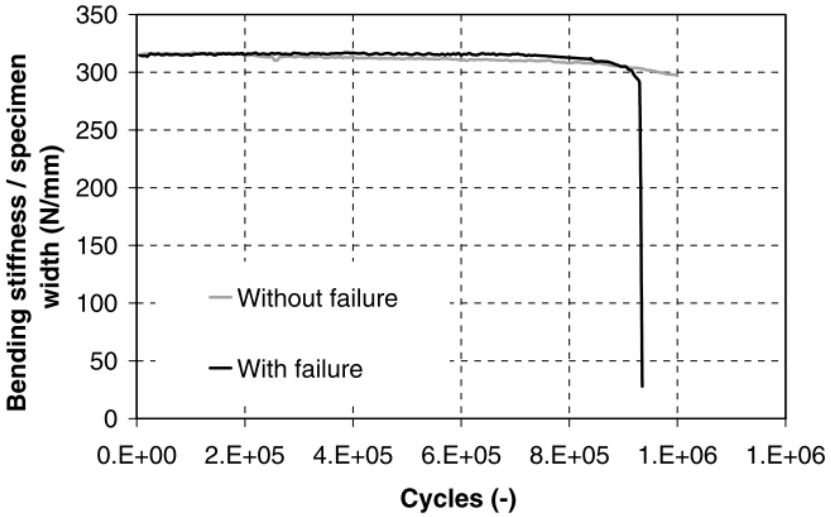

Figure 2.28. Bending stiffness values against number of cycles in fatigue test (Source: (Belingardi, Martella, and Peroni 2007)

The fatigue test results of are characterized with the S-N curve as shown in Figure 2.29. The load is expressed in terms of maximum bending moment M_f normalized with respect the static failure bending moment M_s (Belingardi, Martella, and Peroni 2007).

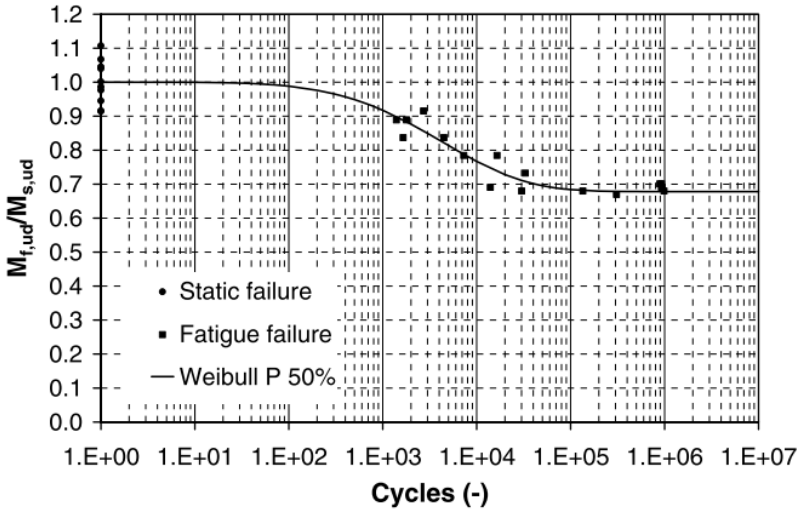

Figure 2.29. S-N diagram of the specimens (Source: (Belingardi, Martella, and Peroni 2007)

Jen and Chang et al. investigated the face thickness effect on bending fatigue life of honeycomb cored sandwich panels. They fabricated the sandwich panels by adhesively bonding of aluminum face sheets and aluminum honeycomb cores. They characterized the fatigue behavior of sandwich structures with three different face thickness with fatigue failure modes and S-N curves. The three types of sandwich panels were identified as Type A, Type B and Type C which has face sheet thickness of 1.0 mm, 1.2 mm, and 1.5 mm, respectively. Main failure modes were found as interfacial debonding for all types of sandwich samples as shown in Figure 2.30. Besides, no significant effect of the thickness of aluminum face sheets on fatigue life of sandwich structures was found in that study as illustrated at the S-N curves of three types of sandwich structures shown in Figure 2.31 (Jen and Chang 2009).

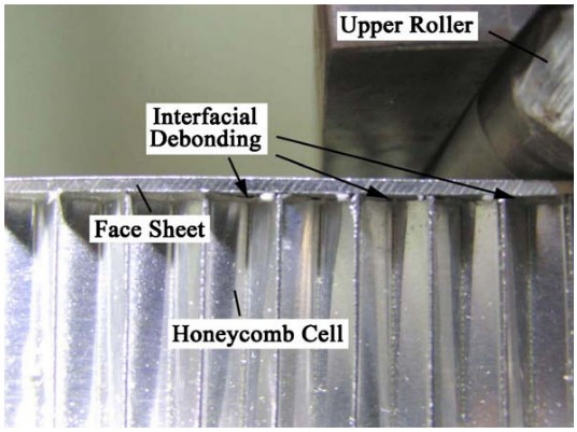

Figure 2.30. Primary fatigue failure mode of sandwich structure (Source: Jen and Chang 2009)

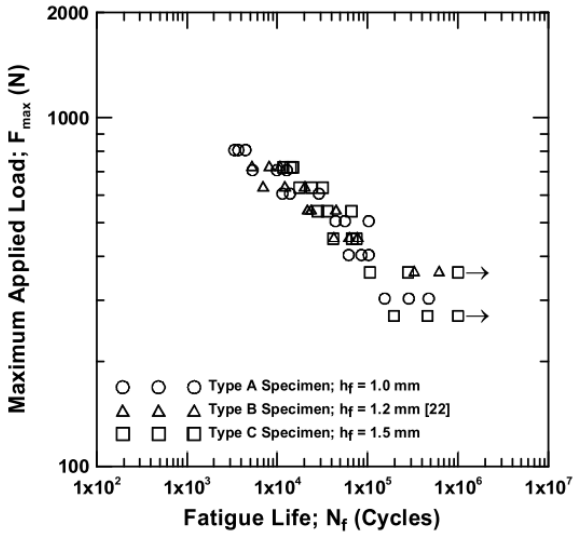

Figure 2.31. S-N curves of three types of sandwich structures (Source: Jen and Chang 2009)

In another study, Jen et al. investigated the effect of amount adhesive on the fatigue strength of honeycomb cored sandwich panels. They used adhesively bonded aluminum honeycomb core with aluminum face sheets in their sandwich panels. They fabricated three groups of sandwich samples which consisted of three different amount of adhesive which were 0.4, 0.7 and 1.0 kg/m^2. Fatigue strength of fabricated sandwich structures were characterized with S-N curves. They also determined the fatigue failure mode of honeycomb bonded sandwich panels.

It was found that fatigue strength of fabricated panels increases as the amount of adhesive on the sandwich panel increases as shown in S-N curves in Figure 2.32 (Jen, Ko, and Lin 2009).

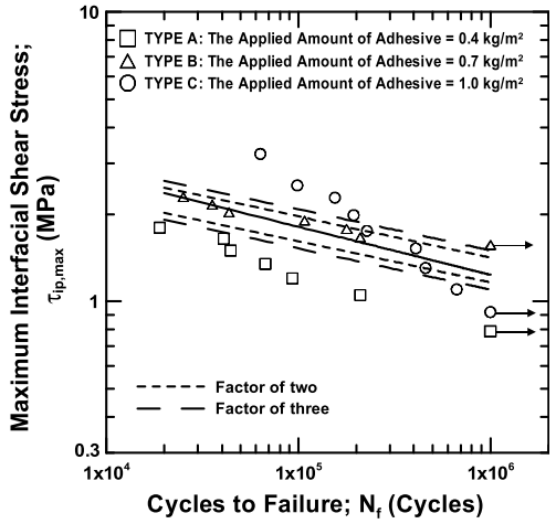

Figure 2.32. S-N curves of three groups of sandwich panels (Source: Jen, Ko, and Lin 2009)

It was also determined that interfacial debonding of core and face sheets were the main failure mode under bending fatigue conditions seen in Figure 2.33 (Jen, Ko, and Lin 2009).

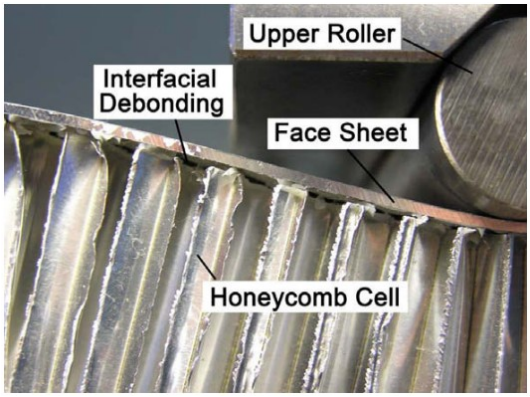

Figure 2.33. Interfacial debonding of aluminum face sheet and honeycomb core (Source: Jen, Ko, and Lin 2009)

Belouettar et al. studied the static and fatigue flexural behavior of honeycomb cored sandwich structures by four-point bending test. They used aluminum and aramid honeycomb core with aluminum face sheets in their fatigue characterization. Static and fatigue failure modes and S-N curves of the structures were obtained.

Load-controlled fatigue tests were carried out with frequency of 2 Hz and stress ratio was selected as 0.1. S-N curves of aluminum honeycomb cored, and aramid honeycomb cored structures were seen in Figure 2.34.

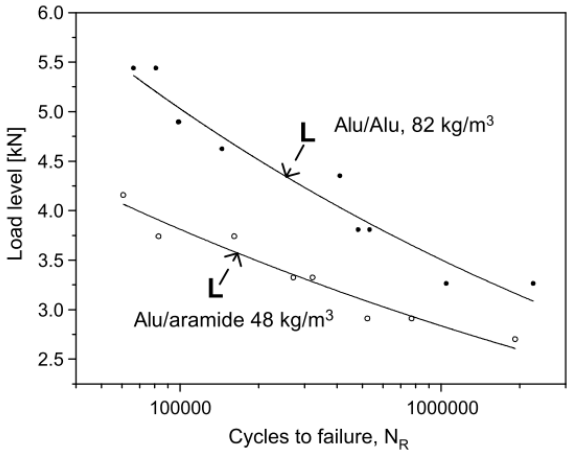

Figure 2.34. Comparison of S-N curves of aramid honeycomb cored and aluminum honeycomb cored sandwich structures (Source: Belouettar et al. 2009)

It was seen that aluminum honeycomb sandwich structures have higher fatigue strength in comparison with aramid honeycomb cored sandwiches according to Figure 2.34. Figure 2.35 illustrated the fatigue failure modes of two types of sandwich structures.

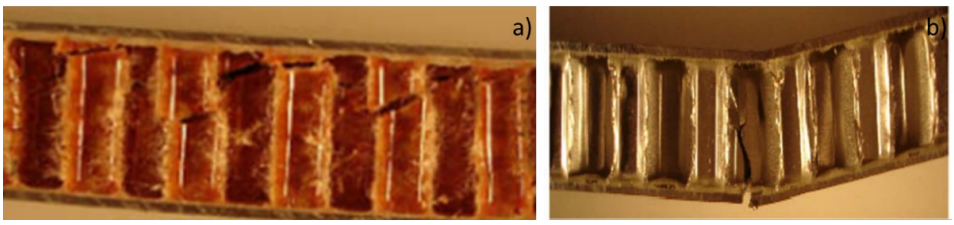

Figure 2.35. Fatigue failure modes of two types of sandwich structures, a) aramid honeycomb, b) aluminum honeycomb (Source: Belouettar et al. 2009)

It was seen that main failure mechanism for aramid honeycomb cored structures is cracking on aramid honeycomb cores while it was both aluminum honeycomb core cracking and aluminum face sheets breakage for aluminum honeycomb cored sandwich structures (Belouettar et al. 2009).

In 2014, another study about the flexural fatigue behavior of sandwich structures fabricated from aluminum honeycomb core and aluminum face sheets by Jen et al. They carried out the tests by constant-amplitude principle and they characterized the fatigue behavior with S-N curve, stiffness degradation and fatigue failure modes. Typical fatigue failure modes were found as buckling of aluminum face sheets and aluminum honeycomb core crushing as shown in Figure 2.36 (Jen, Teng, and Teng 2014).

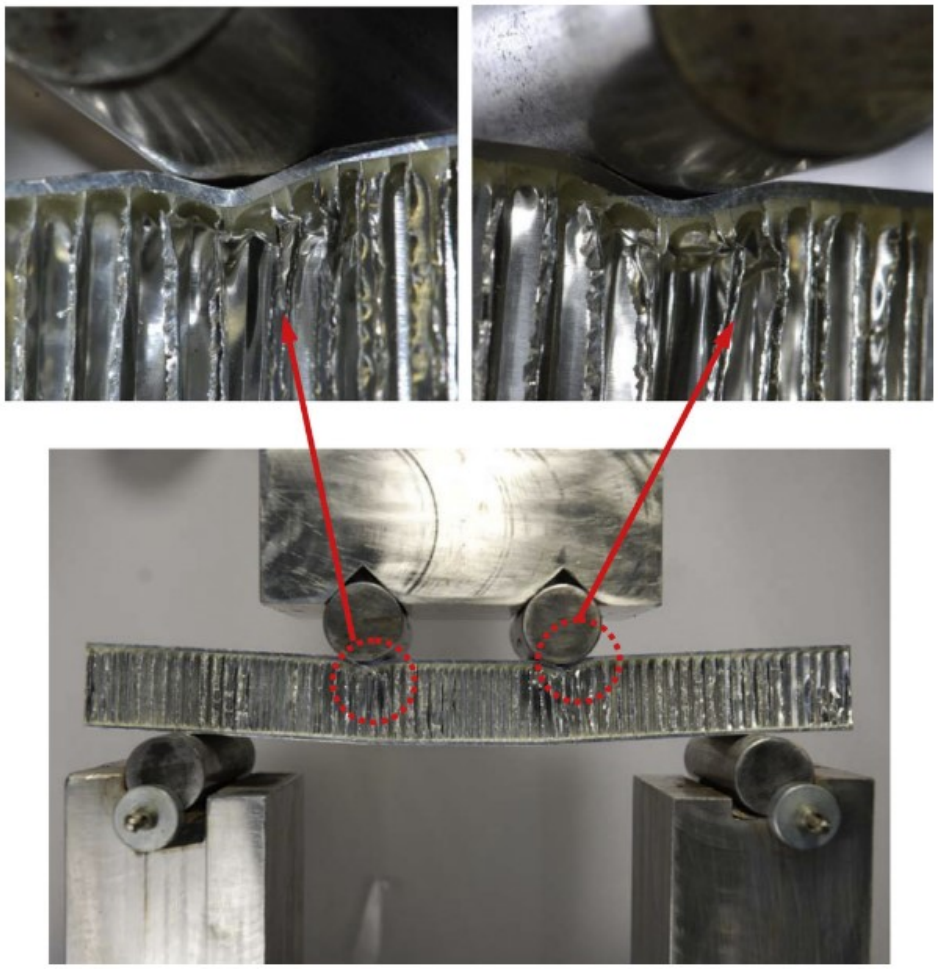

Figure 2.36. Typical fatigue failure modes of investigated sandwich structures (Source: Jen, Teng, and Teng 2014)

Boukharouba et al. developed an analytical model for prediction of fatigue behavior of sandwich panels. They executed displacement-controlled fatigue tests in three point bending test fixture to validate the analytical model. Carbon fiber reinforced polymer face sheets and aramid honeycomb core was utilized to fabricate the sandwich panels. Stiffness reduction curves of the sandwich panels with different load levels are shown in Figure 2.37.

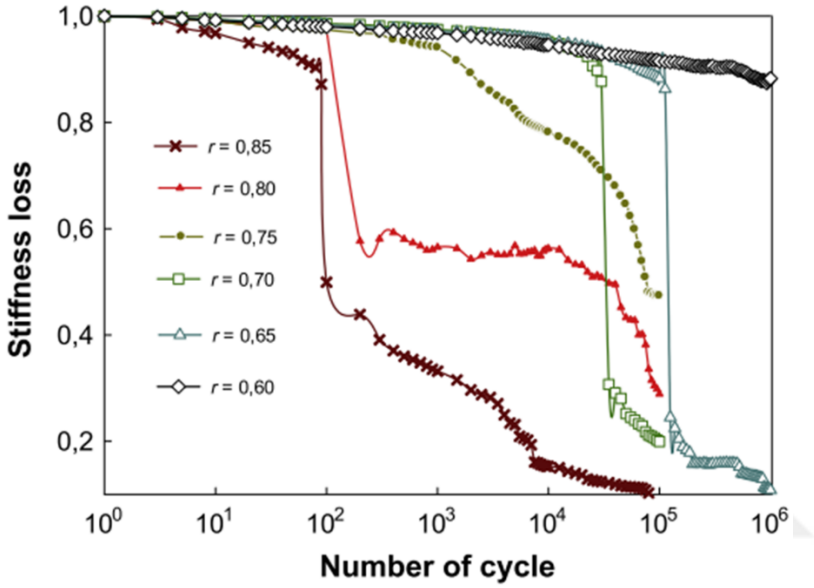

Figure 2.37. Stiffness reduction curves of the sandwich samples with different loading levels (Source: Boukharouba, Bezazi, and Scarpa 2014)

After a few cycles, the stiffness reduction level drops instantly, followed by a slow decrease in stiffness that lasts almost the entire operational life of the specimen. The final phase consists of a sudden load loss until the sandwich beam fails completely. At the end of the study, they compared and validate their analytical model with stiffness loss curves (Boukharouba, Bezazi, and Scarpa 2014).

Abbadi et al. studied the fatigue behavior of honeycomb sandwich panels with and without artificial defects. Aluminum was used as faces and the core structure was made from aluminum alloy or aramid honeycombs folded and glued together forming a hexagonal cell structure. Fatigue tests of without defects samples were carried out under load-control. Frequency of the tests were kept at 2 Hz., and the load ratio R was selected to 0.1. S-N curves and fatigue failure modes were investigated to compare the fatigue

behavior of sandwich panels with aramid and aluminum honeycomb cored. They also characterized the fatigue behavior of sandwich panels with respect to defect situation. Figure 2.38 shows the fatigue failure modes of both aramid and aluminum honeycomb cored sandwich structures according to test results (Abbadi et al. 2015).

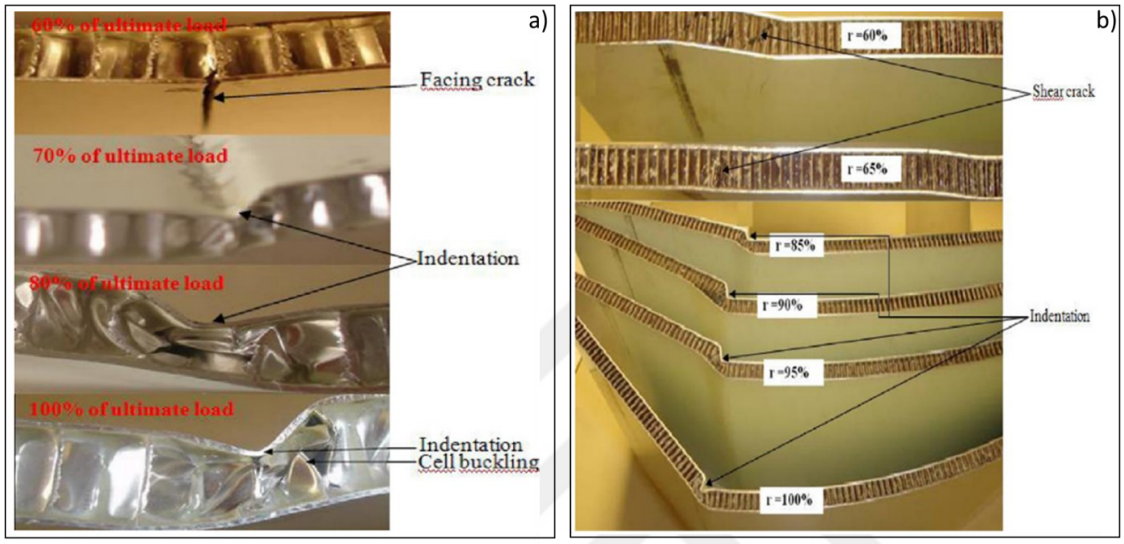

Figure 2.38. Fatigue failure modes of without defect sandwich structures, a) aluminum honeycomb core, b) aramid honeycomb core (Source: Abbadi et al. 2015)

More detailed failure mode investigation was done in that study in comparison with Belouettar et al. (Belouettar et al. 2009) as shown in Figure 2.35 and Figure 2.38. Some other failure modes such as indentation of face sheets and honeycomb cell buckling was observed in that study in addition to Belouettar et al. (Belouettar et al. 2009, Abbadi et al. 2015)

Palomba et al. investigated the collapse modes of aluminum honeycomb sandwich structures under flexural fatigue loading. Aluminum face sheets and aluminum honeycomb core were used to manufacture the sandwich panels. They obtained the S-N curves and fatigue failure modes for different span length under flexural fatigue load. Figure 2.39 shows the S-N curves of sandwich panels with different span dimensions and Figure 2.40 illustrates the fatigue failure mode with respect to span length.

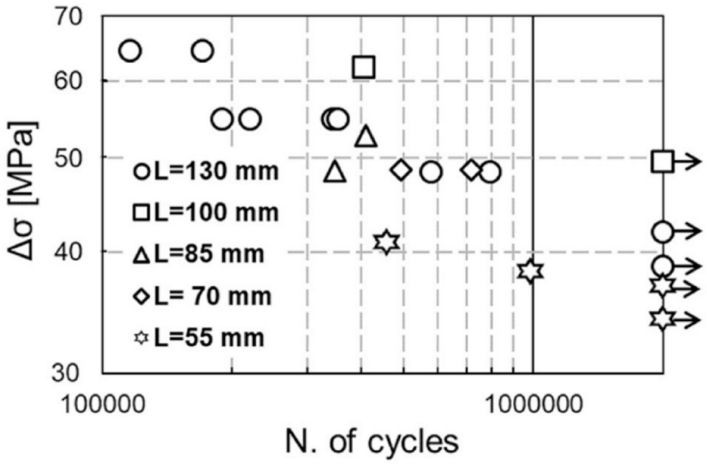

Figure 2.39. S-N curves of sandwich structures with different span length (Source: Palomba, Crupi, and Epasto 2019)

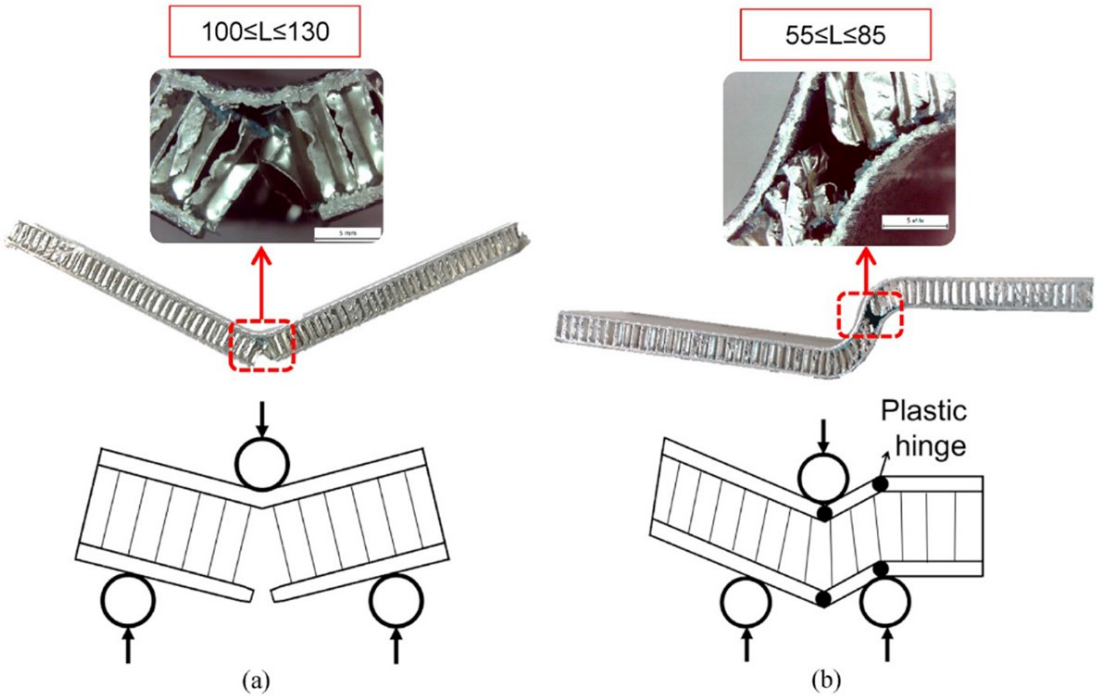

Figure 2.40. Fatigue failure modes of sandwich panels under flexural fatigue loading with different span length a) face sheet failure, b) core shear (Source: Palomba, Crupi, and Epasto 2019)

Decreasing in span length causes the reducing on the fatigue life of sandwich panels as shown in Figure 2.39. Span length also effected the fatigue failure mode as

shown in Figure 2.40. In small length spans, the failure modes were determined as core shear. Skin failure was observed when the span length is greater than 85 mm according to test results (Palomba, Crupi, and Epasto 2019).

Wu et al. made an experimental and numerical study on both static and fatigue behavior of honeycomb cored sandwich structures. The sandwich samples were manufactured by adhesively bonded carbon fiber reinforced polymer and aramid honeycomb core. They investigated flexural and compression fatigue behavior of sandwich panels experimentally. They obtained S-N curves and fatigue failure modes of sandwich panels as well as most of the studies. The S-N curve with the linear fitting of the developed sandwich panels is shown in Figure 2.41.

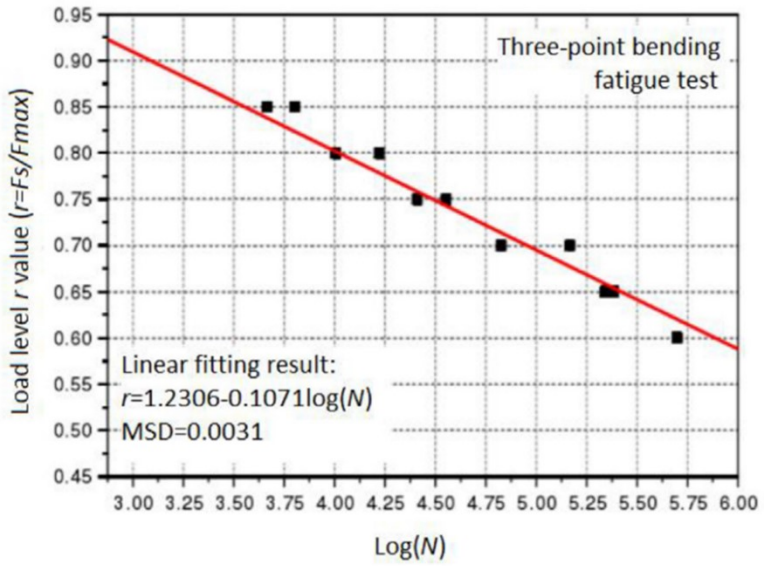

Figure 2.41. S-N curve of three point bending fatigue tests of developed sandwich panels (Source: Wu et al. 2019)

S-N curve of the shows that the fatigue life of the sandwich panels could reach above 500.000 cycles at loading level of 0.6 F_{max}. Figure 2.42 illustrates the flexural fatigue failure modes of developed sandwich panels (Wu et al. 2019).

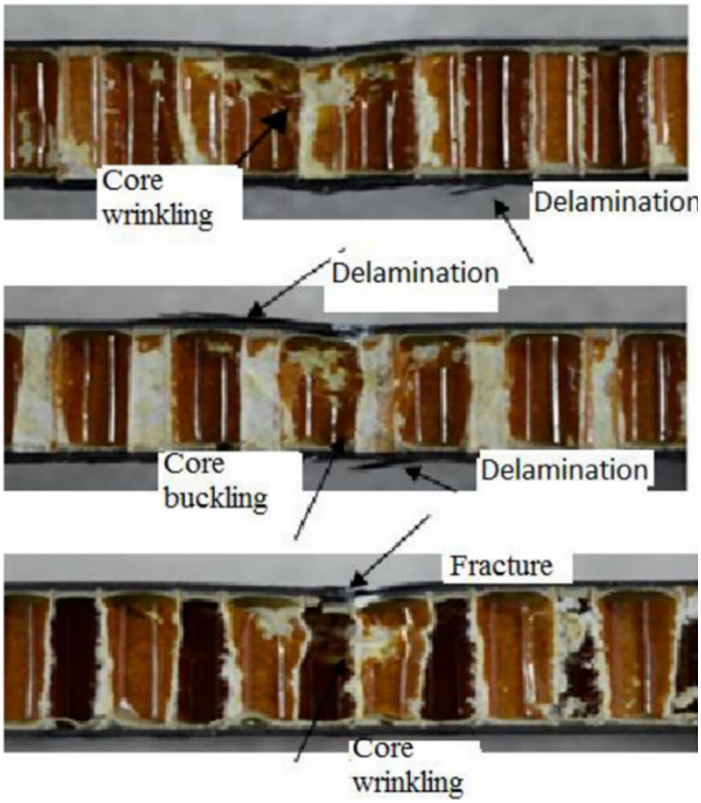

Figure 2.42. Flexural fatigue failure modes of developed sandwich structures (Source: Wu et al. 2019)

As shown in Figure 2.42, core wrinkling, delamination of carbon fiber reinforced polymer face sheets, core buckling, and fracture of composite face sheets were found as failure modes of developed sandwich panels by contrast with Abbadi et al. (Abbadi et al. 2015) and Belouettar et al. (Belouettar et al. 2009). Main reason of that difference was to be considered the greater stiffness of the carbon fiber reinforced polymer face sheets (Abbadi et al. 2015, Belouettar et al. 2009, Wu et al. 2019).

The last study about fatigue failure of the honeycomb cored sandwich structures was made by Ma et al. to our knowledge in 2020. Their investigation includes both numerical and experimental studies. The sandwich panels were made by quartz fabric reinforced cyanate ester face sheets and aramid honeycomb core. They carried out their tests under three point bending load with three different stress ratio which are R=-1, R=0 and R=0. 4 or 5 loading levels were used for each stress levels and S-N curves and flexural fatigue failure modes were obtained. Failure modes and crack growth of those sandwich panels are shown in Figure 2.43 and Figure 2.44, respectively.

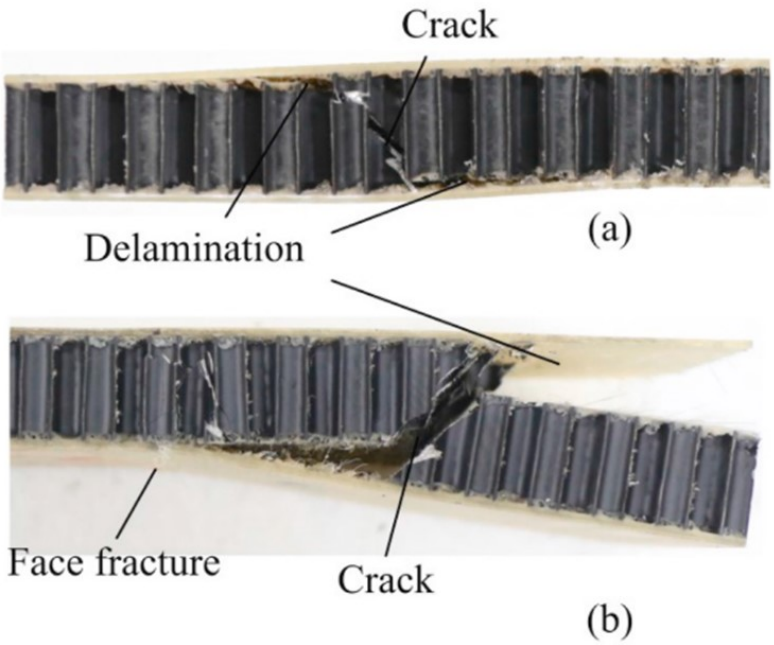

Figure 2.43. Flexural fatigue failure modes of sandwich panels, a) failure modes of the samples, b) fracture in the face sheet and face sheet/core debonding (Source: (Ma et al. 2020)

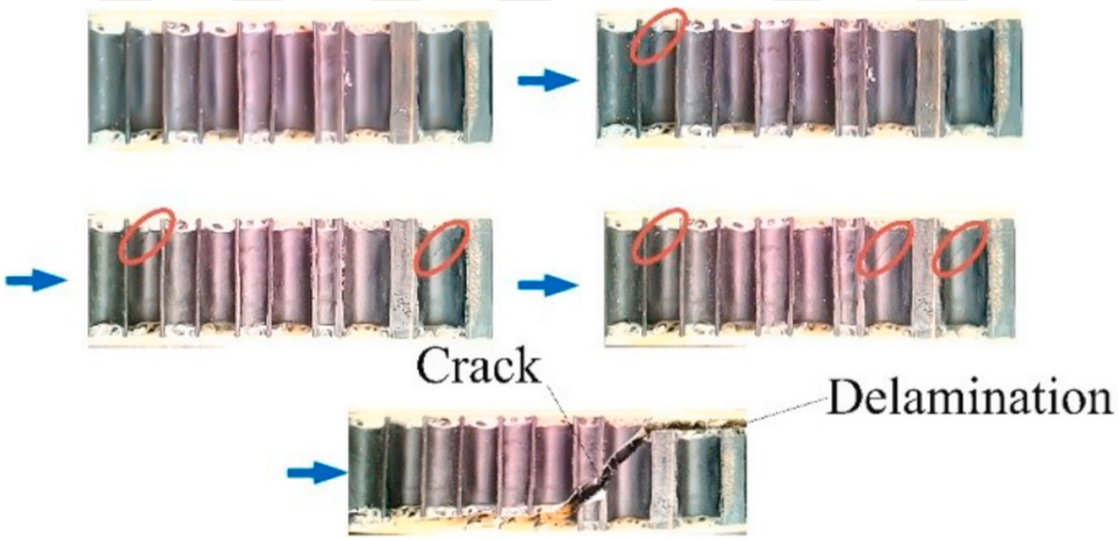

Figure 2.44. Fatigue crack growth story of sandwich panels (Ma et al. 2020)

First failure mode of the sandwich structures was interfacial debonding as shown in crack growth story. The crack formation that initiates at the interface grows into the

core with approximately 45º as shown in Figure 2.44. Failure completed with complete separation of face sheets and honeycomb core as shown in Figure 2.43 (Ma et al. 2020).

As shown in the literature review, there are very limited studies existing in the literature about an experimental approach on fatigue behavior of sandwich structures with carbon fiber reinforced polymer (GFRP) face sheets and aluminum honeycomb core. In the next chapters of the thesis, fatigue behavior of sandwich structures made by GFRP face sheets and aluminum honeycomb core will be investigated.

CHAPTER 3

EFFECT OF AMOUNT OF ADHESIVE ON FATIGUE BEHAVIOR OF ALUMINUM HONEYCOMB CORED SANDWICH PANELS

3.1. Materials

Carbon fiber reinforced polymer (CFRP) matrix composites were used as face material for sandwich panels. Unidirectional carbon fabrics with unit weight of 500 gr/m^2 were supplied from METYX Composites, Turkey. A low viscosity epoxy resin system (Momentive L160, Hexion Inc., Ohio) and its hardener (Momentive H160, Hexion Inc., Ohio) were used as polymer matrix for face sheets. In this section of thesis, aluminum honeycombs with hexagonal cell configuration with the thickness of 21 mm were supplied from Altıgen Panel Aerospace Shipbuilding Panel Industry, Turkey and were utilized as core material for sandwich system. Denlaks PU99 polyurethane based adhesive were used to laminate the carbon fiber reinforced polymer matrix composites with aluminum honeycomb core. In this part of section, sandwich panels were fabricated with three different amounts of adhesive which are 333 g/m^2, 500 g/m^2 and 666 g/m^2 to characterize the effect of amount of adhesive on mechanical characteristic of aluminum honeycomb cored sandwich structures.

3.2. Fabrication of CFRP Faced Aluminum Honeycomb Cored Sandwich Panels

Sandwich panels were manufactured at the Composite Research Laboratory of Izmir Institute of Technology at Mechanical Engineering Department.

Composite face sheets were fabricated by vacuum assisted resin transfer molding (VARTM) process. Four layers of dry carbon fabrics were placed onto a smooth surface with the orientation of [0/90]. VARTM system was closed by a vacuum bag, after all VARTM manufacturing elements were prepared. Epoxy resin and its hardener were

mixed with ratio of 80:20 in mass, respectively. Resin was allowed to inject through the fabrics by the force of vacuum. After completion of the infusion, composite plate was kept in the room temperature for 24 hours. Composite plate was removed after resin curing was completed. A post-curing procedure was applied to the composite part for 16 hours at 60 ºC to obtain superior mechanical properties. Composite plates were cut into by water-cooled diamond saw according to relevant ASTM standard.

Fabricated composite plates were bonded to aluminum honeycomb core with the polyurethane-based adhesive to obtain a sandwich panel. One surface of the face sheets was sanded with a sandpaper to improve the surface area to obtain perfect adhesion between face sheets and honeycomb core interface. Polyurethane adhesive was applied to the surface of face sheets then honeycomb cores were laminated with face sheets under the pressure of 10 kPa. Sandwich structures were cured for 24 hours at 40ºC. At the end of the process, a post-curing was applied to the sandwich structures for 7 days at room temperature. Flow chart of the manufacturing of sandwich panels were mentioned in Figure 3.1.

In section of thesis, sandwich panels with three various amounts of adhesive on the composite face-aluminum honeycomb core interface (333 g/m^2, 500 g/m^2 and 666 g/m^2) were manufactured and characterized. Sandwich panels with amount of adhesive on the face-core interface of 333 g/m^2, 500 g/m^2 and 666 g/m^2 core thickness are named Adh333, Adh500 and Adh666, respectively.

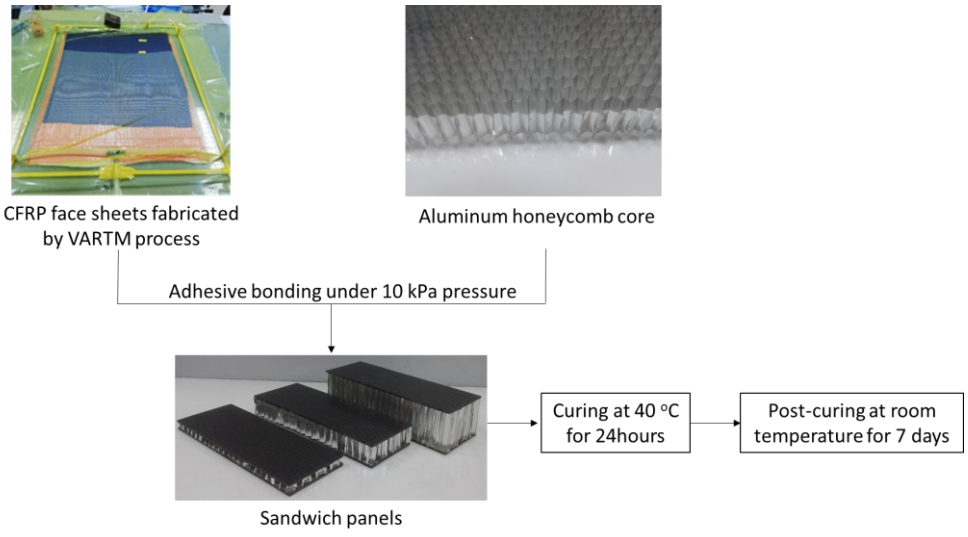

Figure 3.1. Flow chart of the manufacturing process of sandwich panels

3.3. Experimental Studies

3.3.1. Determination of Static Flexural Behavior of Sandwich Panels

Quasi-static flexural behavior of the sandwich panels was characterized by three-point bending test. Three-point bending tests were performed to sandwich panels by using MTS universal servo-hydraulic testing machine with 100 kN load cell in accordance with ASTM C393 standard (International 2016). Static bending tests were applied to sandwich panels not only to determine the static flexural behavior of sandwich panels but also to provide the ultimate flexural load to fatigue tests. Static bending test set-up is shown in Figure 3.2. The loading span was 150 mm, and diameter of rollers was 10 mm. Tests were performed with the rate of 6 mm/min until failure occurs. Three of specimen were tested for each batch of sandwich panels. Load-deflection curves and failure modes of sandwich panels were obtained.

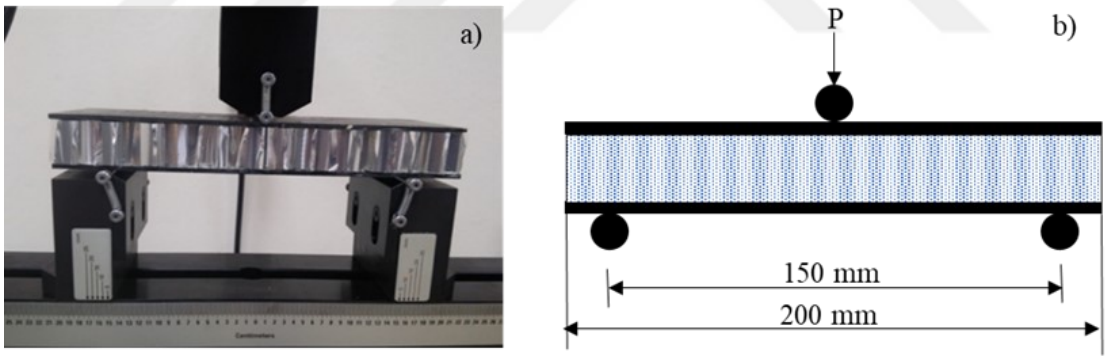

Figure 3.2. a) Test set-up for static bending test of sandwich beams, b) schematic illustration of test set-up

3.3.2. Determination of Fatigue Behavior of Sandwich Panels

Load controlled fatigue tests were performed using MTS servo-hydraulic testing machine under three-point bending load. The test setup was the same as the static flexural tests seen in Figure 3.2. Tests were carried out with respect to 80, 70, 60 and 50% of

ultimate static flexural load (F_{ult}) provided from static three-point bending tests. F_{max} and F_{min} are maximum and minimum load levels subjected on specimens in fatigue tests with sinusoidal waveform, respectively. Load ratio (R) which is defined in (3.1) was selected to 0.1.

$$R = \frac{F_{min}}{F_{max}} \tag{3.1}$$

Frequency (f) was kept at 2 Hz to prevent the specimens from failure by heating. Test was ended when the first failure mode was observed on the specimen which means specimens could not bear the load.

3.4. Results and Discussion

3.4.1. Static Flexural Test Results

Static flexural behavior of sandwich specimens was carried out by three-point bending tests and results were characterized by load-displacement curves and flexural failure modes of sandwich panels.

3.4.1.1. Load-Displacement Curves and Failure Modes

Figure 3.3 shows the load-deflection curve of three distinct samples of sandwich panels which were named Adh333. Three significant points were stated on load-displacement curve of Adh333 panels which were reflected as O, A and B shown in Figure 3.3 to explain the deformation and failure conditions. Point O represents the starting point of the three-point bending test. A linear elastic region was seen up to point A in the load-displacement curve. Slope of the linear-elastic line of the load-displacement curve represents the stiffness of the sandwich panels. Debonding of the composite face and aluminum honeycomb core was observed as initial failure mode which occurs at point A as shown in Figure 3.4(a). $[0/90]_4$ oriented carbon fiber reinforced composite face

sheets enabled the bending deformation of the face sheets without failure so that sandwich panel has maintained its load-bearing capacity at the end of the point A, however stiffness of the panel decreased dramatically, and a steady plateau was seen between point A and point B as shown in Figure 3.3. Shear forces that had been sustained by face-core interface was transferred to the honeycomb core and composite face sheet as compression force and bending force respectively, after debonding of the core-face interface occurred. This phenomenon is the reason of stiffness reduction of sandwich panels. Aluminum honeycomb core and carbon fiber reinforced epoxy face sheets absorbed whole deformation energy generated from bending load between point A and point B, as a result, aluminum honeycomb core crush was observed as second failure mode for sandwich panels coded Adh333 as shown in Figure 3.4(b). Delamination at carbon fiber reinforced epoxy face sheet was the final failure mode for Adh333 panels at point B as shown in Figure 3.4(c). Carbon fiber reinforced epoxy face sheets were completely separated from aluminum honeycomb core due to insufficient amount of adhesive on the core-face interface which causes insufficient bonding strength on the interface.

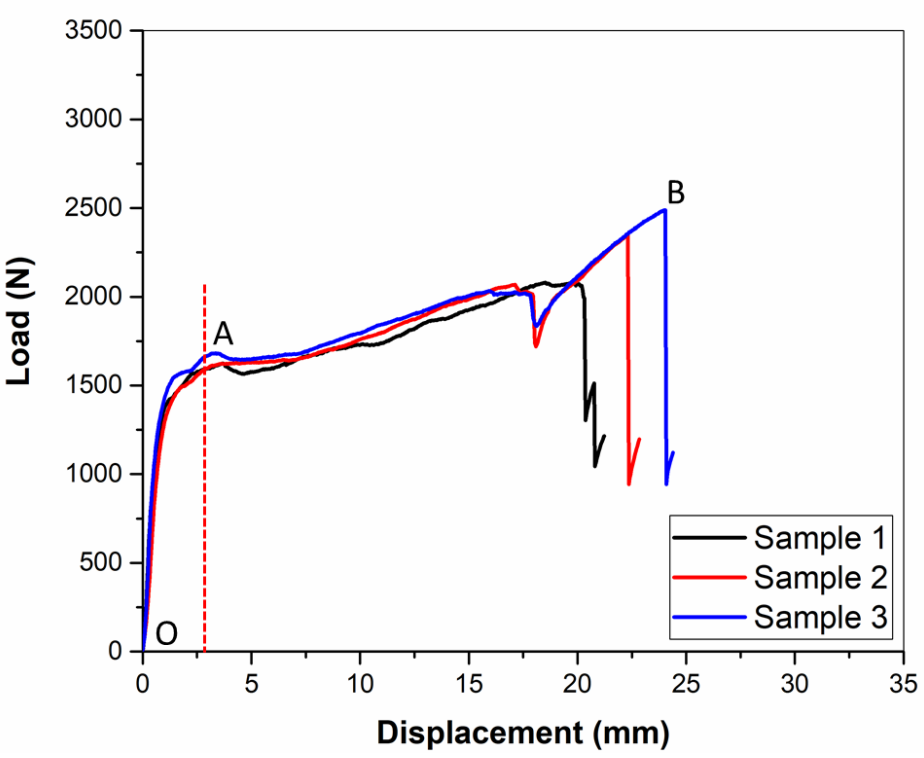

Figure 3.3. Load displacement curves of three samples of Adh333 panels

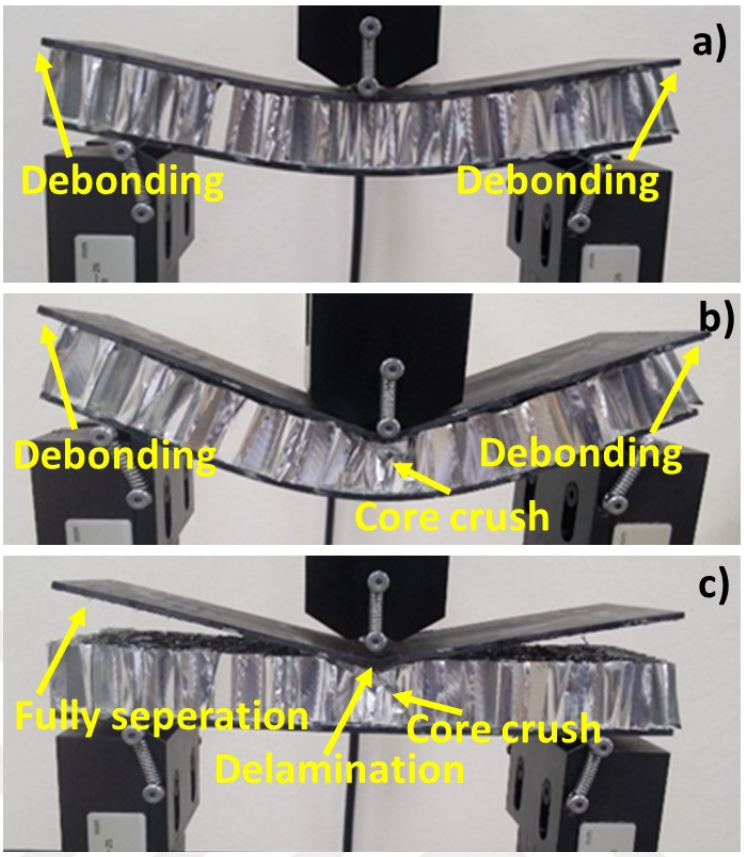

Figure 3.4. Failure modes of Adh333 sandwich panels a) debonding at point A, b) core crush at the steady plateau between point A and point B, d) delamination at point B

The load-displacement curves of three samples of sandwich panels named as Adh500 is shown in Figure 3.5. Significant points were marked on load-displacement curves of those samples as well. Likewise, a linear elastic region was observed between point O and point A on the load-displacement curve of Adh500 samples. Peak load was seen at point A after linear elastic region end, then load decreased dramatically up to point C. That was because debonding on the interface between composite face and aluminum honeycomb core occurred between point A and point C as shown in Figure 3.6(a). Debonding on the interface appeared on the one edge of the interface and crack has grown from the edge to the middle of the sample. Shear load on the interface was carried by areas of the interface that have not been collapsed yet. Shear load on the collapsed area of the interface was transferred to the aluminum honeycomb core and composite faces as compression load and the bending load respectively as well. Aluminum honeycomb core crush was observed between point C to point B as another failure mode of the sandwich panels which were named as Adh500 as shown in Figure 3.6(b). Aluminum honeycomb

core and [0/90] oriented composite faces have high strain energy capability during failure. Due to this reason, although stiffness of the sandwich panels decreases, sandwich panels kept their load-bearing capacity and out-of-plane load that was carried by sandwich samples increased between point C to point B. Load decreased significantly in point B due to delamination of the composite faces as shown in Figure 3.6(c). It was revealed that most of the strain energy generated by out-of-plane flexural forces was absorbed from composite faces due to sudden decreasing after delamination.

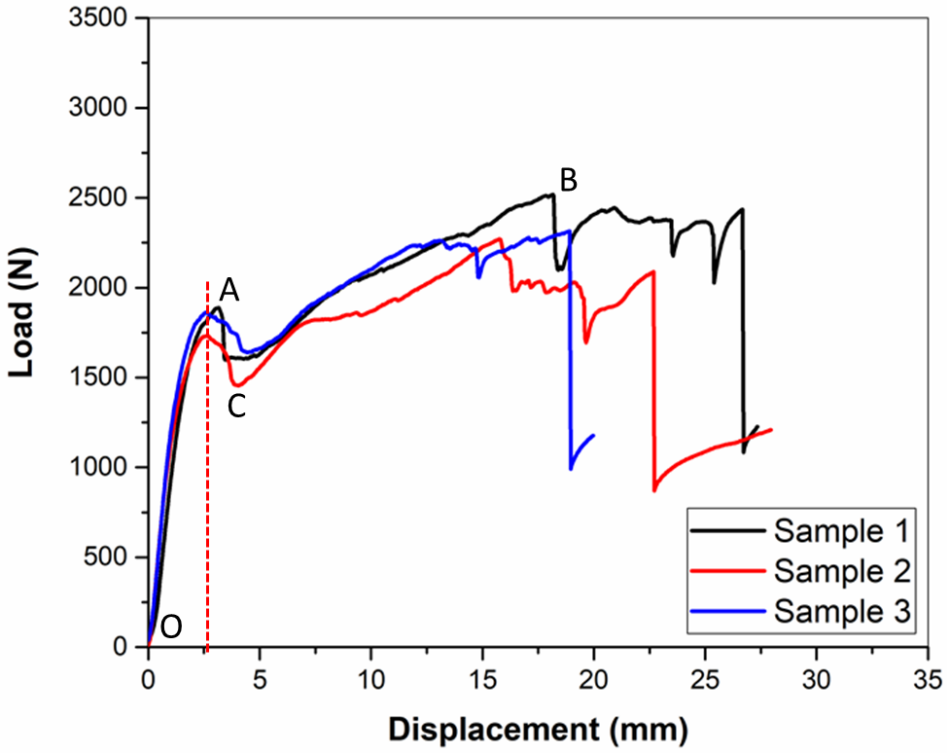

Figure 3.5. Load-displacement curves of three samples of Adh500 panels

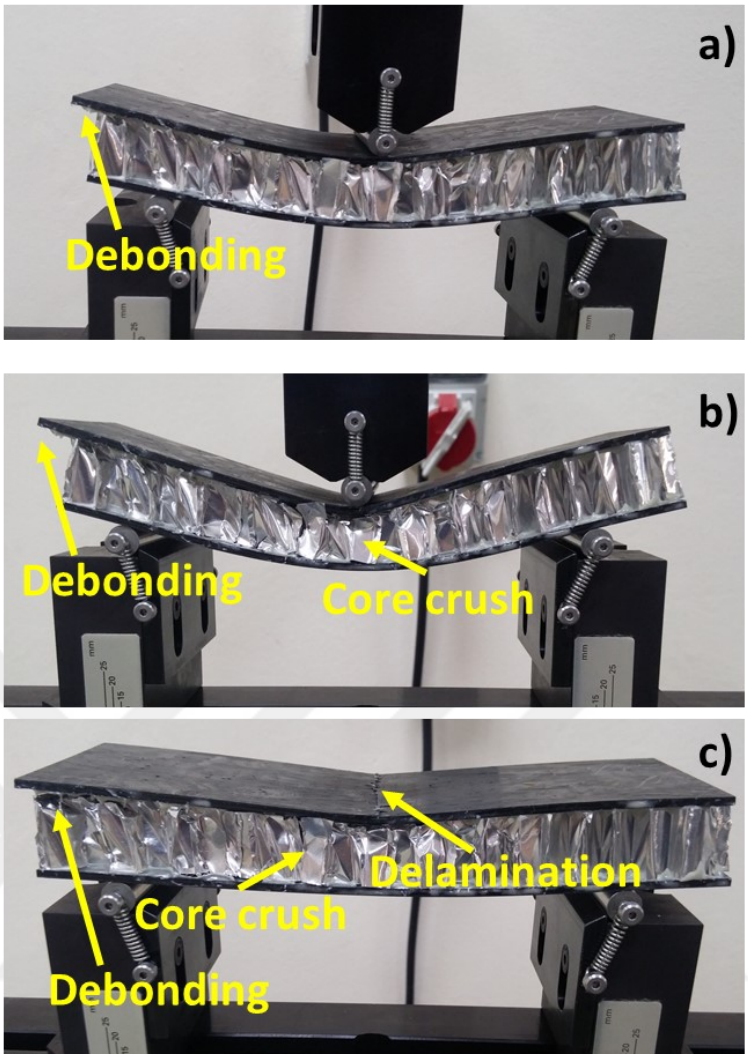

Figure 3.6. Failure modes of Adh500 sandwich panels a) debonding at point A, b) core crush between point A and point B, c) delamination at point B

Load-displacement curves of three distinct samples of Adh666 sandwich panels are illustrated in Figure 3.7. Four significant points were marked on load-displacement curves. Similar with the other two groups of samples (Adh333 and Adh500), the linear-elastic region was determined between point O and point A. However, core crush was seen as the first failure mode of Adh666 samples under flexural load at the point A as shown in Figure 3.8(a). Interfacial debonding on the composite face-aluminum honeycomb core interface was prevented by the adhesive layer which had sufficiently thickness to interact the wall of aluminum honeycomb core. There was some of load decreasing between point A and point C after aluminum honeycomb core crushing occurred. Adh666 sandwich panels has kept their load-bearing capacity after point C

similarly with other two groups of samples. On the other hand, it was seen at the load displacement curves of the Adh666 panels, stiffness of the panels was significantly decreased although the bending load on the panels increased. The final failure mode was determined as delamination on carbon fiber reinforced polymer face sheets as illustrated in Figure 3.8(b) in point B. It was observed that load decreased dramatically when the delamination on the composite face sheet occurred.

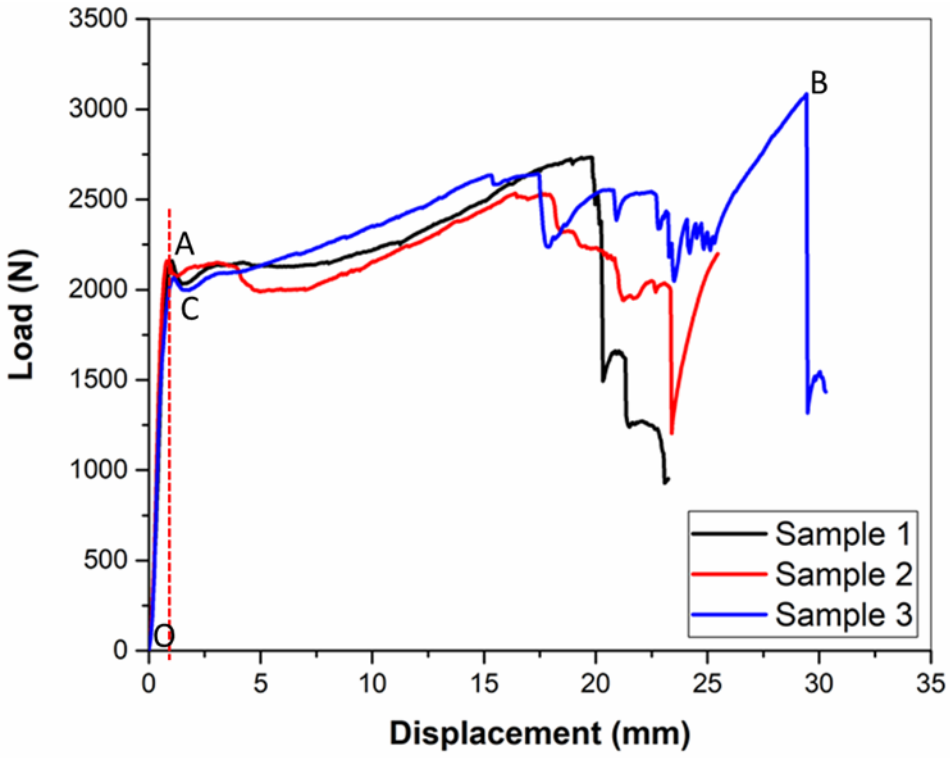

Figure 3.7. Load-displacement curves of three samples of Adh666 panels

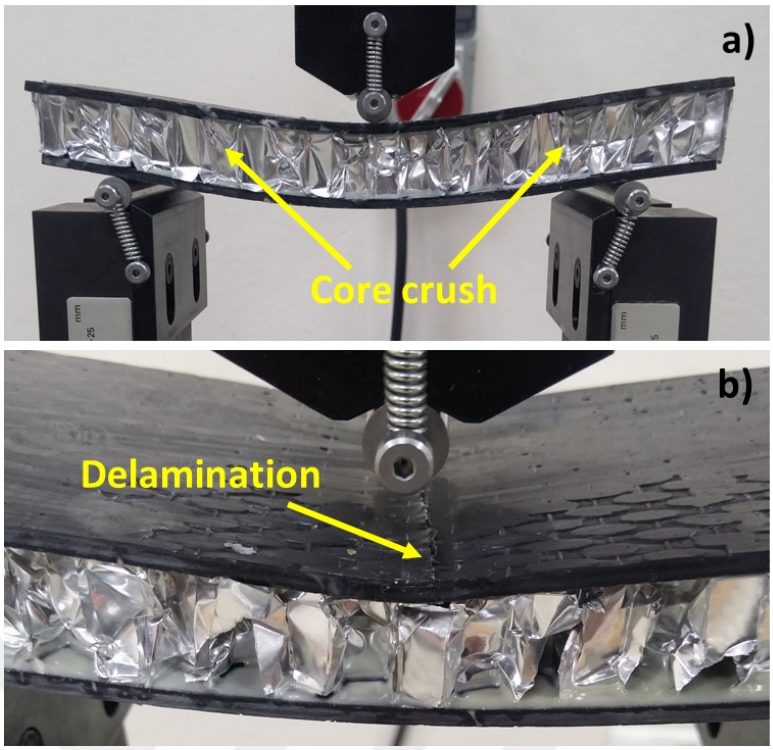

Figure 3.8. Failure modes of Adh666 sandwich panels a) core crush at point A and b) delamination at point B

3.4.1.2. Comparison of the Static Bending Behavior of The Sandwich Panels with Various Amount of Adhesive

Mechanical behavior under quasi-static bending load of developed sandwich panels contains different amounts of adhesives for bonding the composite face sheets and aluminum honeycomb core were discussed regarding to failure modes and load displacement curves in section 3.4.1.1. Figure 3.9 shows the representative load-displacement curves of three different sandwich panels with various amount of adhesive layer. A linear-elastic line was observed for whole load-displacement curves as aforementioned in section 3.4.1.1. A yield point was determined as soon as the linear elastic region finished for all types of sandwich panels. Stiffness of the panels significantly decreased at the yield point where the first failure mode was seen. Therefore, load values at the yield point were described as failure load for whole types of sandwich panels.

Figure 3.10 shows the average failure loads with standard deviation of three types of sandwich panels which contains different amounts of adhesives in their face-core interface. As shown in the figure, average failure loads of Adh333, Adh500 and Adh666 sandwich panels were 1633.82 ± 31.66 N, 1807.34 ± 67.81 N and 2112.82 ± 33.57 N, respectively. The average failure load of the Adh666 panels is 14% and 22% higher than Adh500 and Adh333 sandwich panels, respectively due to the different failure modes of the sandwich panels. Initial failure modes were determined as interfacial debonding for Adh333 and Adh500 panels yet core crushing for Adh666 panels. Turning the initial failure mode from interfacial debonding to core crushing provides superior quasistatic bending strength to Adh666 sandwich panels.

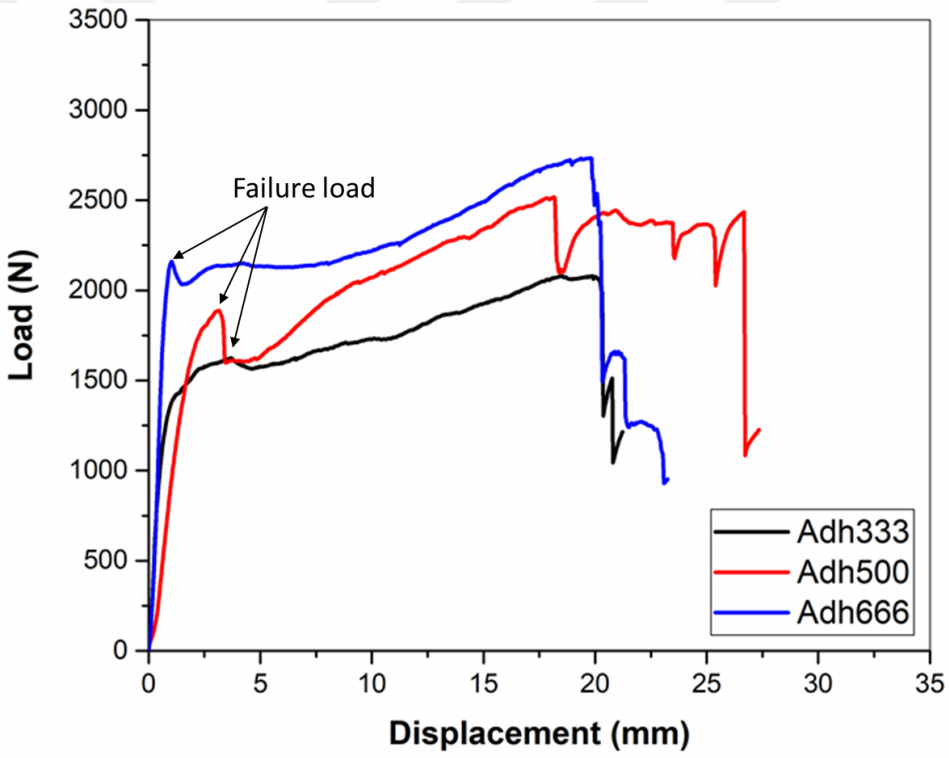

Figure 3.9. Representative load-displacement curve of Adh333, Adh500 and Adh666 sandwich panels

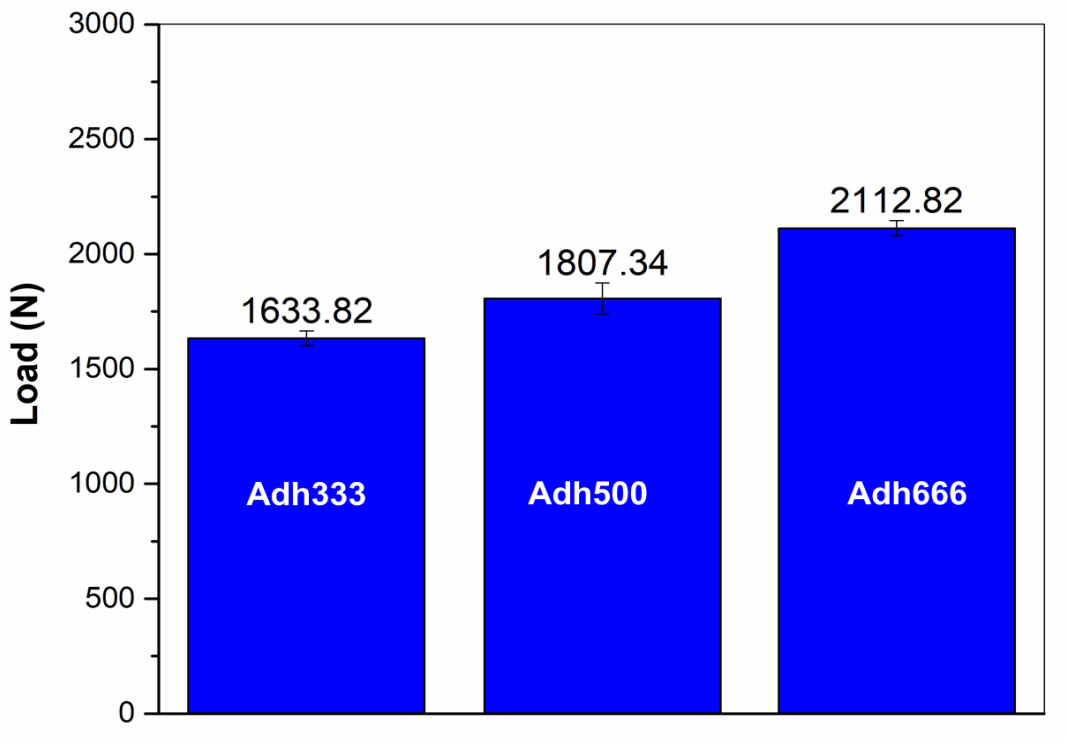

Figure 3.10. Comparison of average failure loads of Adh333, Adh500 and Adh666 sandwich panels with standard deviations

3.4.2. Fatigue Test Results

Effect of amount of adhesive on the composite face-aluminum honeycomb interface on fatigue behavior of sandwich panels were characterized by stiffness reduction, fatigue failure modes and Wöhler Curves (S-N Curves) in this section.

3.4.2.1. Stiffness Reduction and Fatigue Failure Modes

Stiffness reduction evaluation is a convenient method to characterize the fatigue behavior of the sandwich structures (El Mahi et al. 2004, Mathieson and Fam 2014, Belingardi, Martella, and Peroni 2007, Bezazi, Pierce, and Worden 2007). This method was one of the beneficial methods to follow the failure propagation on the samples. Stiffness reduction was characterized with normalized stiffness, which is defined as follows,

$$Normalized\ Stiffness = \frac{k}{k_0} \tag{3.2}$$

where the k is stiffness of the specimen in any cycle and k_0 is stiffness value on the first cycle of the fatigue test.

Figure 3.11-Figure 3.14 shows the stiffness reduction curves of Adh333 sandwich samples curves with respect to number of cycles with different load levels. Stiffness reduction curves of Adh333 sandwich samples shows similar characteristic for all load levels as shown in figures. Stiffness reduction curves may be divided into three regions. A rapid reduction of the stiffness in the first few cycles on the tests was observed on the first region of the curves. It can be explained with a failure initiation on the microscopic level (Essassi et al. 2020); however, samples have conserved their load-bearing capacity. In the second region, a slow and steady stiffness reduction was observed with in the samples. This region represents the failure propagation of the sandwich samples. In the beginning of the third region, samples have lost their entire load-bearing capacity and a sudden decrease was seen on the stiffness reduction curves. The corresponding number of cycles in that sudden decrease of the stiffness indicates the completion of the fatigue failure. Thus, this cycle was identified as failure cycles of the samples.

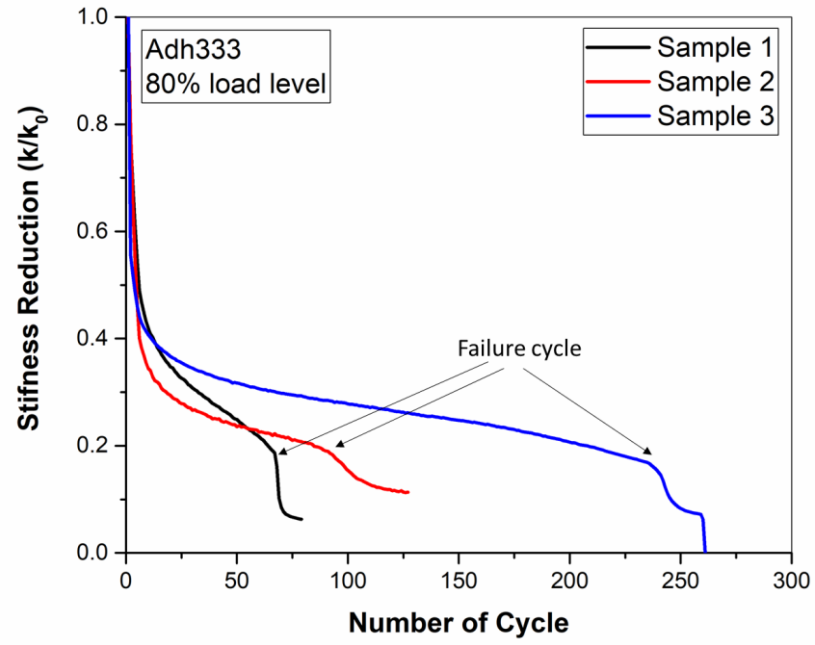

Figure 3.11. Stiffness reduction curves of Adh333 sandwich samples, for 80% of ultimate flexural load

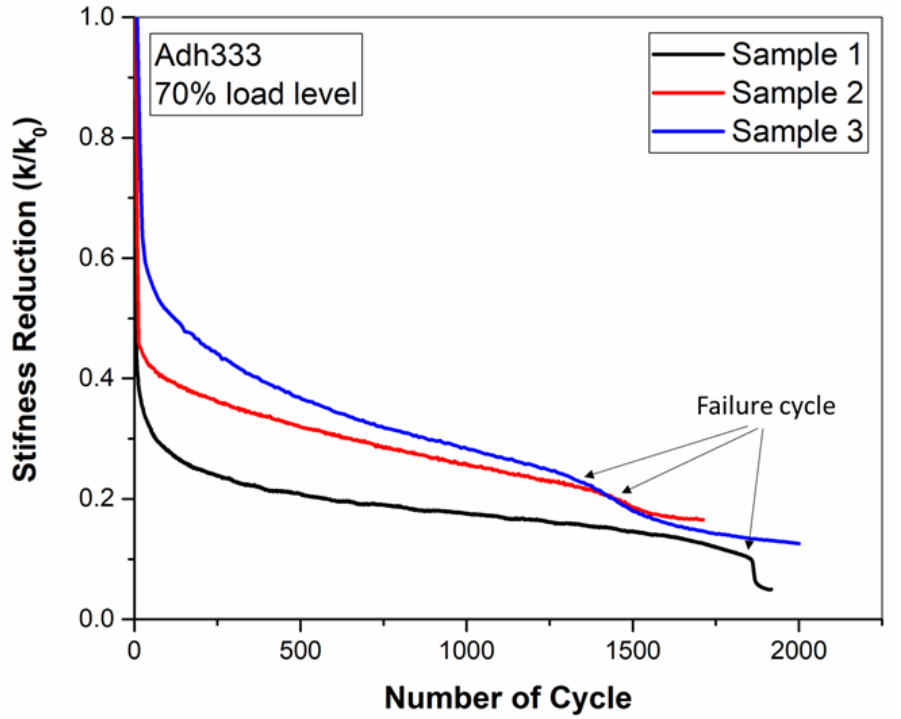

Figure 3.12. Stiffness reduction curves of Adh333 sandwich samples, for 70% of ultimate flexural load

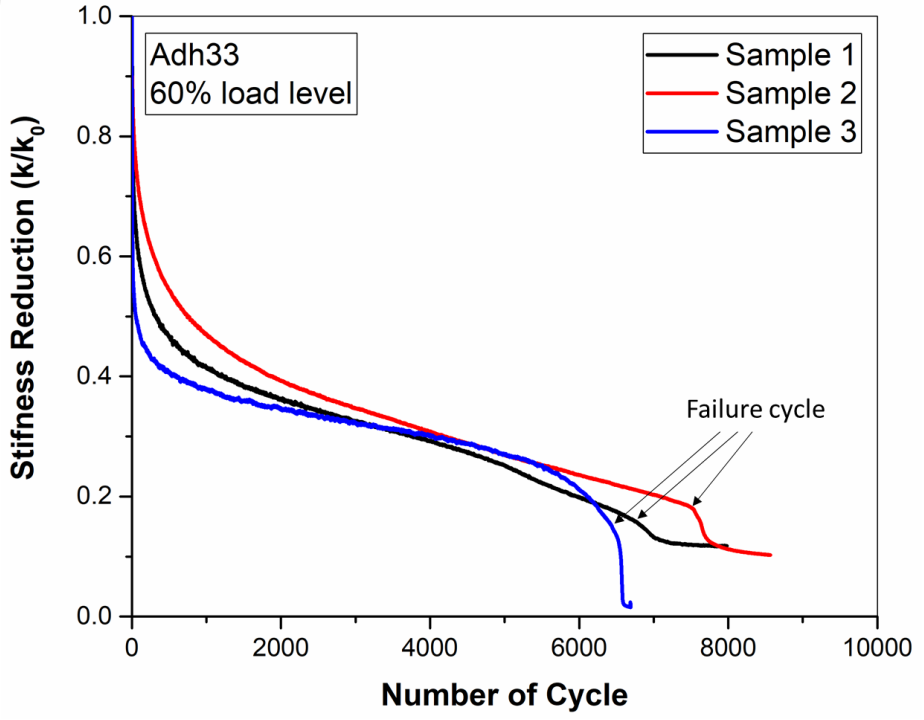

Figure 3. 13. Stiffness reduction curves of Adh333 sandwich samples, for 60% of ultimate flexural load

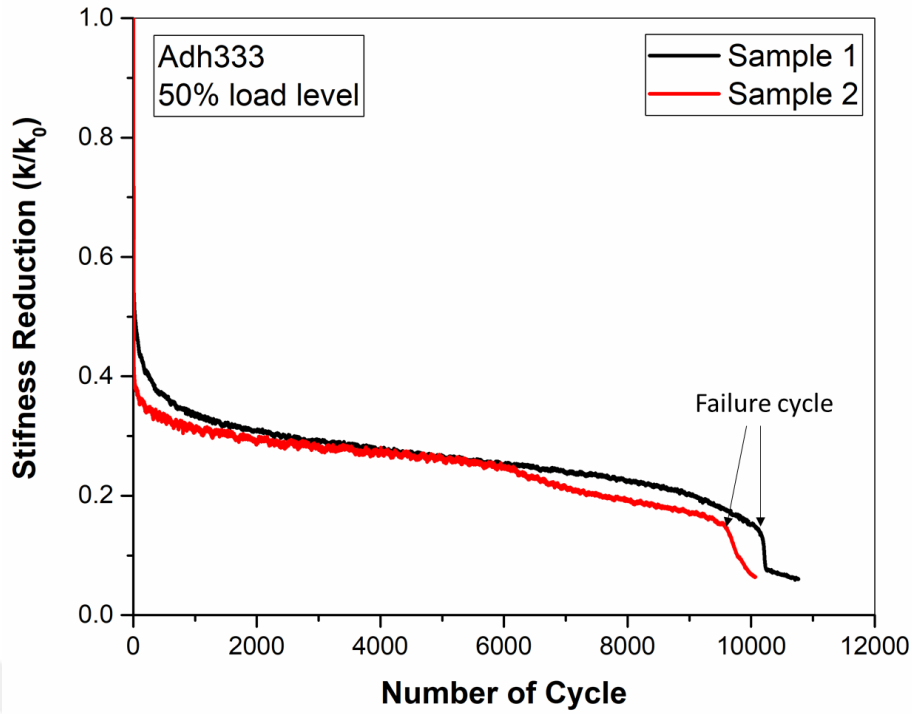

Figure 3.14. Stiffness reduction curves of Adh333 sandwich samples, for 50% of ultimate flexural load

Analysis of fatigue failure modes is a useful method to understand the fatigue failure propagation on the samples (Zenkert and Burman 2011, Banghai, Zhibin, and Fangyun 2015, Kulkarni et al. 2004, Wahl et al. 2014). Figure 3.15 shows the fatigue failure modes of Adh333 samples with various loading levels. In the few cycles of the tests, any visible failure on the sandwich samples was not observed although the rapid reduction of the stiffness appeared on the stiffness reduction curves. Failure initiation on the sandwich samples caused that rapid stiffness reduction at the beginning cycles of the tests as aforementioned before. Sandwich structures kept their load-bearing capacity during the first and second region of the stiffness reduction curves although the progressive failure had begun. At the end of the second region of the load-displacement curves, crack propagation and progressive failure has completed. Initial failure mode of the Adh333 panels was determined as interfacial debonding for all loading levels as shown in Figure 3.15. Interfacial debonding occurred in the low cycles of the tests even for the low load levels due to lack of adhesive on the core-face interface. It was appeared from failure mode analysis that insufficient adhesive layer on the interface could not bear the shear forces which were resultant of the bending load. Interfacial debonding was also

found as main fatigue failure mode of the general sandwich structures in most of the study (Abbadi et al. 2015, Jen, Ko, and Lin 2009, Shi et al. 2014, Ma et al. 2020). It also proves that failure of the sandwich structures becomes in the low cycles of the tests if the core-face interface has insufficient shear strength. Core crushing is also observed as a failure mode of Adh333 samples as shown in Figure 3.15. Core crush occurred due to interfacial debonding. Bending load on the sandwich structures could not been transferred to the shear load on the core-face interface after interfacial debonding occurred. That causes all the bending load was transferred to the aluminum honeycomb as compression load. That is the reason of core crushing appeared where the interfacial debonding occurred on the sandwich panels as shown in Figure 3.15. The cycle that progressive fatigue failure completed was assumed as failure cycle as shown in Figure 3.11-Figure 3.14 because the structure has lost its whole load-bearing capacity. Failure cycles of the Adh333 panels in different loading conditions are listed in the Table 3.1.

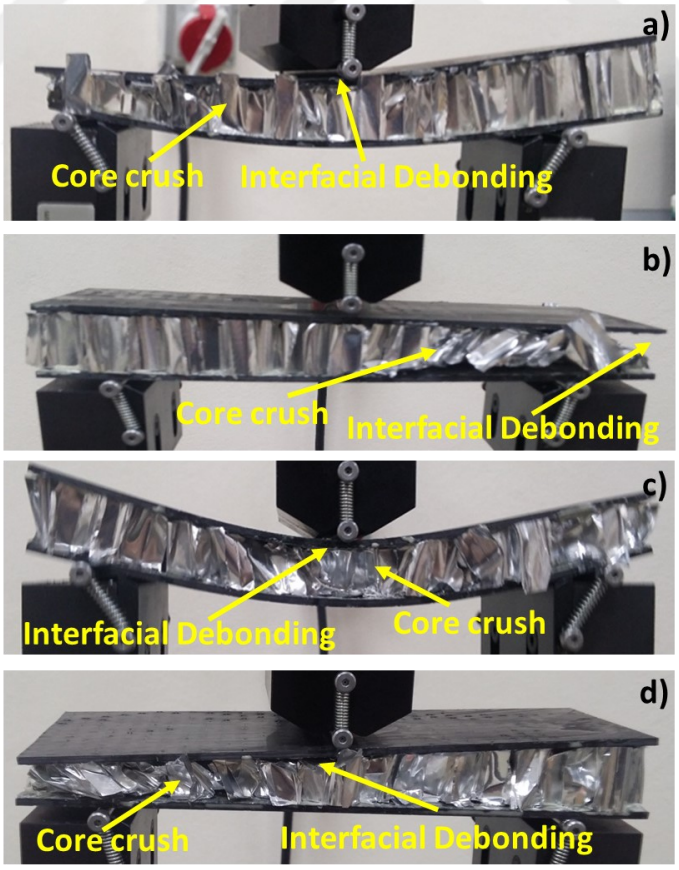

Figure 3.15. Fatigue failure modes of the Adh333 sandwich panels for different loading conditions, a) 80% of the F_{ult}, b) 70% of the F_{ult}, c) 60% of the F_{ult}, d) 50% of the F_{ult}

Table 3.1 Failure cycles of Adh333 panels for each load levels

Load Levels	80% of Ult. Load	70% of Ult. Load	60% of Ult. Load	50% of Ult. Load
Number of Failure Cycles	68 93 240	1862 1440 1408	6849 7574 6528	10205 9635

Figure 3.16-Figure 3.19 show the stiffness reduction curves of Adh500 sandwich samples curves with respect to number of cycles with different load levels. Stiffness reduction curves of Adh500 panels represents similar characteristic with Adh333 panels. Failure cycle was identified on the cycle that progressive fatigue failure completed as well. Failure cycles were shown in Figure 3.16-Figure 3.19.

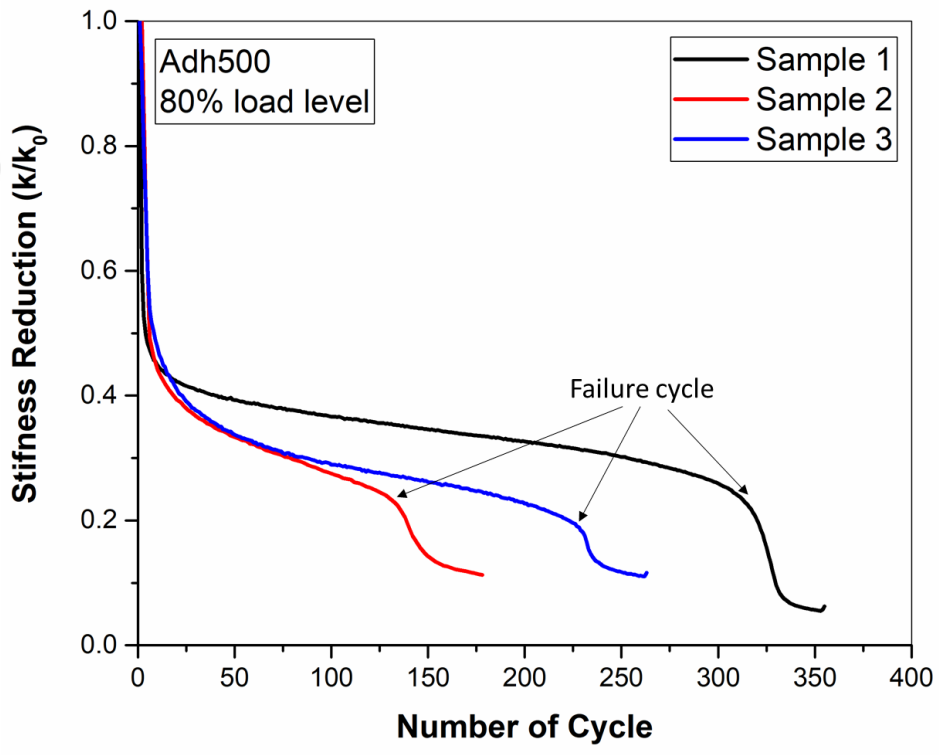

Figure 3.16. Stiffness reduction curves of Adh500 sandwich samples, for 80% of ultimate flexural load

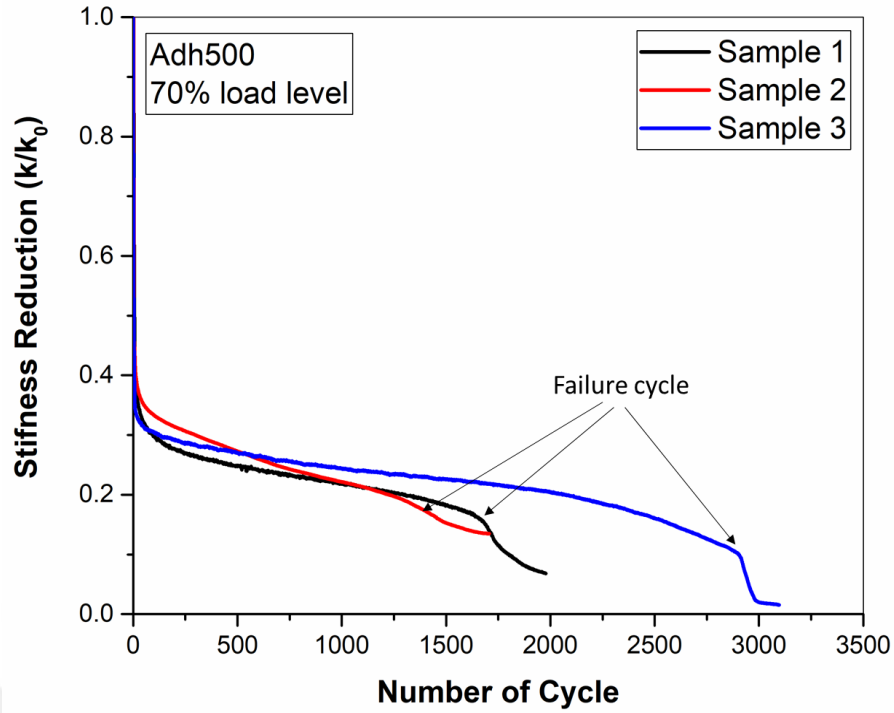

Figure 3.17. Stiffness reduction curves of Adh500 sandwich samples, for 70% of ultimate flexural load

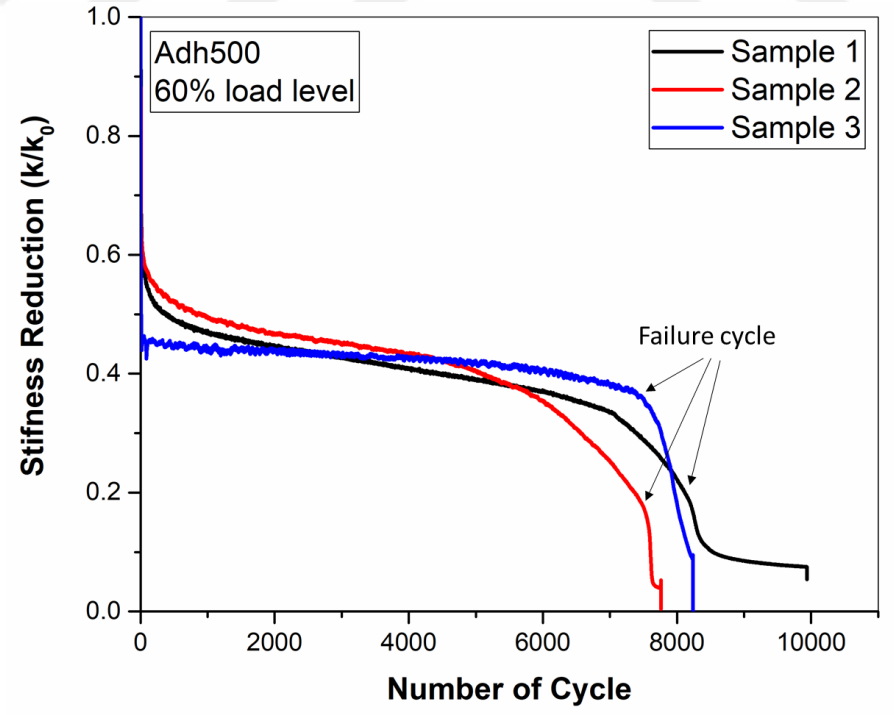

Figure 3.18. Stiffness reduction curves of Adh500 sandwich samples, for 60% of ultimate flexural load

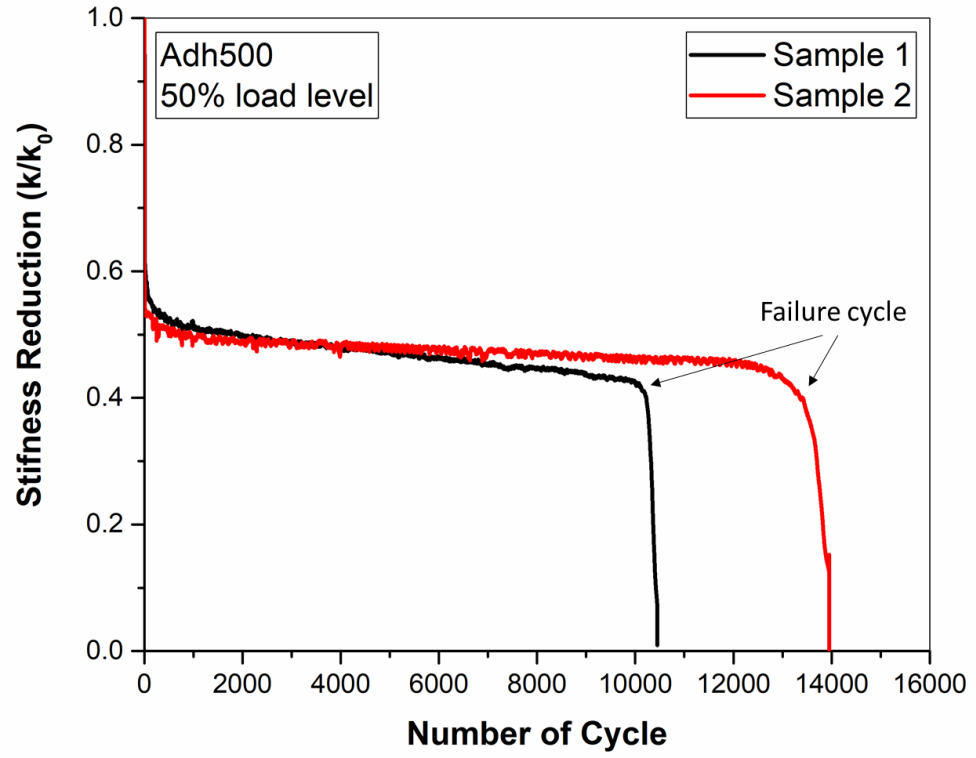

Figure 3.19. Stiffness reduction curves of Adh500 sandwich samples, for 50% of ultimate flexural load

Figure 3.20 shows the fatigue failure modes of Adh500 samples with various loading levels. First failure mode was observed as interfacial debonding for all load levels as seen in Figure 3.20. Failure of core crushing occurred next after interfacial debonding similarly with Adh333 panels and static flexural test results. Besides, failure propagation mechanisms of the Adh500 panels were seen as similar as Adh333 panels. Thus, Adh500 panels has shown low cycle fatigue behavior like Adh333 panels. Failure cycles of Adh500 panels were listed in Table 3.2 Despite showing similar failure propagation and failure mode characteristic, fatigue life of the Adh500 panels determined slightly higher than Adh333 panels. Main reason of this increment is the difference of the severity of the interfacial debonding failure. Relatively thicker adhesive layer on the face-honeycomb core interface provided higher resisting interface against shear loads generated from bending load. However, that increment on the interface strength was insufficient to shift the failure mode and failure mechanism on the sandwich panels so that structure has shown low cycle fatigue characteristic as well.

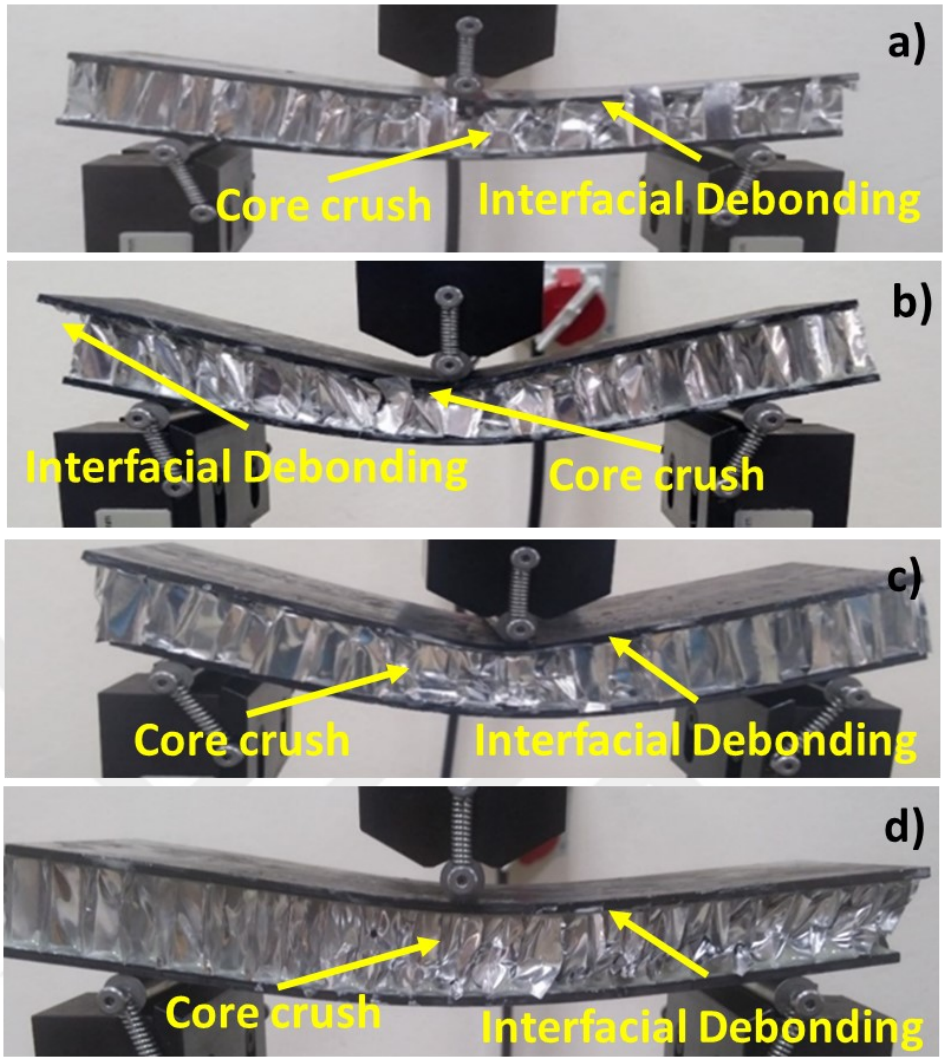

Figure 3.20. Fatigue failure modes of the Adh500 sandwich panels for different loading conditions, a) 80% of the F_{ult}, b) 70% of the F_{ult}, c) 60% of the F_{ult} , d) 50% of the F_{ult}

Table 3.2. Failure cycles of Adh500 panels for each load levels

Load Levels	80% of Ult. Load	70% of Ult. Load	60% of Ult. Load	50% of Ult. Load
Number of Failure Cycles	321 138 231	1704 1416 2918	7810 7555 7750	10240 13507

Figure 3.21-Figure 3.24 show the stiffness reduction curves of Adh666 sandwich samples curves with respect to number of cycles with different load levels. Stiffness reduction curves in load levels 80% and 70% consist of three regions as well as Adh333 and Adh500 sandwich panels. Initial rapid stiffness reduction was observed in Adh666 panels in the beginning of the tests at those load levels. The slope of the curve in the second region indicates the failure propagation rate so that relatively slow failure propagation occurs for Adh666 panels in accordance with stiffness reduction curves. Stiffness reduction curve of the load levels of 60% of ultimate flexural force includes two regions. Initial stiffness reduction was not seen on these samples and failure propagation lasts up to higher number of cycles. Failure was completed in a critical number of cycles when the stiffness of the sandwich panels was dramatically dropped. Failure cycles of Adh666 panels were identified in Figure 3.21-Figure 3.24. Adh666 samples was not exposed any fatigue failure on the 50% of ultimate flexural load level up to above one million cycles as shown in Figure 3.24. That load level was supposed as the fatigue limit for Adh666 panels.

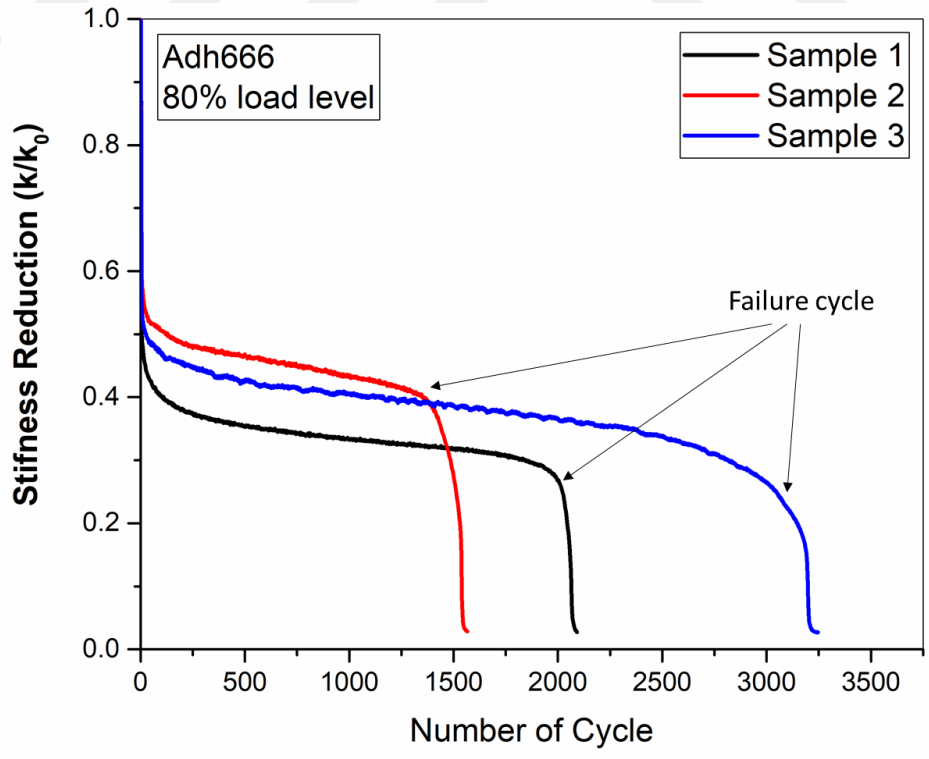

Figure 3.21. Stiffness reduction curves of Adh500 sandwich samples, for 80% of ultimate flexural load

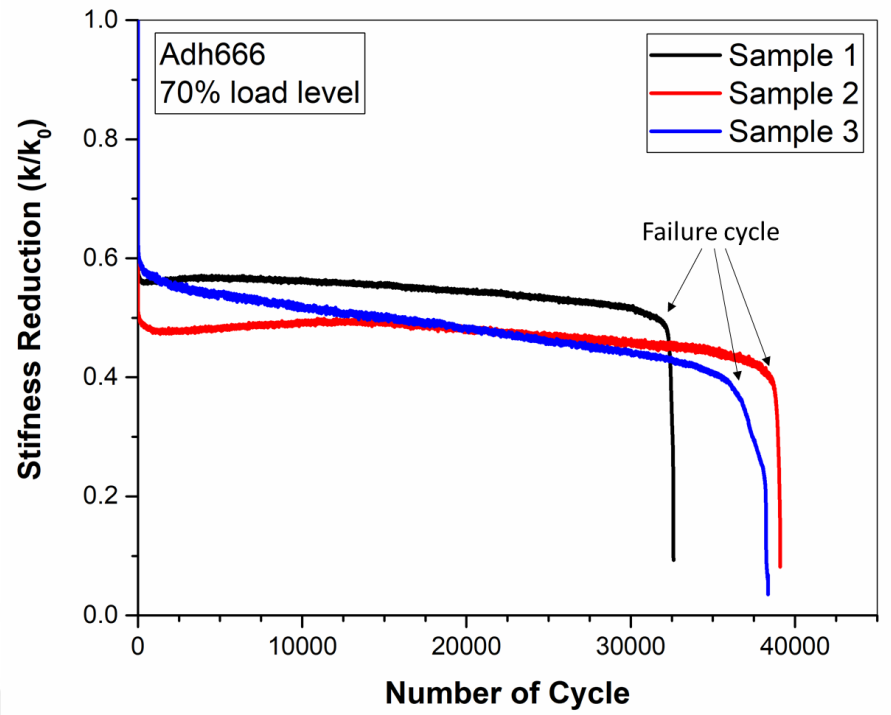

Figure 3.22. Stiffness reduction curves of Adh500 sandwich samples, for 70% of ultimate flexural load

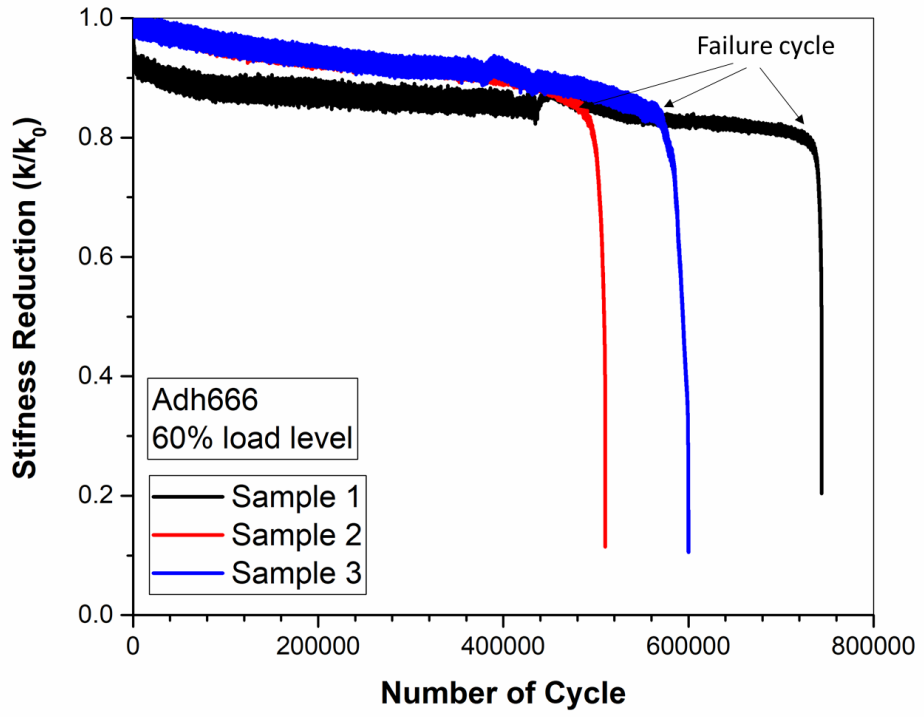

Figure 3.23. Stiffness reduction curves of Adh500 sandwich samples, for 60% of ultimate flexural load

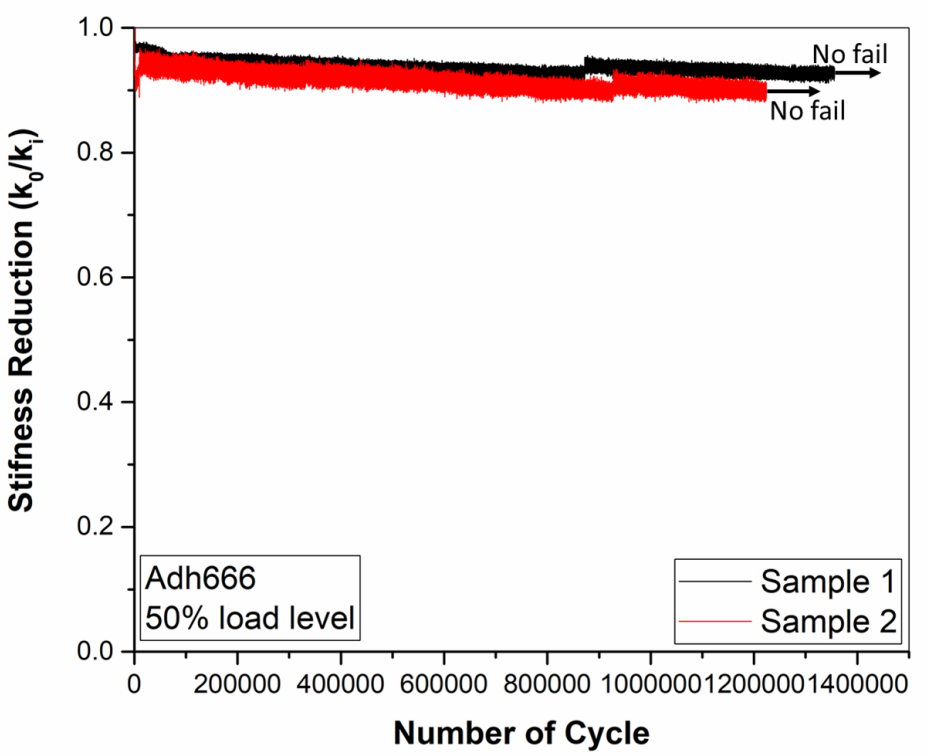

Figure 3.24. Stiffness reduction curves of Adh500 sandwich samples, for 50% of ultimate flexural load

Analyzing the fatigue failure modes of Adh666 panels illuminated to understand the significant increasing on the fatigue life of the Adh666 panels in comparison with Adh333 and Adh500 panels. Figure 3.25 illustrates the fatigue failure modes of Adh666 panels under different loading conditions. Interfacial debonding on the face-honeycomb core interface was not observed on the whole loading levels for Adh666 panels. Core crushing was only fatigue failure mode that was determined on the experimental study. Increasing amount of adhesive makes a high strength interface on the composite face-aluminum honeycomb core interface so that the shear load generated from out of plane bending load could be carried by that interface. This provides a balanced load transfer between composite face, aluminum honeycomb core and face-core interface. Thus, initial failure mode was shifted from interfacial debonding to aluminum honeycomb core crush. Adh666 panels has reached significantly higher number of cycles without failure due to shifting of failure mode. Adh666 panels were not damaged at the 50% load levels tests up to one million cycles. Those loading levels were supposed to be fatigue limit for

Adh666 sandwich panels. Table 3.3 shows the failure cycles of the Adh666 panels with different loading conditions.

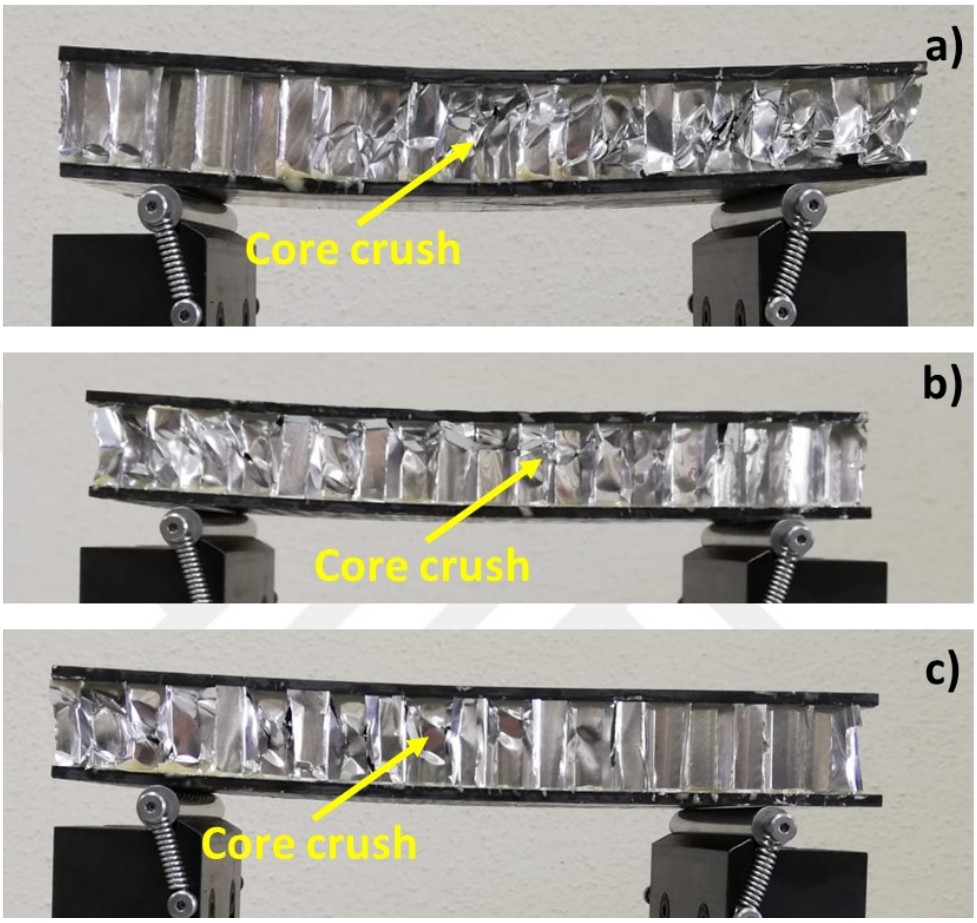

Figure 3.25. Fatigue failure modes of the Adh666 sandwich panels for different loading conditions, a) 80% of the F_{ult}, b) 70% of the F_{ult}, c) 60% of the F_{ult} , d) 50% of the F_{ult}

Table 3.3. Failure cycles of Adh666 panels for each load levels

Load Levels	80% of Ult. Load	70% of Ult. Load	60% of Ult. Load	50% of Ult. Load
Number of Failure Cycles	2028	32210	725775	No failure
	1492	38346	559689	No failure
	2155	36780	479263	

3.4.2.2. Wöhler Curves of Developed Sandwich Panels

Fatigue life is an important parameter for characterization of fatigue behavior of sandwich panels which can be indicated by Wöhler curves (S-N curves). Figure 3.26 illustrates the Wöhler curves of Adh333, Adh500 and Adh666 sandwich panels. Wöhler curves were generated with maximum applied load levels (F_{max}/F_{ult}) and number of failure cycle (N_f) of sandwich beams. Wöhler curves were given in logarithmic scale for all developed sandwich panels in the same graph due to better comparing. A linear curve fitting was made into Wöhler curves to state the relation between maximum load level and number of failure cycle which is defined as;

$$\frac{F_{max}}{F_{ult}} = A - B log N \tag{3.3}$$

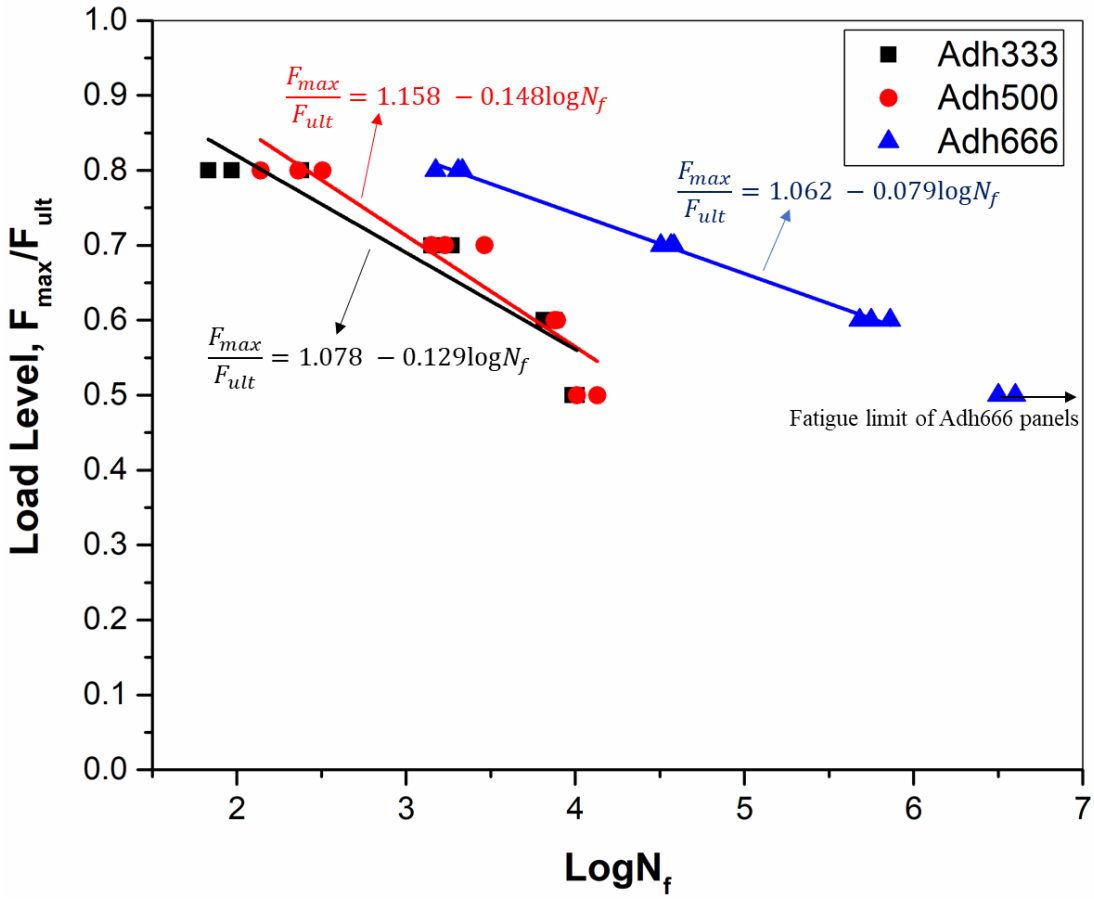

Figure 3.26. Wöhler curves of Adh333, Adh500 and Adh666 panels with linear fitting.

The relationship between maximum applied load and number of cycles were expressed for Adh333, Adh500 and Adh666 sandwich panels according to (3.4), (3.5) and (3.6), respectively as follows,

$$\frac{F_{max}}{F_{ult}} = 1.078 - 0.129logN \tag{3.4}$$

$$\frac{F_{max}}{F_{ult}} = 1.158 - 0.148logN \tag{3.4}$$

$$\frac{F_{max}}{F_{ult}} = 1.062 - 0.079logN \tag{3.5}$$

In these equations, F_{max} is a maximum load applied to the sandwich panels in fatigue tests in each load levels, F_{ult} is an ultimate static flexural load of each sandwich beams and N_f is a number of failure cycle.

The parameter B and parameter A are fitting parameters in (3.3). Parameter B is the value that indicates the fatigue degradation rate of the sandwich panels (Essassi et al. 2020). Parameter B was found as close values for Adh333 and Adh500 sandwich panels. Nearly 12% of difference caused by fitting error. The reason of Adh333 and Adh500 panels having similar B parameter is that both panels have the same failure fatigue modes. Failure occurred in low cycles of the tests for Adh333 and Adh500 sandwich panels due to high fatigue degradation rate.

B parameter of Adh666 panels was found as nearly %90 lower than Adh333 and Adh500 panels. This can be explained by any failure was not observed on the composite face-aluminum honeycomb core interface of Adh666 panels in any load levels. The Adh666 panels have high fatigue resistance due to shifting the fatigue failure mode from interfacial debonding to core crush. The panels have reached their fatigue limit in 50% load level since it has been observed that the failure did not occur in 10^6 cycles as shown in Figure 3.26.

CHAPTER 4

EFFECT OF CORE THICKNESS ON FATIGUE BEHAVIOR OF ALUMINUM HONEYCOMB CORED SANDWICH PANELS

4.1. Materials

Face material is carbon fiber reinforced polymer (CFRP) in this study as well as Chapter 3. 500 g/m^2 unit weight of unidirectional carbon fabrics and epoxy matrix system (Momentive L160, Hexion Inc., Ohio) and its hardener (Momentive H160, Hexion Inc., Ohio) were used to fabricate the face sheets. In this section of thesis, aluminum honeycomb structures with hexagonal cell configuration with various thicknesses of 6 mm, 21 mm and 46mm were supplied from Altıgen Panel Aerospace Shipbuilding Panel Industry, Turkey and were selected as core material to determine the core thickness effect on quasi-static and fatigue behavior of aluminum honeycomb cored sandwich panels. 666 g/m^2 amount of Denlaks PU99 polyurethane based adhesive were used to laminate the carbon fiber reinforced polymer matrix composites with aluminum honeycomb core.

4.2. Fabrication of CFRP faced Aluminum Honeycomb Cored Sandwich Panels

Sandwich panels with various cores thicknesses were fabricated at the Composite Research Laboratory in Izmir Institute of Technology Mechanical Engineering Department.

Vacuum assisted resin transfer molding (VARTM) method were used to fabricate the composite face sheets with the orientation of $[0/90]_4$. Face sheets fabrication method was explained in Chapter 3.

Sandwich panels were fabricated by adhesively bonding of composite face sheets and aluminum honeycomb cores. Polyurethane (PU) adhesive was used with the amount of 666 g/m^2 to laminate the composite face sheets and aluminum honeycomb core due to

finding better adhesion properties on Chapter 3. 10 kPa pressure was applied on sandwich panels after implementing PU adhesive and left for curing for 24 hours at 40ºC. At the end of the process, a post-curing was applied to the sandwich structures for 7 days at room temperature.

In this section of thesis, sandwich panels with three various core thicknesses (6mm, 21 mm and 46 mm) were manufactured and characterized. Sandwich panels core thicknesses of 6 mm, 21mm and 46 mm are named CT6, CT21 and CT46 respectively.

4.3. Experimental Studies

4.3.1. Determination of Effect of Core Thickness on Static Flexural Behavior of Sandwich Panels

Three-point bending tests were performed to the sandwich panels to determine the core thickness effect on flexural properties of honeycomb cored sandwich structures in accordance with ASTM C393 test standard (International 2016). Tests were implemented on MTS universal servo-hydraulic testing machine with 100 kN load cell. Three-point bending test set-up is shown in Figure 3.2. Distance between rolling supports was 150 mm while diameter of the rollers was 10 mm. Tests were maintained until failure was completed and test rate was 6 mm/min as specified in ASTM C393. Static bending test results provided the fatigue test to ultimate flexural load of each sandwich panels with different core thickness. Besides, load-deflection curves, flexural failure modes and failure story of the sandwich panels with different core thickness were revealed.

4.3.2. Determination of Shear Properties of Aluminum Honeycomb Core Materials

Shear properties of aluminum honeycomb core materials were measured with core shear tests according to ASTM C273 test standard (Standard 2013). Tests were performed in MTS servo-hydraulic testing machine on the tensile test fixture with a special testing apparatus as seen in Figure 4.1. Aluminum honeycomb cores with thickness of 6 mm, 21

mm and 46 mm were tested. Test rate was 0.5 mm/min according to test standard. Three of samples were tested for each group of sandwich panels. Effect of core thickness on shear properties of the aluminum honeycomb cores were characterized by load-displacement curves and core shear strength values. Calculation of core shear stress is given in (4.1)

$$\tau = \frac{P}{Lb} \tag{4.1}$$

In equation 4.1, τ is core shear stress, P is load on the specimen, L is length of the specimen and b is width of the specimen.

Figure 4.1. Core shear test set-up with special testing apparatus according to ASTM C273

4.3.3. Determination of Effect of Core Thickness on Fatigue Behavior of Sandwich Panels

Core thickness effect on fatigue behavior of adhesively bonded honeycomb cored sandwich panels were characterized by load-controlled fatigue tests using MTS servo-hydraulic testing machine with three-point bending test fixture. Loads on the fatigue tests were applied to the sandwich panels with sinusoidal waveform in four particular load levels which are 80, 70, 60, 50% of ultimate flexural load provided from static flexural tests. Load ratio (R) which is the ratio of F_{max} and F_{min} and test frequency (f) was selected to 0.1 and 2 Hz., respectively. Fatigue tests were maintained until the sandwich panels has lost their entire load-bearing capacity.

4.4. Results and Discussions

4.4.1. Results of Effect of Core Thickness on Static Flexural Behavior of Sandwich Panels

Effect of core thickness of adhesively bonded aluminum honeycomb cored sandwich panels on the quasi-static flexural behavior was characterized by three-point bending tests and load-displacement curves and flexural failure modes of sandwich panels were obtained and discussed.

4.4.1.1. Load-Displacement Curves and Failure Modes

Figure 4.2 shows the load-deflection curves of three samples of CT6 sandwich panels. Four letters were marked on load-displacement curve of CT6 sandwich panels on significant points which were reflected as O, A, B and C shown in Figure 4.2 to explain the deformation history and failure conditions. Origin of the load-displacement curve was represented by point O. In the beginning of the test a linear elastic region was observed until point A. The tangent of the curve between point O and point A indicates the stiffness of the sandwich panel. First failure was seen as core crushing on the aluminum

honeycomb core and it observed in the point A as shown in Figure 4.3(a). After initial failure mode was observed at point A, it was seen that flexural load decreased to point C and then started to rise again. The reason of that rising is that flexural load had carried by the aluminum honeycomb core transferred to the [0/90] oriented carbon fiber reinforced composite face sheets, and those composite face sheets could easily bear the bending load up to point B by plate deflection. Interfacial debonding was not observed as static bending failure mode on CT6 sandwich panels. The interface between aluminum honeycomb core and composite face sheets could sustain the shear load generated as a resultant of out of plane bending load. Carbon fiber reinforced polymer (CFRP) face sheets could bear the bending load on the structure up to their flexural strength and when the applied bending load exceeded the bending strength of the CFRP face sheets, then delamination was observed on the composite face sheets corresponding on point B at the load-displacement curves of CT6 panels as shown in Figure 4.3(b). At that point, CT6 sandwich panels lost their entire load-bearing capacity.

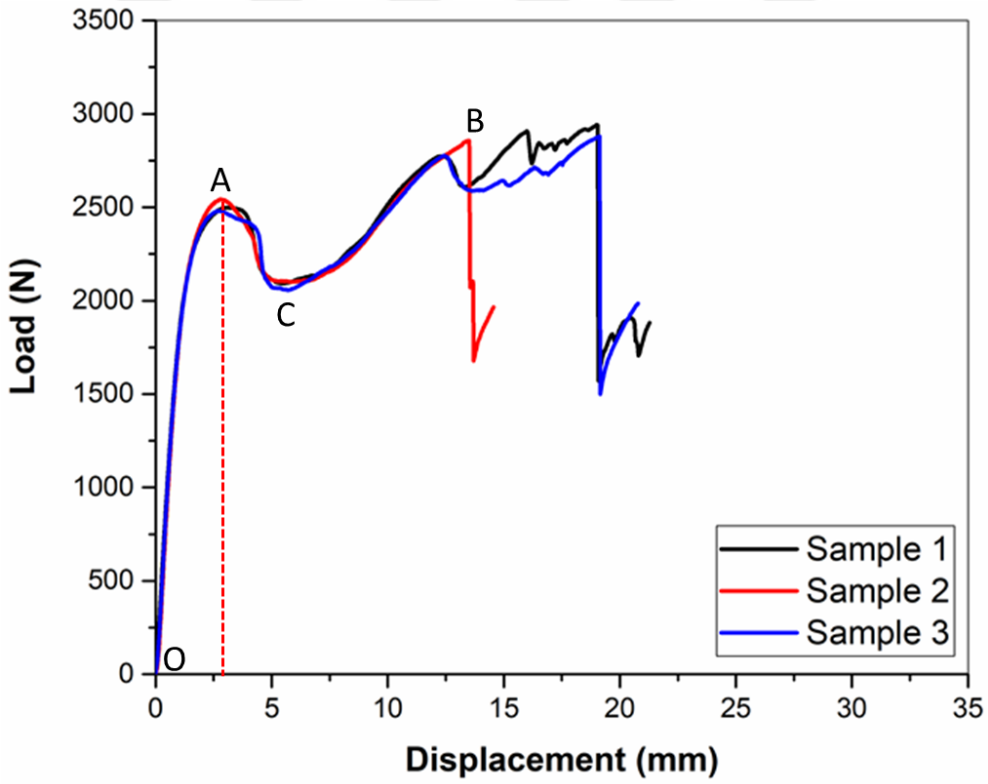

Figure 4.2. Load displacement curves of three samples of CT6 panels

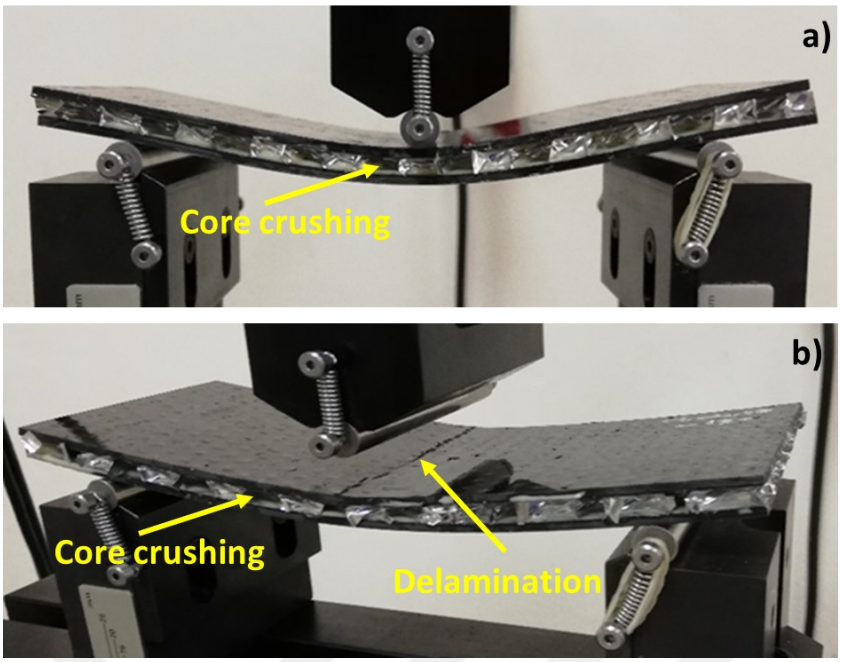

Figure 4.3. Failure modes of CT6 sandwich panels a) core crushing at point A, b) delamination at point B

The load-displacement curves of three samples of CT21 sandwich panels is shown in Figure 4.4. Point O, point A, point B and point C were marked on the load-displacement curve as well. The load-displacement curve of CT21 sandwich panels begin with a linear elastic region between point O and point A as well as load-displacement curve of CT6 sandwich panels. Aluminum honeycomb core crushing was found as the first failure mode which occurred in point A as shown in Figure 4.5(a). Load decreased to point C after first failure was seen on the aluminum honeycomb core as shown in Figure 4.4. It can be seen from Figure 4.4that the load decreasing after the first failure was seen less than that of the CT6 sandwich panels. It was observed that the load increased after point C due to strain energy capability of aluminum honeycomb core and CRFP face sheets. Aluminum honeycomb core absorbed the strain energy generated by flexural loading by crushing after point C while CFRP face sheets absorbed it by deflecting. Failure on the interface between aluminum honeycomb core and CFRP face sheets was not observed due to the adhesive layer carried the shear load. Bending stress on the CFRP face sheets exceeded the flexural strength of CFRP face sheets and caused the delamination as shown in Figure 4.5(b). Delamination is the final failure mode obtained from CT21 sandwich panels.

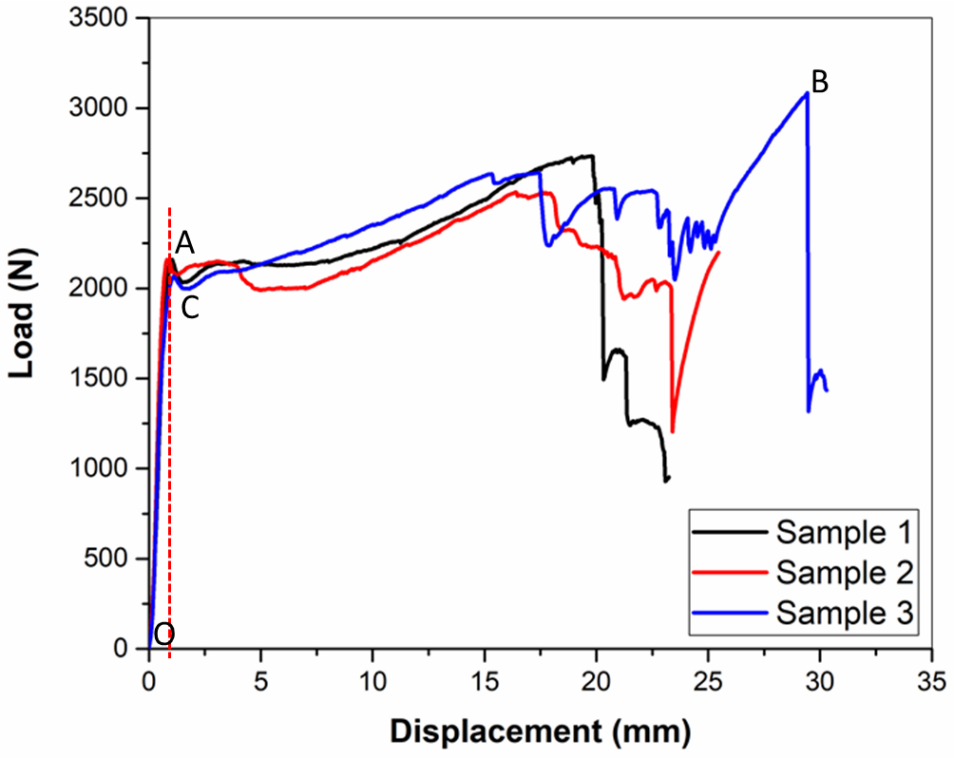

Figure 4.4. Load-displacement curves of three samples of CT21 panels

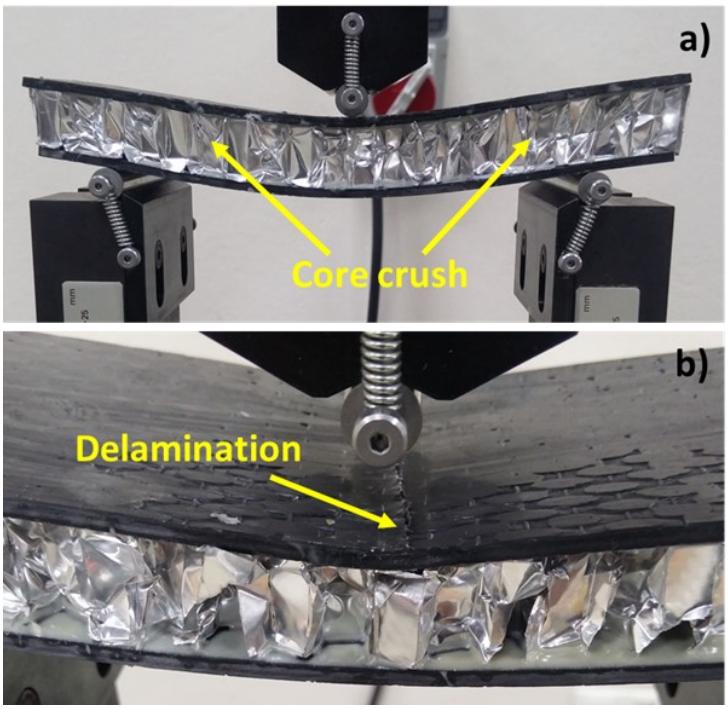

Figure 4.5. Failure modes of CT21 sandwich panels a) core crushing at point A, b) delamination at point B

Figure 4.6 shows the load-displacement curves of CT46 sandwich panels. It was seen that load-displacement curve characteristic of CT46 sandwich panels were quite similar to load-displacement curve characteristic of CT21 sandwich panels. Load-displacement curves of the CT46 sandwich samples begin showing a linear-elastic characteristic between point O and point A. First failure mode was observed as core crushing which occurred in point A. Load dramatically decreased to point C and then began to increase up to point B. The reason of that increasing was that aluminum honeycomb core absorbed the strain energy by crushing like CT21 panels. Unlike the other two groups of sandwich panels (CT6 and CT21), interfacial debonding at the edge of the panels was determined as the failure mode for CT46 panels as shown in Figure 4.7(b). Interfacial debonding occurred between point C and point B. This was because the high thickness aluminum honeycomb core produced high shear stress at the edges of the sandwich panels after the aluminum honeycomb core crushing appeared. As with CT21 and CT6 sandwich panels, CFRP face sheets carried the bending load by deflecting up to point B. Delamination was seen on the CFRP face sheets when the flexural load on the CFRP face sheets exceeded to ultimate bending strength of CFRP face sheets.

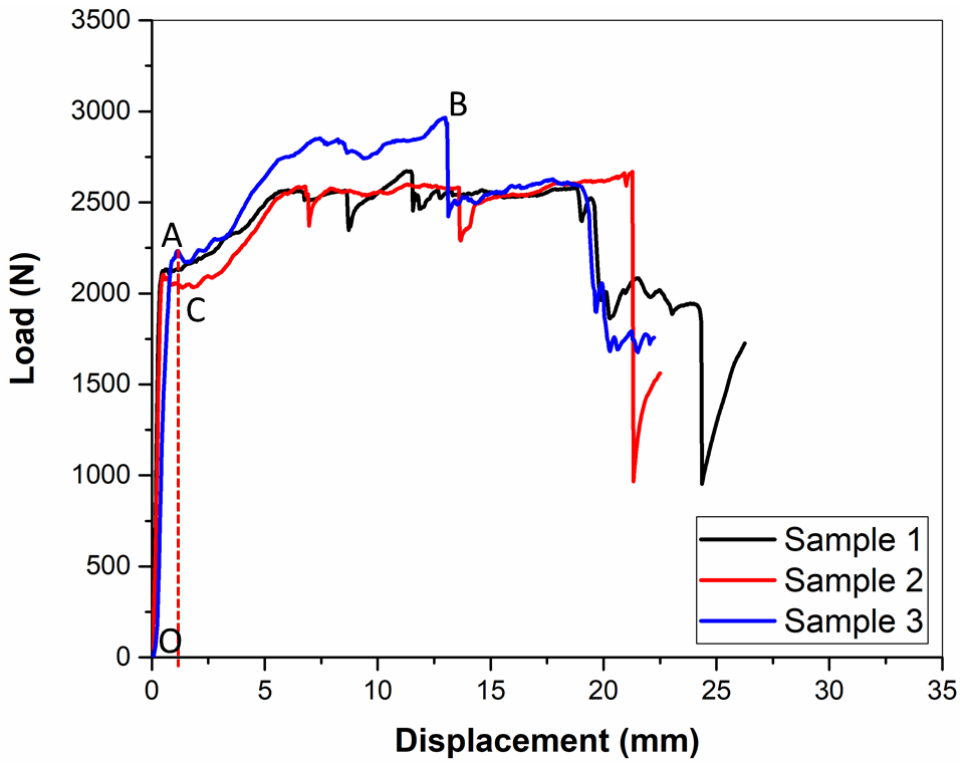

Figure 4.6. Load-displacement curves of three samples of CT46 panels

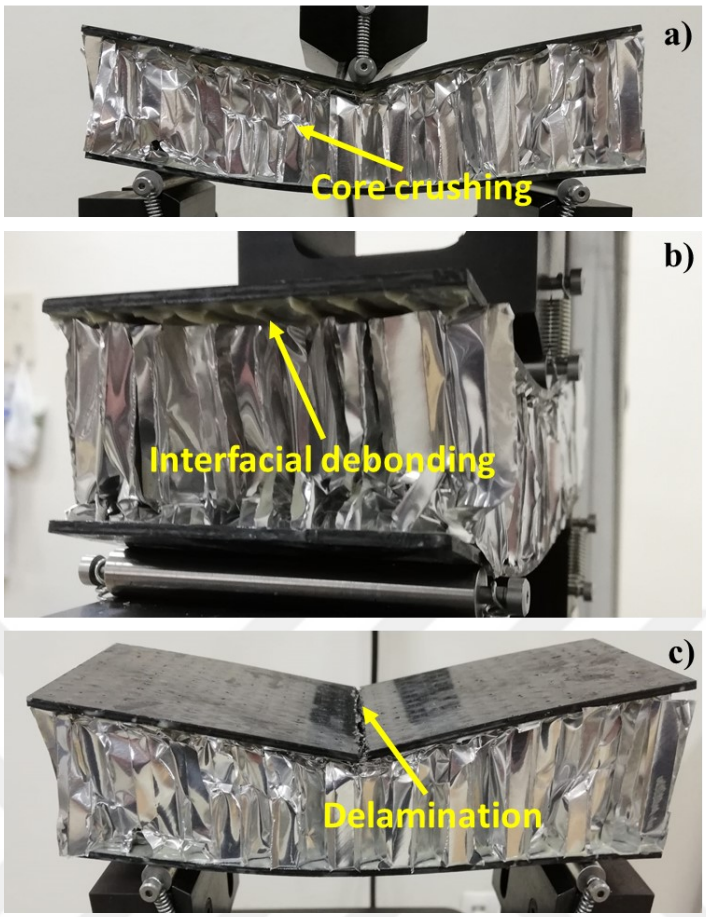

Figure 4.7. Failure modes of CT46 sandwich panels a) core crushing at point A, b) interfacial debonding between point C and point B and c) delamination at point B

4.4.1.2. Comparison of the Static Flexural Behavior of The Sandwich Panels with Various Core Thickness

Quasi-static three point bending tests were carried out to the sandwich panels with different core thickness on two purposes:

1- Providing the ultimate flexural load data to the fatigue tests.
2- Determining the effect of core thickness on flexural behavior of sandwich panels.

Figure 4.8 shows the representative load-displacement curves of sandwich panels with three various core thickness. All load-displacement curves begin with a linear-elastic region which was mentioned in section 4.4.1.1. The slope of that curve represents the stiffness of the sandwich panels. A peak load was observed at the end of the linear-elastic

region. That corresponds to first failure for whole sandwich panels. It was seen from load-displacement curves that stiffness of the panels was significantly decreased even though load on the sandwich panels increased. Thus, the load that first failure was determined was identified as ultimate failure load of the sandwich panels and provided to the fatigue tests.

The average failure loads with standard deviations of the sandwich panels with three different core thickness are shown Figure 4.9. Average failure loads of CT6, CT21 and CT46 sandwich panels were measured as 2507.76 ± 25.95 N, 2119.01 ± 47.34 N and 2153.95 ± 57.28 N, respectively. The average failure load of CT6 sandwich panels is 15% and 14% higher than CT21 and CT46 sandwich panels, respectively although CT6 sandwich panels have lower moment of inertia. This can be explained by the shear stress increasing with distance from the neutral axis of the beam. Higher shear stress on the interface between aluminum honeycomb core and composite face sheets caused the interfacial debonding on the CT46 sandwich panels and it decreases the ultimate flexural load of the CT46 panels. Core shear tests were implemented on the sandwich samples to prove that theory.

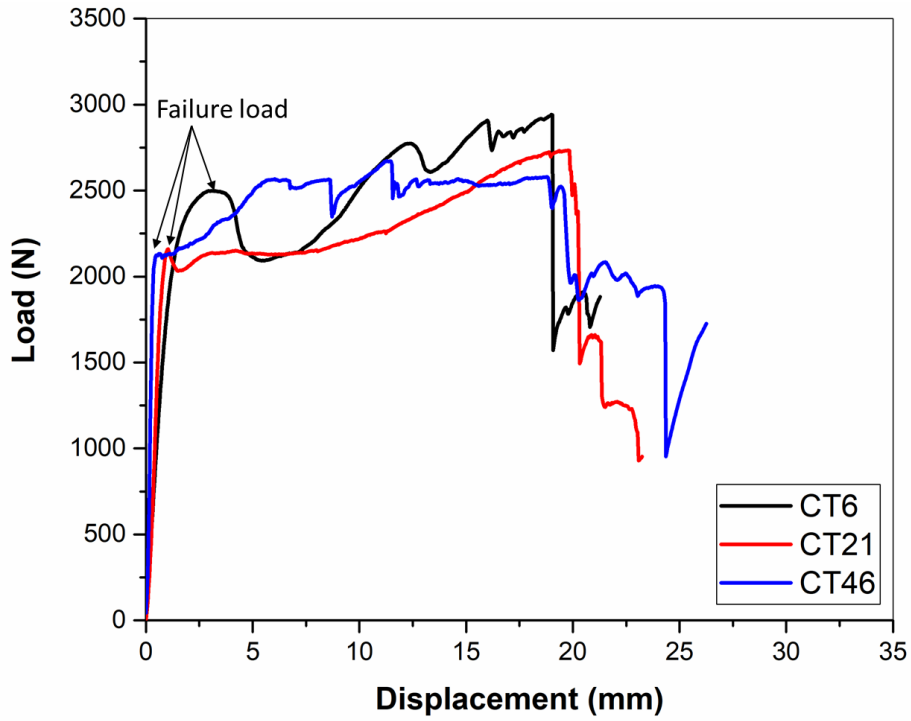

Figure 4.8. Representative load-displacement curves of CT6, CT21 and CT46 sandwich panels

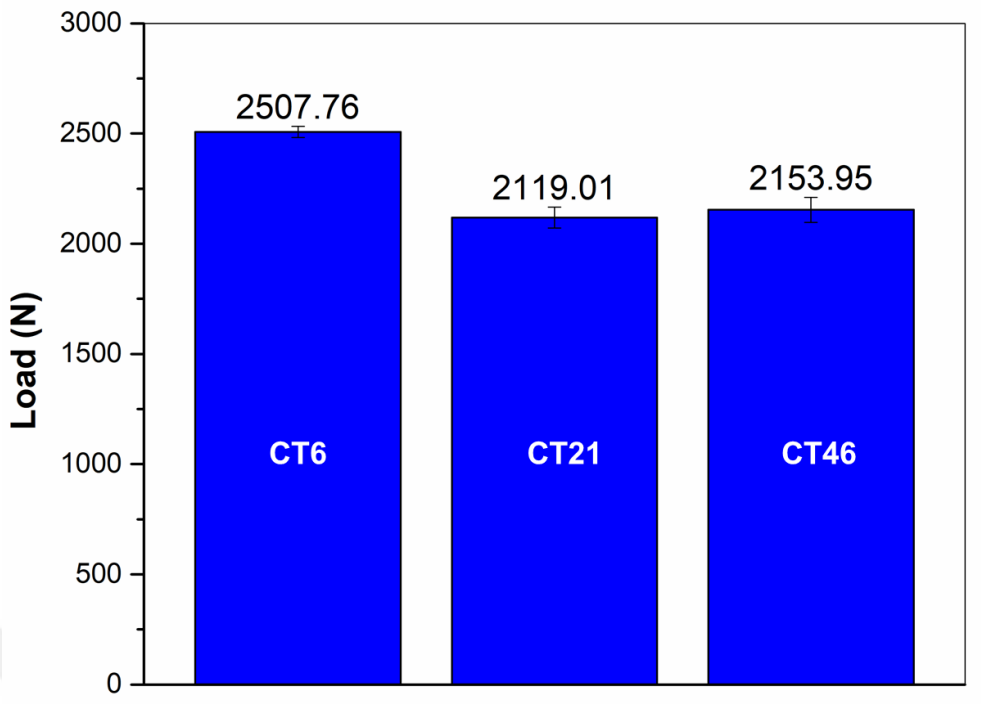

Figure 4.9. Comparison of average failure loads of CT6, CT21 and CT46 sandwich panels with standard deviations

4.4.2. Results of Core Shear Behavior of Aluminum Honeycomb Cores with Different Core Thickness

Shear properties of aluminum honeycomb core materials with different core thickness were characterized with core shear test according to ASTM C273 test standard. Load-displacement curves and shear strength of the aluminum honeycomb cores were reported in this section.

4.4.2.1. Load-Displacement Curves and Shear Strength of Aluminum Honeycomb Core Materials

In section 4.4.1, effect of core thickness on quasi-static flexural behavior of adhesively bonded honeycomb cored sandwich structures were investigated experimentally. It was determined from three point bending tests, CT6 panels have higher ultimate flexural load than CT21 and CT46 sandwich panels despite their lower core

thickness and moment of inertia. Examination of flexural failure modes of sandwich panels revealed that interfacial debonding was observed at the end of the CT46 sandwich panels as a failure mode shown in Figure 4.7(b). Thus, it was thought that shear load on the core-face interface increased on those sandwich panels as the thickness of the aluminum honeycomb core increased. Core shear behavior of sandwich panels with three different core thickness were measured to prove that consideration.

Figure 4.10-Figure 4.12 illustrates the core shear loads of CT6, CT21 and CT46 sandwich panels with respect to displacement, respectively. Load-displacement curves characteristic were found as similar for whole types of sandwich panels. Samples reached a peak load after a linear curve and load was dramatically decreased when the shear failure occurred. That load was identified as the shear failure load as shown in figures. Only shear failure was accepted as a failure mode according to ASTM C 273 test standard. Figure 4.13 shows the failure modes of aluminum honeycomb cores with different core thickness obtained from the tests. Shear failure was seen on whole tested sandwich panels as shown in Figure 4.13.

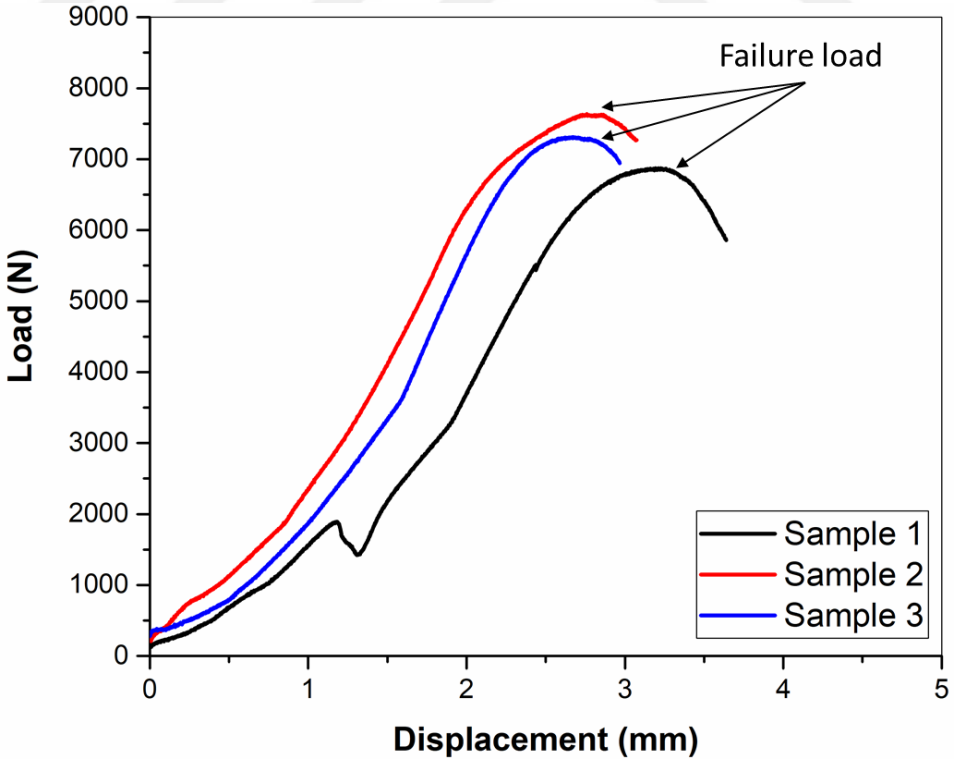

Figure 4.10. Load-displacement curves of three samples of CT6 sandwich panels

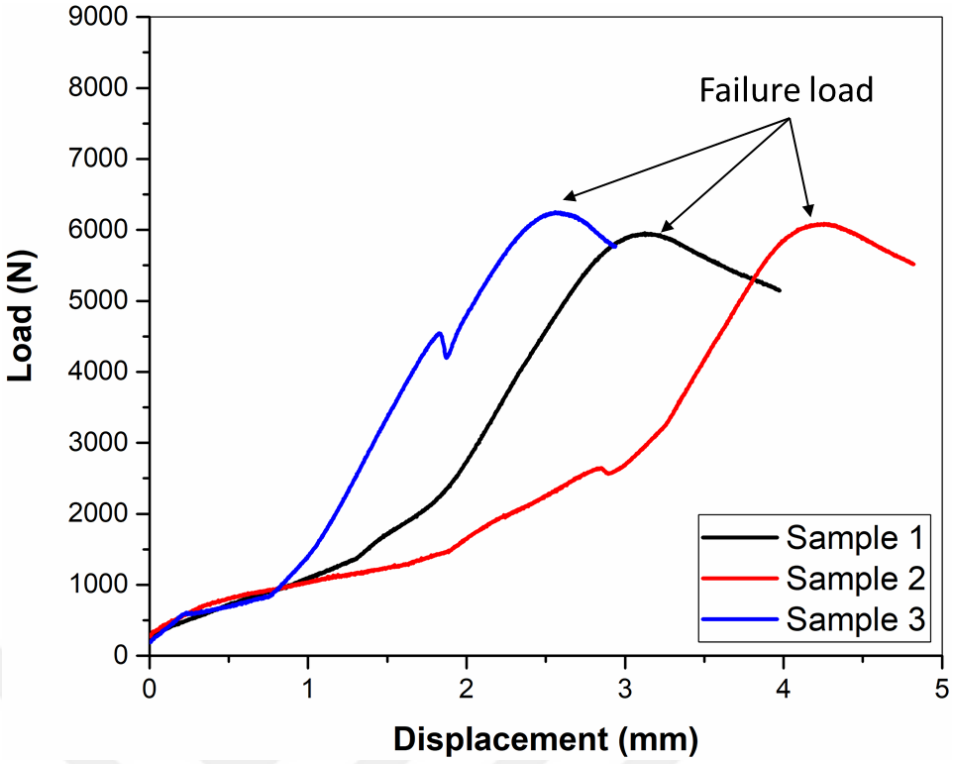

Figure 4.11. Load-displacement curves of three samples of CT21 sandwich panels

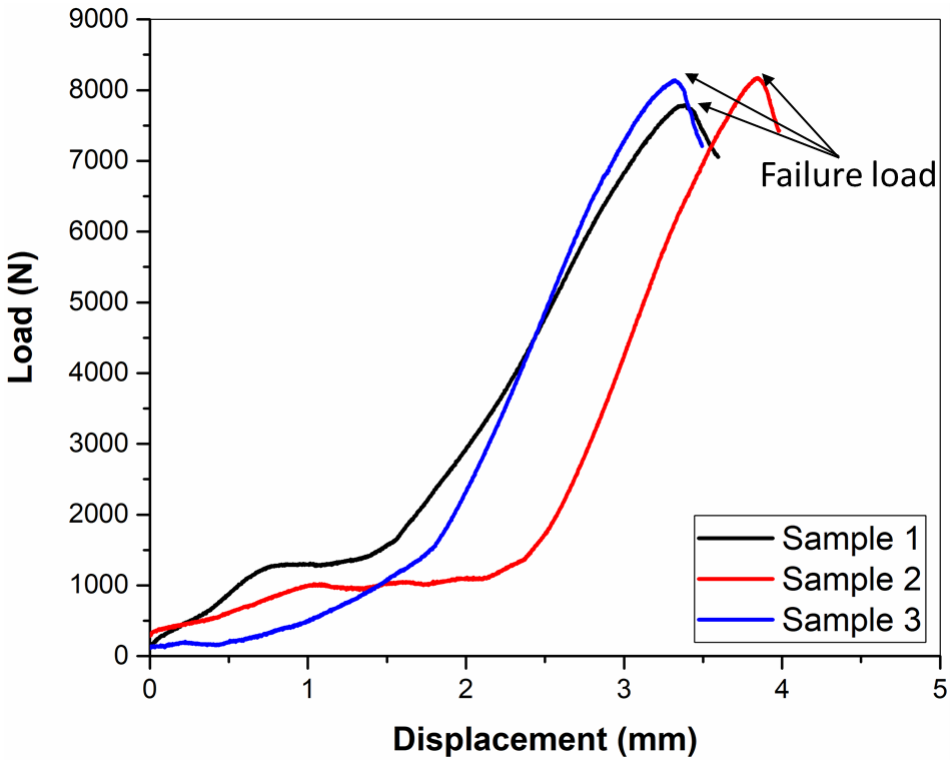

Figure 4.12. Load-displacement curves of three samples of CT46 sandwich panels

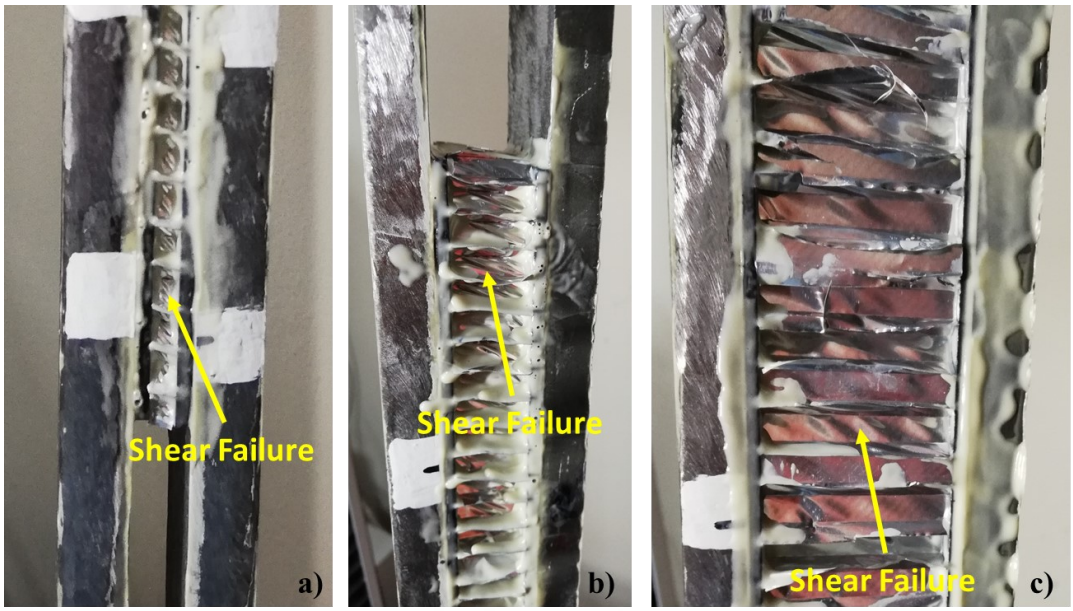

Figure 4.13. Failure modes of aluminum honeycomb cores at core shear tests, a) CT6 sandwich panels, b) CT21 sandwich panels, c) CT46 sandwich panels

Core shear strength of sandwich panels with different core thickness were measured according to equation 4.1. Figure 4.14 shows the comparison of core shear strength of sandwich panels with three different core thickness. Average core shear strength of CT6, CT21 and CT46 sandwich panels were measured as 909.24 ± 39.22 kPa, 483.96 ± 9.54 kPa and 458.99 ± 9.91 kPa, respectively. It was found that core shear strength of CT6 sandwich panels is 46% and 49% higher than core shear strength of CT21 and CT46 sandwich panels, respectively. This can be explained by the fact that shear stress on the aluminum honeycomb core increase as the aluminum honeycomb core thickness increases. Those results also explain the reason why the ultimate flexural load of the CT6 sandwich panels were found higher than the ultimate flexural load of the CT21 and CT46 sandwich panels. Core shear strength of the CT21 and CT46 sandwich panels were found to be close to each other and those results were also correlated with the results of ultimate flexural load results of those panels.

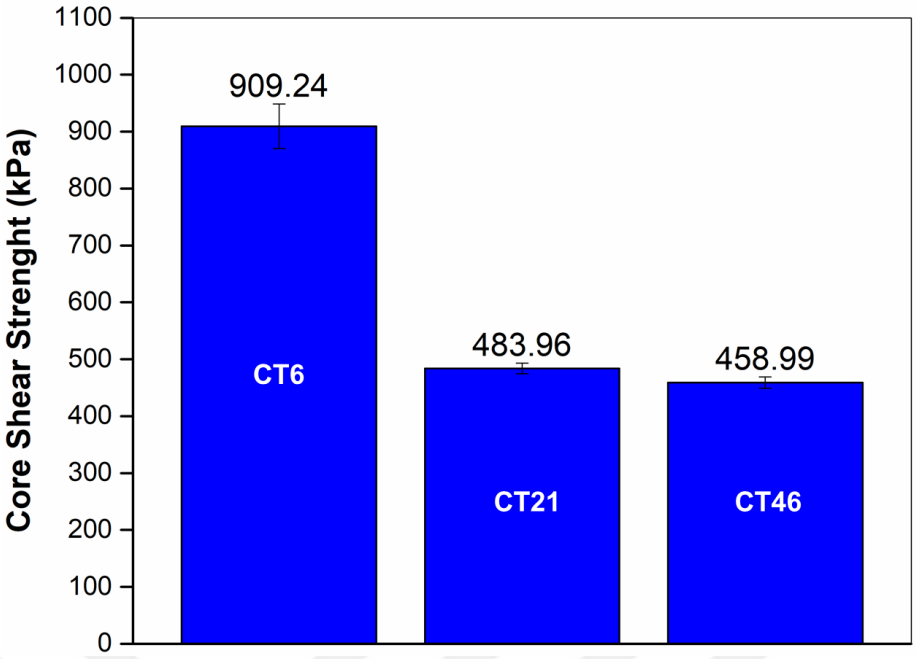

Figure 4. 14. Core shear strength of the CT6, CT21 and CT46 sandwich panels.

4.4.3. Fatigue Test Results

In this section of the thesis, fatigue test results of the honeycomb cored sandwich structures with different core thickness were reported. Fatigue behavior of sandwich panels with different core thickness were characterized by stiffness reduction, fatigue failure modes and Wöhler Curves (S-N Curves) as well as in Chapter 3.

4.4.3.1. Stiffness Reduction and Fatigue Failure Modes

Stiffness reduction method was used to define the failure cycle of the sandwich structures in this study as well as in Chapter 3. Stiffness reduction method provides not only to define the failure cycle of the specimen both also to enable to follow the fatigue failure propagation by stiffness reduction curve with respect to number of cycles. To recall that normalized stiffness equation which shows the rate of stiffness reduction given in (4.2),

$$Normalized\ Stiffness = \frac{k}{k_0} \quad (4.2)$$

where the k is stiffness of the specimen in any cycle and k_0 is the initial stiffness value of sandwich panel.

Figure 4.15-Figure 4.18 shows the stiffness reduction curves of CT6 sandwich panels in different load levels. Stiffness reduction curves show that CT6 samples shows a progressive fatigue failure characteristic during the testing for all load levels. Stiffness reduction curves consist of three regions. A sharp decreasing in stiffness was observed in the beginning of the test in each stress levels. It shows that fatigue failure process begins as cyclic load was implemented to the sandwich panels. However, structures have conserved their load-bearing capacity although that sharp reduction in their stiffness. A linear reduction with a constant slope was seen in the second region of the stiffness reduction curves. Fatigue failure process completed with the sudden decreasing at the end of the second region of the curve. Sandwich samples has lost their entire load-bearing capacity at that cycle and progressive fatigue failure process was completed. The cycle which corresponds the failure process has been done was identified as failure cycle of CT6 sandwich panels.

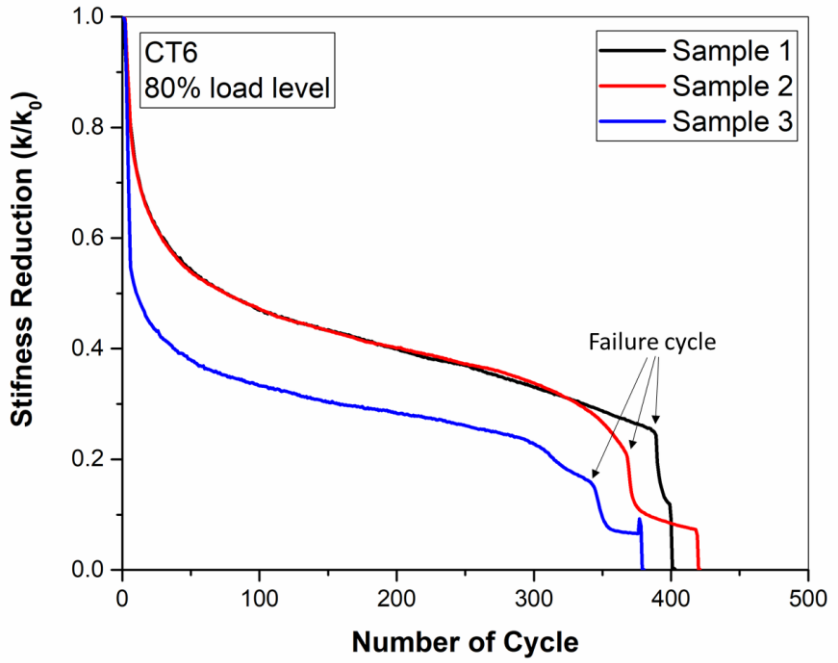

Figure 4.15. Stiffness reduction curves of CT6 sandwich samples, for 80% of ultimate flexural load

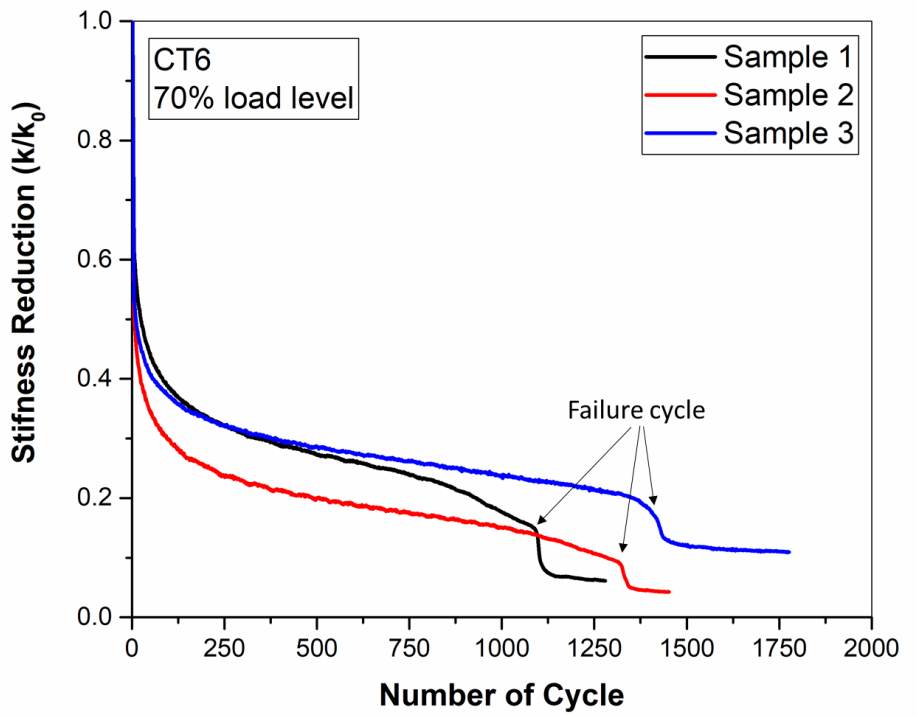

Figure 4. 16. Stiffness reduction curves of CT6 sandwich samples, for 70% of ultimate flexural load

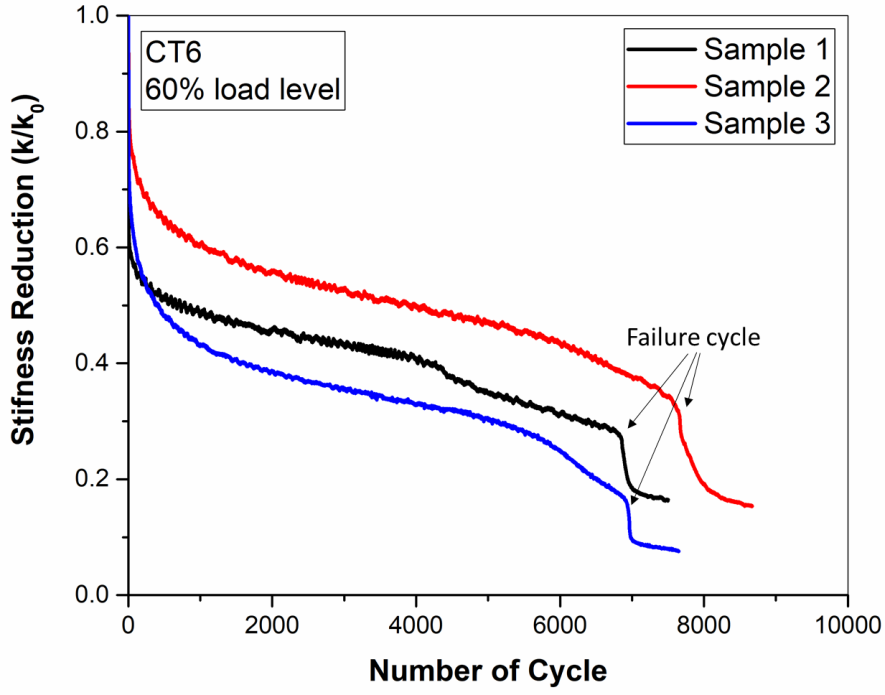

Figure 4.17. Stiffness reduction curves of CT6 sandwich samples, for 60% of ultimate flexural load

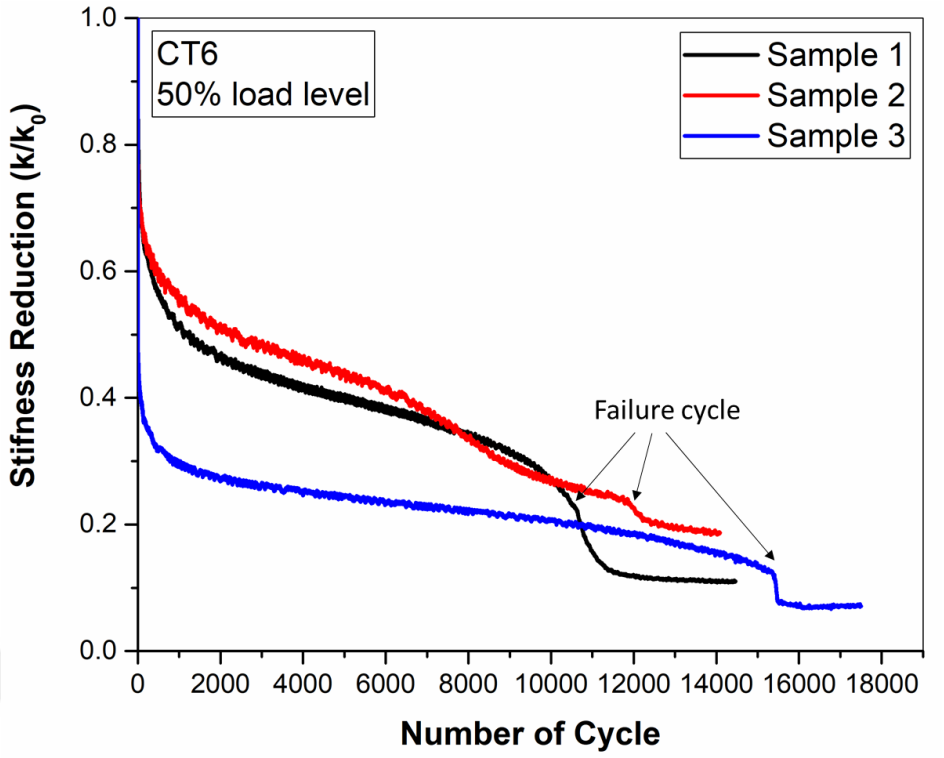

Figure 4.18. Stiffness reduction curves of CT6 sandwich samples, for 50% of ultimate flexural load

Figure 4.19 shows the fatigue failure modes of the CT6 sandwich panels. Any visible failure mode or cracks on sandwich samples was not seen in the first and second region of the stiffness reduction curves although the stiffness reduction was observed. Aluminum honeycomb core crushing was observed when the stiffness of the sample is dramatically decreased which corresponds the end of the second region in stiffness reduction curves. Crack propagation continued after the first failure mode occurred and visible cracks that formed by the growth of core crushing were observed on aluminum honeycomb core as shown in Figure 4.19. There was no failure existing in honeycomb core-composite face sheet interface under fatigue loads due to good adhesion between aluminum honeycomb core and composite face sheets in any loading levels. A rapid progressive failure occurred on CT sandwich panels and structure could not bear the load after first failure occurred. Table 4.1 shows the failure cycles of each CT6 sandwich panels in various load levels. CT6 sandwich panels show the low cycle fatigue behavior as seen in Table 4.1. It can be explained by the fact that the low thickness aluminum honeycomb core could not bear the flexural load as it could not sufficiently increase the

moment of inertia. Otherwise, other structural elements on the sandwich panels which are aluminum honeycomb core-composite face sheets interface and composite face sheets succeeded to carry the shear load and bending load respectively and any failure was not observed on those structures.

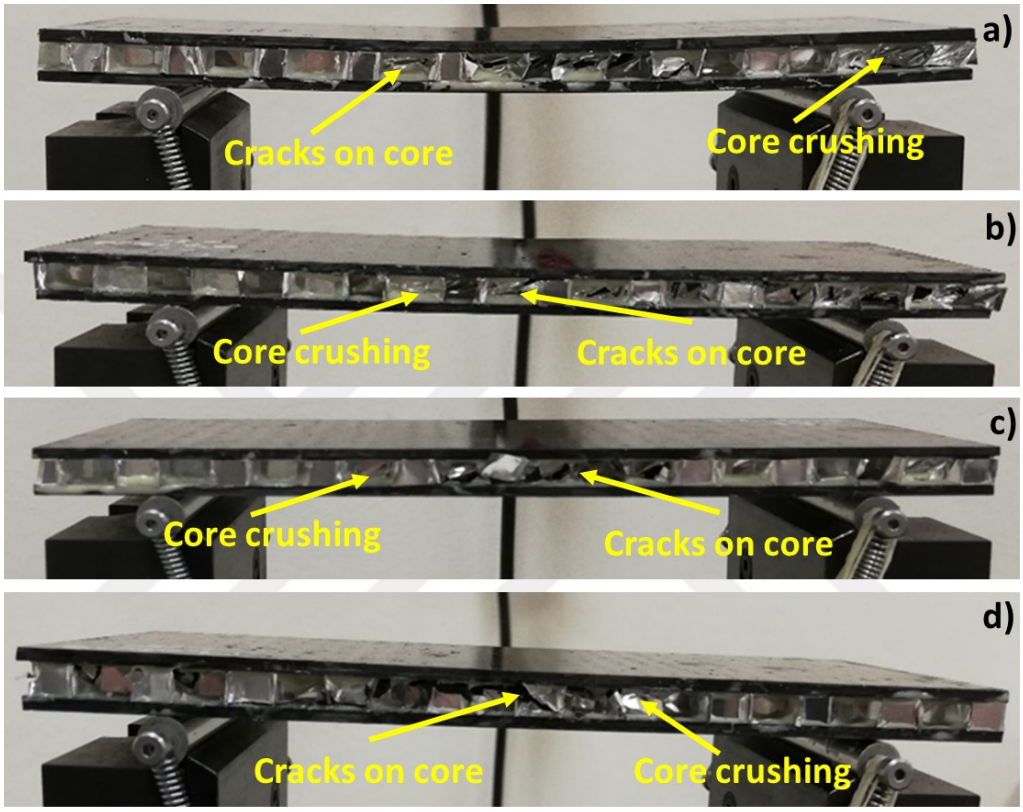

Figure 4.19. Fatigue failure modes of the CT6 sandwich panels for different loading conditions, a) 80% of the F_{ult}, b) 70% of the F_{ult}, c) 60% of the F_{ult} , d) 50% of the F_{ult}

Table 4.1. Failure cycles of CT6 panels for each loading levels

Load Levels	80% of Ult. Load	70% of Ult. Load	60% of Ult. Load	50% of Ult. Load
Number of Failure Cycles	389	1097	6868	15442
	368	1331	7634	12001
	347	1423	6946	10619

Figure 4.20-Figure 4.23 shows the stiffness reduction curves of CT21 sandwich panels with respect to number of cycles with different load levels. Stiffness reduction curves of CT21 panels represents similar characteristic with CT6 panels. Failure cycle was identified on the cycle that progressive fatigue failure completed as well. Failure cycles were shown in Figure 4.20-Figure 4.23.

Two types of stiffness reduction curve were obtained from CT21 sandwich panels. Stiffness reduction curves of 80% and 70% of ultimate flexural load loading levels consist of three regions. Initial stiffness reduction in the few cycles of the test were seen on those panels. In the second region of curves, a linear stiffness reduction curve was observed as shown in Figure 4.20 and Figure 4.21. Rate of the stiffness reduction was indicated with the tangent of the stiffness reduction curves so that it can be said that stiffness reduction occurred slowly in comparison with CT6 sandwich panels in the second region of stiffness reduction curves. Stiffness of the CT21 panels were suddenly decreased at the end of the second region of the curves and failure process completed. That cycle was identified as the failure cycle for each sandwich panels.

Stiffness reduction curve of 60% of ultimate flexural load loading level consists of two regions as shown in Figure 4.22. Initial stiffness reduction was not seen in that load level unlike the other loading levels. Stiffness reduction of the panels occurred with a constant slope line for all samples of that loading level. At the end of the line, a sharp decreasing which indicates the completion of the fatigue failure was seen. That cycle shows the fatigue failure cycle for CT21 sandwich samples on 60% of ultimate flexural load loading level. At 50% of ultimate flexural load loading level, neither stiffness reduction nor a visual failure mode was not observed until one million cycles. In those cycles, test was terminated, and those panels were assumed to reach their fatigue limit.

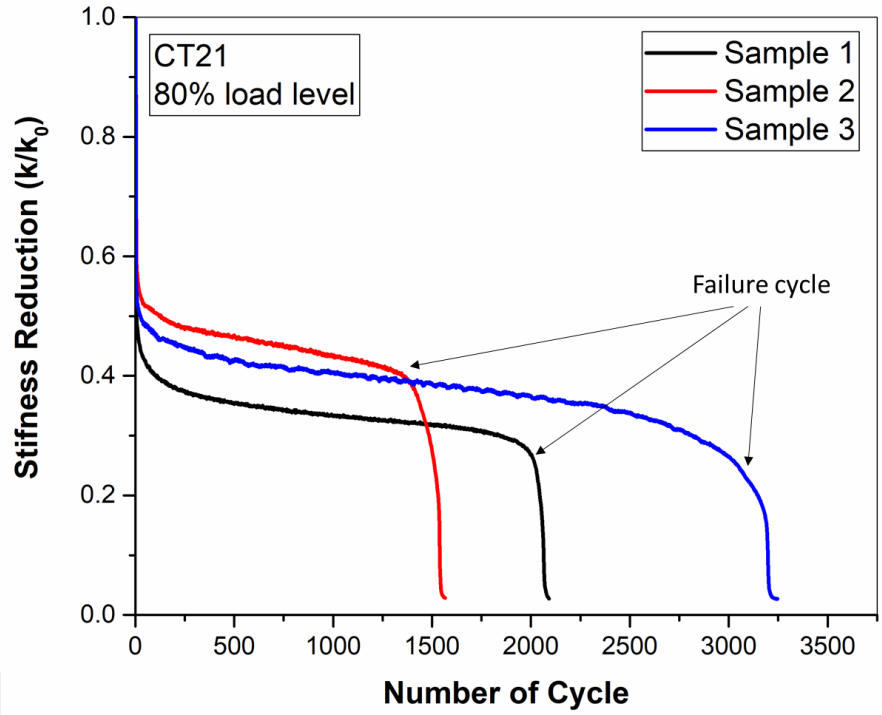

Figure 4.20. Stiffness reduction curves of CT21 sandwich samples, for 80% of ultimate flexural load

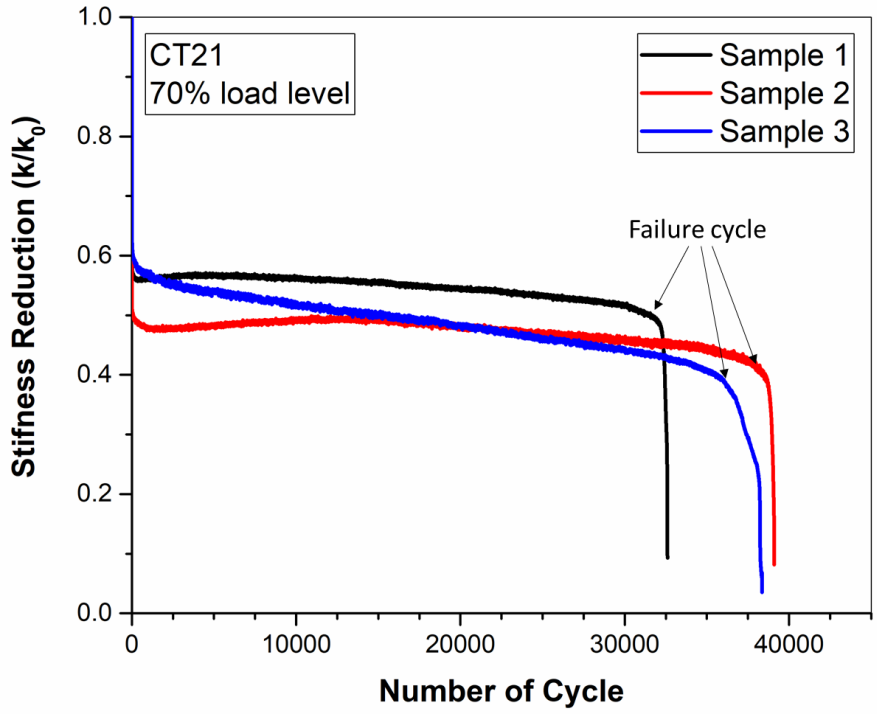

Figure 4.21. Stiffness reduction curves of CT21 sandwich samples, for 70% of ultimate flexural load

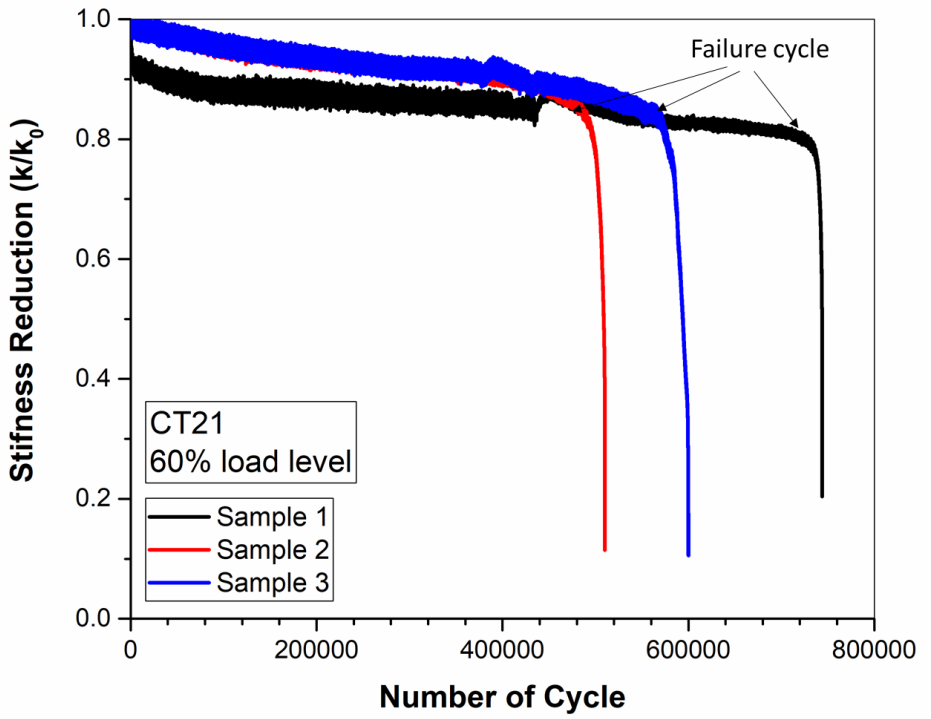

Figure 4.22. Stiffness reduction curves of CT21 sandwich samples, for 60% of ultimate flexural load

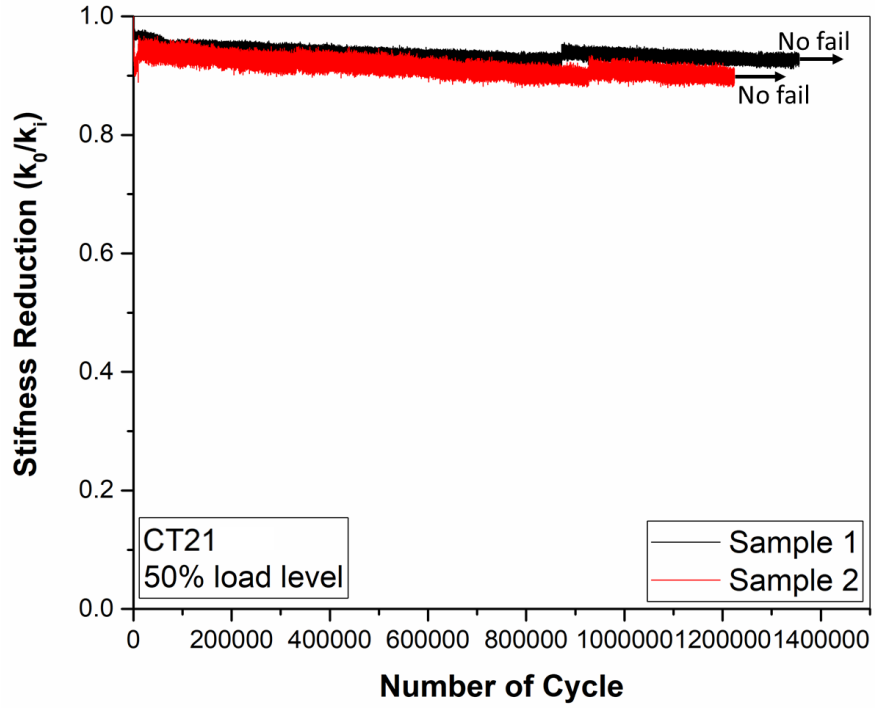

Figure 4.23. Stiffness reduction curves of CT21 sandwich samples, for 50% of ultimate flexural load

Figure 4.24 shows the fatigue failure modes of CT21 sandwich panels regarding to different loading levels. Core crushing is the only failure mode determined until fatigue failure was completed for CT21 sandwich panels for all loading levels. Sandwich panels containing 21 mm thickness of aluminum honeycomb core were found as thick enough to generate a sufficient moment of inertia against bending load on those panels. Shear loads which were resultant from out of plane bending load was carried by aluminum honeycomb core and composite face interface was carried by adhesive layer. 666 g/m^2 amount of adhesive layer generated a sufficient interface against the shear loads so that any failure mode was not observed in aluminum honeycomb core composite face sheet interface. Effect of amount of adhesive on the interface on the fatigue strength of the panels were investigated in Chapter 3. Bending load carried by carbon fiber reinforced polymer matrix composite (CFRP) face sheets were so low in comparison with CFRP's ultimate flexural strength so that any fatigue failure was not observed on CFRP face sheets neither. Table 4.2 shows the fatigue failure cycles of CT21 sandwich panels. CT21 panels shows high cycle fatigue characteristics due to strong enough adhesive layer on the interface and containing thick enough aluminum honeycomb core.

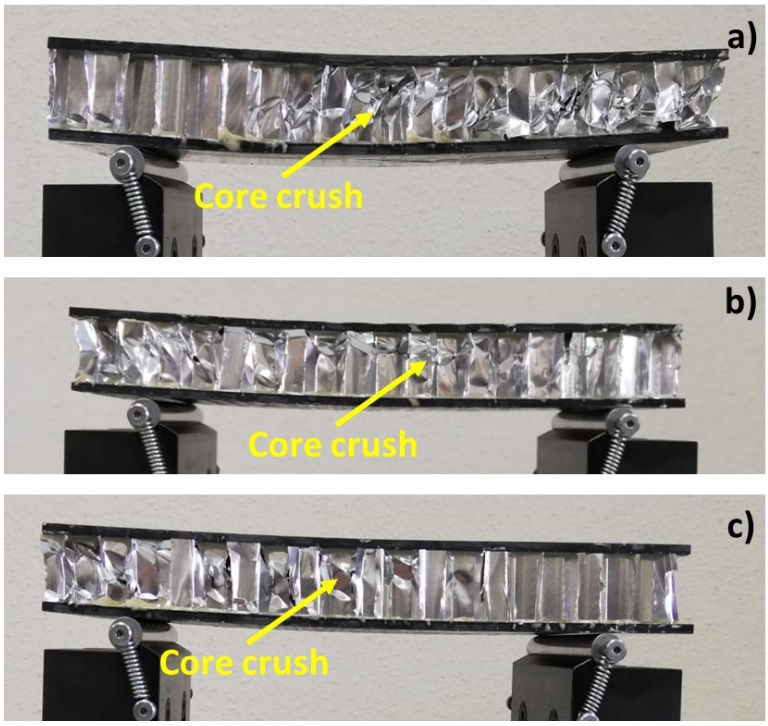

Figure 4.24. Fatigue failure modes of the CT21 sandwich panels for different loading conditions, a) 80% of the F_{ult}, b) 70% of the F_{ult}, c) 60% of the F_{ult}

Table 4.2. Failure cycles of CT21 panels for each loading levels

Load Levels	80% of Ult. Load	70% of Ult. Load	60% of Ult. Load	50% of Ult. Load
Number of Failure Cycles	2028 1492 2155	32210 38346 36780	725775 559689 479263	No fail No fail

Figure 4.25-Figure 4.28 shows the stiffness reduction curves for CT46 samples in each load levels. It was found that stiffness reduction curves of CT46 sandwich panels were similar with stiffness reduction curves of CT21 sandwich panels. Stiffness reduction process continued with a constant rate during the tests after the first stiffness reduction on the beginning of the test in all loading levels. It was seen that sandwich panels kept their load-bearing capacity until a critical cycle in which the stiffness of the samples instantaneously decreased. That cycle was identified as failure cycle for CT46 samples due to the fatigue failure process completed.

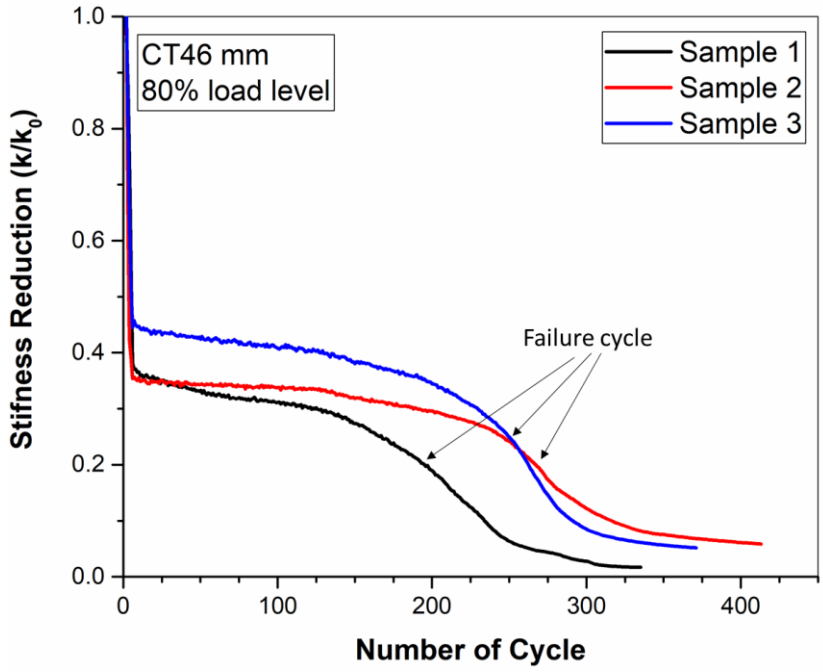

Figure 4.25. Stiffness reduction curves of CT46 sandwich samples, for 80% of ultimate flexural load

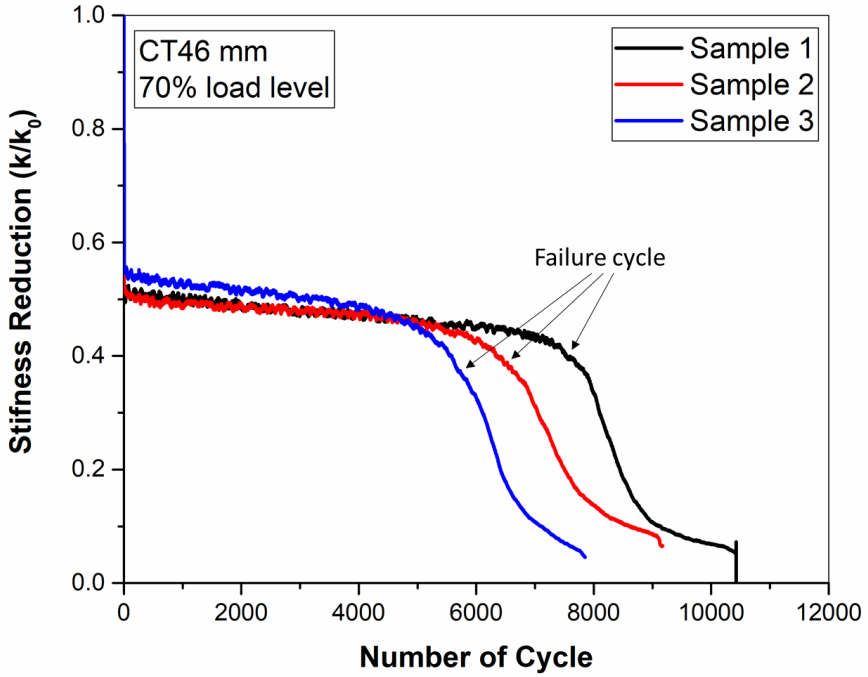

Figure 4.26. Stiffness reduction curves of CT46 sandwich samples, for 70% of ultimate flexural load

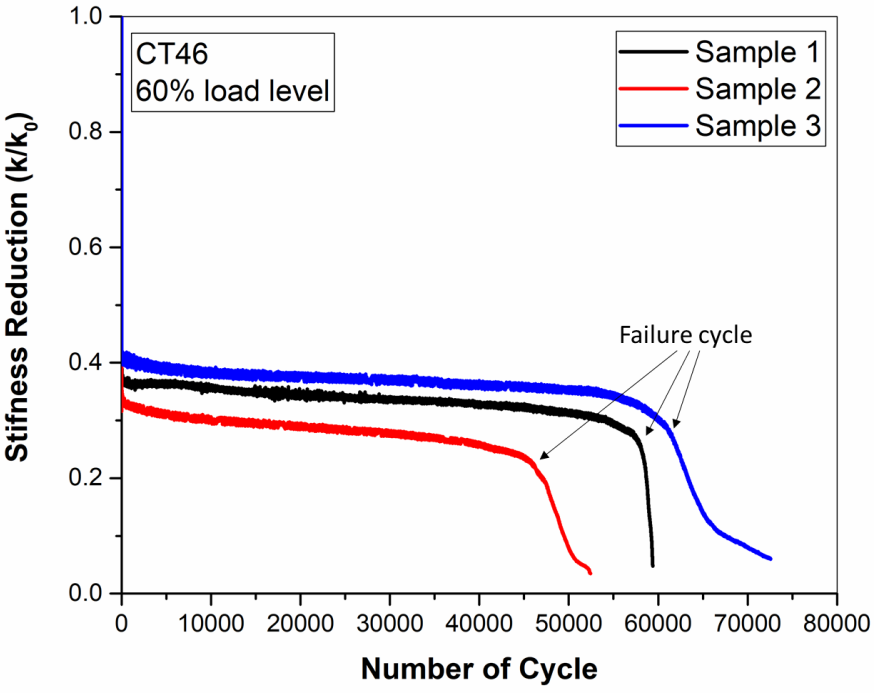

Figure 4.27. Stiffness reduction curves of CT46 sandwich samples, for 60% of ultimate flexural load

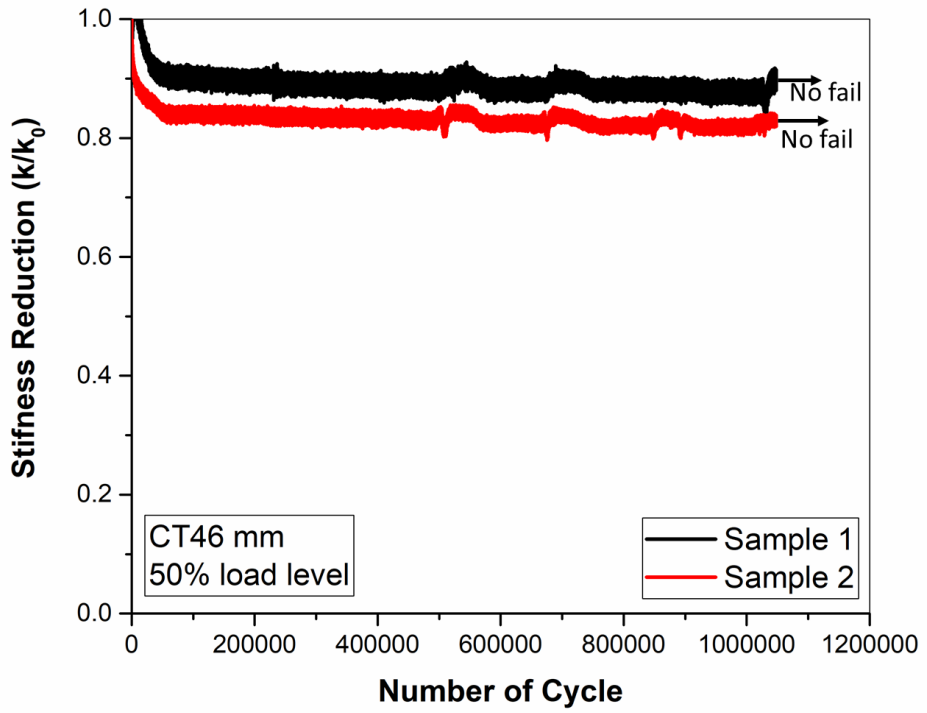

Figure 4.28. Stiffness reduction curves of CT46 sandwich samples, for 50% of ultimate flexural load

Figure 4.29 illustrates the fatigue failure modes of CT46 sandwich panels. It was observed that from analyzing the fatigue failure modes of CT46 sandwich panels, a buckling was formed on the aluminum honeycomb core in the few cycles of the tests for all loading levels. That buckled area formed on the compression side on the aluminum honeycomb core near the edges for whole samples on the fatigue tests. Initial buckling area acted as a stress raiser and become a crack initiator on the surface on the aluminum honeycomb core. It was observed that crack growing due to initially bucked on the aluminum honeycomb surface continued up to high cycles of the tests so that it was proved that formation of the buckling on the aluminum honeycomb surface is the driving force of the failure of CT46 sandwich panels for loading levels 80%, 70% and 60% of ultimate flexural load. When the crack length on the aluminum honeycomb core surface reached a critical level, then structure could not bear the bending load anymore and an instantaneous drop in the stiffness reduction curves was seen. Besides, core crushing was seen on the sandwich panels with crack propagation during the tests. Fatigue failure process was completed with the instant dropping was seen on the stiffness reduction curves.

However, Initial buckling formation was not seen on the sandwich panels on loading levels of 50% of ultimate flexural load so that it was observed that CT46 sandwich panels were not failed on that loading levels. It also proves that initial buckling formation was the driving force of the fatigue failure process for CT46 sandwich panels despite the CT46 panels had an enormous moment of inertia in comparison with CT21 sandwich panels. The fact that there is no stiffness reduction in the sandwich panels under that loading levels also proves that circumstances as seen in Figure 4.28.

Table 4.3 shows the failure cycles of each sandwich samples in various load levels. Failure cycles of the CT46 sandwich panels were seen as lower than CT21 sandwich panels although they had more moment of inertia. That phenomenon occurs due to the failure mode difference between those two types of sandwich panels. As aforementioned before, stress accumulation on the compression side of the CT46 panels causes the formation of a buckled area on the aluminum honeycomb core surface and that buckled area acted as crack initiator. Therefore, in the higher loading levels CT46 sandwich panels was failed on lower cycles of the test than CT21 sandwich panels. In the lower loading levels, formation of initial buckling was not seen and CT46 sandwich panels reached their fatigue limits as shown in Table 4.3.

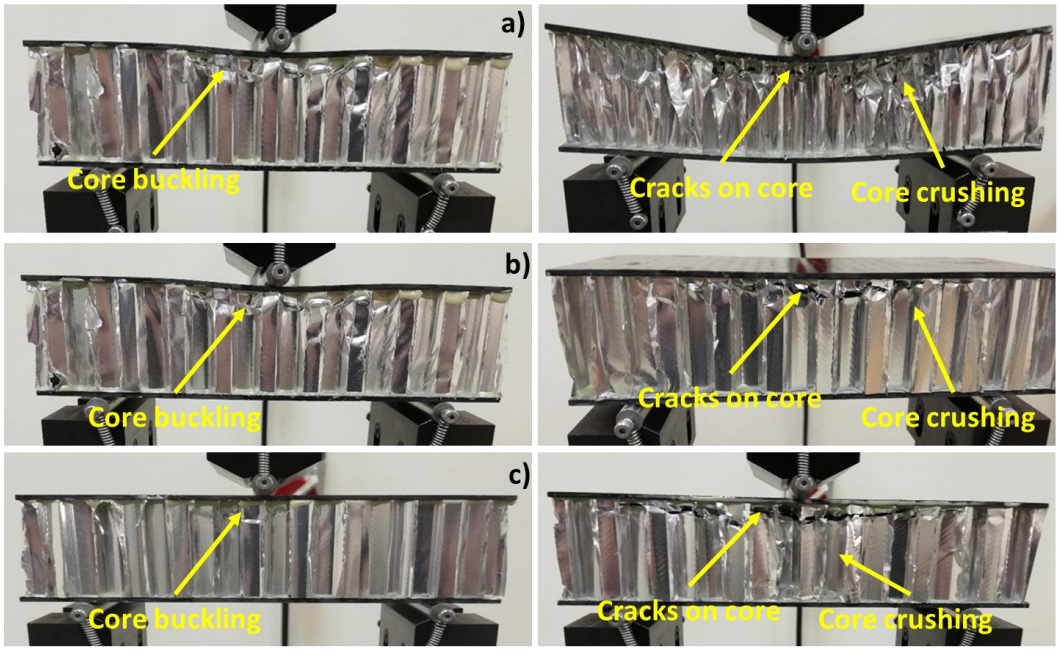

Figure 4.29. Fatigue failure modes of the CT46 sandwich panels for different loading conditions, a) 80% of the F_{ult}, b) 70% of the F_{ult}, c) 60% of the F_{ult}

Table 4.3. Failure cycles of CT46 panels for each loading levels

Load Levels	80% of Ult. Load	70% of Ult. Load	60% of Ult. Load	50% of Ult. Load
Number of Failure Cycles	192	5132	36006	No fail
	263	6147	58040	No fail
	256	7384	56008	

4.4.3.2. Wöhler Curves of The Sandwich Panels with Different Core Thickness

Wöhler curves (SN curves) are most utilized method to characterize and compare the experimental data of fatigue tests of different structural elements includes sandwich panels. Wöhler curves of CT6, CT21 and CT46 sandwich panels are shown in Figure 4.30. The method using to generate Wöhler curves were explained in Chapter 3. Wöhler curves of the CT6, CT21 and CT 46 sandwich panels were demonstrated in logarithmic scale in the same graph to understand the difference between them. The relation between load level and number of fatigue cycle were obtained with a linear relation defined at (4.3).

$$\frac{F_{max}}{F_{ult}} = A - B log N_f \tag{4.3}$$

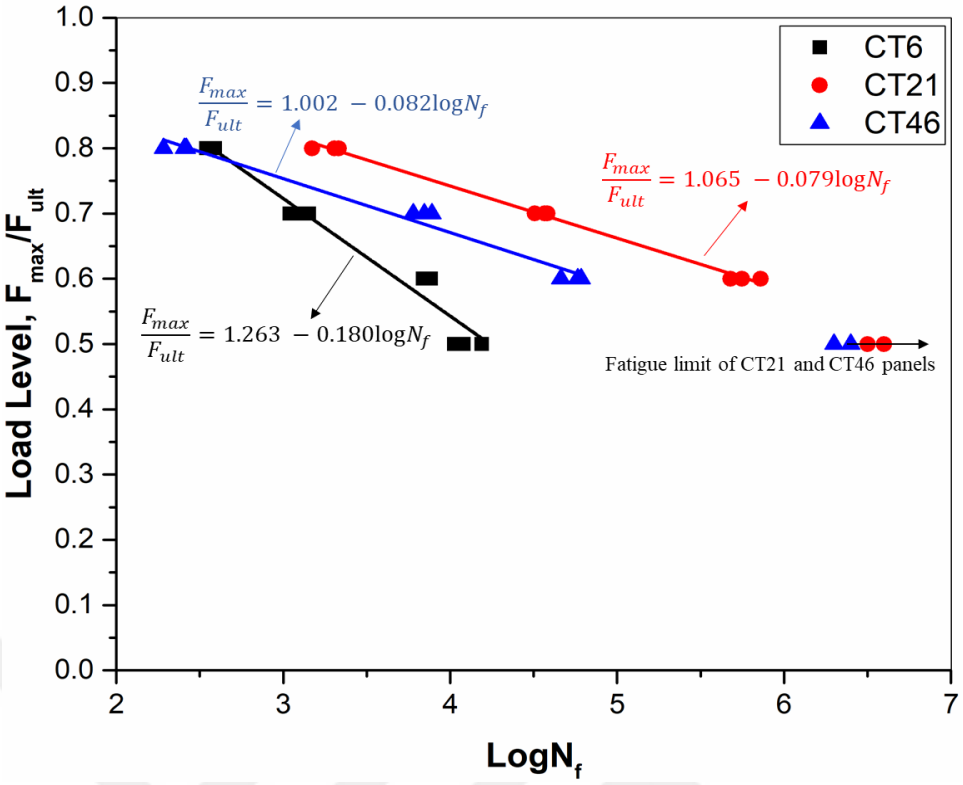

Figure 4.30. Wöhler curves of CT6, CT21 and CT46 panels with linear fitting

The linear expression between the applied load level and the fatigue failure cycles of CT6, CT21 and CT46 sandwich panels are shown in (4.4), (4.5) and (4.6) respectively.

$$\frac{F_{max}}{F_{ult}} = 1.263 - 0.180logN \tag{4.4}$$

$$\frac{F_{max}}{F_{ult}} = 1.065 - 0.079logN \tag{4.5}$$

$$\frac{F_{max}}{F_{ult}} = 1.002 - 0.082logN \tag{4.6}$$

In these equations, F_{max} is the maximum load applied on the fatigue tests, F_{ult} is ultimate flexural load of sandwich panels and N_f is the fatigue failure cycle.

The A and B constants as the linear curve fitting parameters in equation 4.3. The fatigue degradation rate of the sandwich panels is represented by coefficient B in equation

4.3 (Boukharouba, Bezazi, and Scarpa 2014, Essassi et al. 2020). It was found that CT6 sandwich panels which had the highest B coefficient according to test results had the highest fatigue degradation rate among three group of sandwich panels. It shows that the CT6 sandwich panels had the lowest fatigue strength despite their high ultimate static flexural load. Reason of those results that the 6 mm thickness of aluminum honeycomb core of CT6 panels were insufficient to bear the flexural fatigue load and crushed in low cycle of the tests. Furthermore, it was found by analyzing the failure mode, lots of cracks on aluminum honeycomb core of CT6 sandwich structures appeared in the low cycles of the tests made the contribution to rapid fatigue degradation. For all these reason, low cycle fatigue behavior has been observed in CT6 sandwich panels.

Coefficient B of CT21 sandwich panels was found slightly higher than that of CT46 sandwich panels. That was because the fatigue failure cycle of the CT46 sandwich panels is significantly lower than that of CT21 sandwich panels at higher load levels. It can be explained by the buckling formation on the lower cycles of the testing of CT46 sandwich panels at higher load levels. Those buckling formations behave as crack initiator and fatigue failure process has completed before expected number of failure cycle. CT46 panels reached the fatigue limit on the tests performed on 50% loading levels in which the buckling formation was not observed. CT21 sandwich panels has the lowest coefficient B has the highest fatigue strength among three groups of sandwich panels. CT21 panels reached fatigue limits on the 50% load level tests as CT46 sandwich panels.

CHAPTER 5

CONCLUSION AND FUTURE WORKS

5.1. Conclusions

Growing demand for low weight structures in engineering applications has raised the usage of carbon fiber reinforced polymer composites in recent years. CFRP structures are especially using in aerospace, automotive, marine and defense applications in which the weight reduction is critical. One of the types of usage of the GFRP composites is to be face sheets on the sandwich panels. Sandwich panels are essential structural elements which are both low-weight and high strength and stiffness with their huge moment of inertia in bending applications. They also have high crashworthiness properties for their high potential of absorbing energy. All these factors make the CFRP faced sandwich structures a great nominee for using as a structural element in aerospace, automotive, defense and marine industries.

Fatigue is the primary failure cause for the structural elements using under fluctuating loading in their application areas such as aerospace, automotive and marine applications. Thus, it has been significant to study on fatigue behavior of sandwich structures in the last decades. This thesis deals with to characterize the fatigue behavior of sandwich structures with aluminum honeycomb core and carbon fiber reinforced polymer face sheets.

Aluminum honeycomb cored CFRP based sandwich panels were fabricated with different amount of adhesive on face-core interface. Effect of amount of adhesive on mechanical behavior of fabricated sandwich panels under quasi-static and cyclic flexural load was experimentally investigated. Load-displacement curves and failure modes under quasi-static flexural load were obtained from three-point bending tests. Interfacial debonding was determined as first failure mode for both Adh333 and Adh500 sandwich panels. However, first failure mode shifted to core crushing for Adh666 sandwich panels. This phenomenon makes the ultimate flexural load of Adh666 sandwich panels 14% and 20% higher than Adh500 and Adh333 sandwich panels, respectively. Core crushing and

composite face sheet delamination were also observed as failure modes under quasi-static flexural load after first failure occurred.

Effect of amount of adhesive on fatigue behavior of the fabricated sandwich panels were characterized with flexural fatigue tests under different load levels. Stiffness reduction curves and fatigue failure modes were experimentally obtained. SN curves for all types of sandwich panels were generated with test results. In parallel with quasi-static flexural tests, interfacial debonding was found as first failure mode for Adh333 and Adh500 sandwich panels while core crushing for Adh666 sandwich panels. Interfacial debonding caused that Adh333 and Adh500 sandwich panels shows low cycle fatigue behavior. Adh666 sandwich panels containing relatively strong adhesive layer its face-core interface shows significantly higher fatigue resistance on comparison with Adh333 and Adh500 sandwich panels in the same load levels. In 50% of F_{ult} load level, Adh666 panels reached their fatigue limit by preventing from failure despite one million cycle of load was exposed. To sum up, amount of adhesive on the face-core interface has significant effect on both quasi-static and fatigue behavior of adhesively bonded sandwich structures due to providing strong face-core interface.

Core thickness effect on the static and fatigue flexural behavior of aluminum honeycomb cored carbon fiber reinforced polymer-based sandwich panels were examined. Aluminum honeycomb cored CFRP based sandwich panels were fabricated with three different core thickness. Static flexural behavior of fabricated sandwich panels was characterized by load-displacement curves and failure modes. First failure mode was observed to be core crushing for all three groups of sandwich panels on static flexural tests. CT46 sandwich panels also shown interfacial debonding as the static flexural failure mode due to high shear strength on the end of aluminum honeycomb core. CFRP face sheet's delamination was found as the last failure mode for all groups of samples. Static flexural strength of CT6 sandwich panels were found to be %15 and %16 higher than CT21 and CT46 sandwich panels, respectively. That was because the shear stress on aluminum honeycomb cores increases with distance from neutral axis. Hence, CT21 and CT46 sandwich panels have lower static flexural strength than CT6 sandwich panels due to their higher moment of inertia. Core shear strength test was implemented on the aluminum honeycomb cores to prove that. It was clearly observed that core shear strength of aluminum honeycomb core of CT6 panels are nearly double to other two groups.

Effect of core thickness on fatigue behavior of aluminum honeycomb cored sandwich structures were experimentally investigated. Fatigue test under different

loading levels were carried out to sandwich panels. Core thickness effect on fatigue behavior of the aluminum honeycomb cored sandwich panels were characterized by fatigue failure modes and SN curves. Aluminum honeycomb core crushing were found to be the first failure modes fore CT6 sandwich panels. It was observed that 6 mm aluminum honeycomb core could not bear the fatigue loading until high cycles of the test since a low cycle fatigue characteristic were determined. It was also seen that visible cracks were formed on aluminum honeycomb core on CT6 panels. First and only failure mode for CT21 sandwich panels was found to be the core crushing. CT21 panels also provides a sufficient moment of inertia to bear the flexural fatigue load thanks to their 21 mm thickness of aluminum honeycomb core. A buckling formation was observed on the honeycomb core of CT46 sandwich panels in the few cycles of the tests. It was seen that the structure has maintained its load-bearing capacity although the buckling formation acted as the stress raiser and crack initiator. As the result of this, CT46 sandwich panels has lower fatigue life than CT21 sandwich panels in high loading levels. In 50% of ultimate flexural load loading level, both CT21 and CT46 sandwich panels reached their fatigue limit as they did not fail over 1 million cycles.

5.2. Future Works

In this thesis, characterization of fatigue behavior of carbon fiber reinforced polymer matrix composite-based aluminum honeycomb cored sandwich structures was experimentally investigated with aspect of amount of adhesive and core thickness. There is still limited knowledge in the literature although the attention on those structures is increasing in several application areas as aforementioned. For future studies, following subjects are recommended to investigate;

- A numerical and analytical model can be developed to predict the fatigue life of carbon fiber-based aluminum honeycomb cored sandwich panels.
- In the literature, it was seen that stress ratio effects on fatigue behavior of different types of sandwich structures were studied yet stress ratio effects on CFRP based aluminum honeycomb core sandwich structures are still unknown. Besides, an experimental study with different frequency can be done to determine the frequency effect on fatigue behavior.

- GFRP based sandwich structures are commonly using in aerospace applications and exposed to various climatic conditions. Climatic aging effect on fatigue behavior of GFRP based sandwich structures could be studied as future work.
- Effect of different environmental conditions such as dusty, salty etc. environments on fatigue behavior of carbon fiber-based sandwich structures are available to investigate. In addition to this, moisture effect on fatigue behavior of GFRP based sandwich structures can be studied.
- Lastly, impact effect on fatigue strength of CFRP based sandwich structures is recommended to study.

REFERENCES

Abbadi, A, C Tixier, J Gilgert, and Z Azari. 2015. "Experimental study on the fatigue behaviour of honeycomb sandwich panels with artificial defects." *Composite Structures* 120:394-405.

Alsubari, S, MYM Zuhri, SM Sapuan, MR Ishak, RA Ilyas, and MRM Asyraf. 2021. "Potential of natural fiber reinforced polymer composites in sandwich structures: A review on its mechanical properties." *Polymers* 13 (3):423.

Ansari, Md Touhid Alam, Kalyan Kumar Singh, and Mohammad Sikandar Azam. 2018. "Fatigue damage analysis of fiber-reinforced polymer composites—A review." *Journal of Reinforced Plastics and Composites* 37 (9):636-654.

Anwar, Waqas, M Zubair Khan, Asif Israr, Shahid Mehmood, and Nazeer A Anjum. 2017. "Effect of structural dynamic characteristics on fatigue and damage tolerance of aerospace grade composite materials." *Aerospace Science and Technology* 64:39-51.

Atas, Cesim, and Umut Potoğlu. 2016. "The effect of face-sheet thickness on low-velocity impact response of sandwich composites with foam cores." *Journal of Sandwich Structures & Materials* 18 (2):215-228.

Banghai, Jiang, Li Zhibin, and Lu Fangyun. 2015. "Failure mechanism of sandwich beams subjected to three-point bending." *Composite structures* 133:739-745.

Bari, Dipak D, and PS Bajaj. 2014. "Theoretical Flexural Behaviour of Sandwich Panel Using Composite Materials." *IJRET Int. J. of Res. in Engng. and Techn* 3 (04).

Belingardi, G, P Martella, and L Peroni. 2007. "Fatigue analysis of honeycomb-composite sandwich beams." *Composites Part A: applied science and manufacturing* 38 (4):1183-1191.

Belouettar, S, A Abbadi, Z Azari, R Belouettar, and P Freres. 2009. "Experimental investigation of static and fatigue behaviour of composites honeycomb materials using four point bending tests." *Composite Structures* 87 (3):265-273.

Bezazi, Abderrezak, S Gareth Pierce, and Keith Worden. 2007. "Fatigue life prediction of sandwich composite materials under flexural tests using a Bayesian trained artificial neural network." *International Journal of Fatigue* 29 (4):738-747.

Birman, Victor, and George A Kardomateas. 2018. "Review of current trends in research and applications of sandwich structures." *Composites Part B: Engineering* 142:221-240.

Blok, LG, J Kratz, D Lukaszewicz, S Hesse, C Ward, and Christos Kassapoglou. 2017. "Improvement of the in-plane crushing response of CFRP sandwich panels by through-thickness reinforcements." *Composite Structures* 161:15-22.

Boukharouba, Wahid, Abderrezak Bezazi, and Fabrizio Scarpa. 2014. "Identification and prediction of cyclic fatigue behaviour in sandwich panels." *Measurement* 53:161-170.

Brocca, Michele, Zdeněk P Bažant, and Isaac M Daniel. 2001. "Microplane model for stiff foams and finite element analysis of sandwich failure by core indentation." *International Journal of Solids and Structures* 38 (44-45):8111-8132.

Burman, M, and D Zenkert. 1997. "Fatigue of foam core sandwich beams—1: undamaged specimens." *International journal of fatigue* 19 (7):551-561.

Callister, William D, and David G Rethwisch. 2018. *Materials science and engineering: an introduction*. Vol. 9: Wiley New York.

Campbell, Flake C. 2010. *Structural composite materials*: ASM international.

Catapano, Anita, and Marco Montemurro. 2014. "Optimal design of sandwich plates with honeycomb core." *Major topics of the full argumentations are the following*:222.

Cecchini, Andres, and Juan Rivera Yusif. 2019. "Fatigue life prediction of shear failure dominated foam cored sandwich composite hull panels under variable water-slamming conditions." *Composite Structures* 227:111282.

Chawla, Krishan K. 2012. *Composite materials: science and engineering*: Springer Science & Business Media.

Chemami, A, K Bey, J Gilgert, and Z Azari. 2012. "Behaviour of composite sandwich foam-laminated glass/epoxy under solicitation static and fatigue." *Composites Part B: Engineering* 43 (3):1178-1184.

Cheon, Jinsil, and Minkook Kim. 2021. "Impact resistance and interlaminar shear strength enhancement of carbon fiber reinforced thermoplastic composites by introducing MWCNT-anchored carbon fiber." *Composites Part B: Engineering* 217:108872.

Clyne, Trevor William, and Derek Hull. 2019. *An introduction to composite materials*: Cambridge university press.

Coskun, Onur, and Halit S Türkmen. 2012. "Bending fatigue behaviour of laminated sandwich beams." Advanced Materials Research.

Curtis, PT. 1991. "Tensile fatigue mechanisms in unidirectional polymer matrix composite materials." *International journal of fatigue* 13 (5):377-382.

Dai, Jin, and H Thomas Hahn. 2003. "Flexural behavior of sandwich beams fabricated by vacuum-assisted resin transfer molding." *Composite structures* 61 (3):247-253.

Daniel, Isaac M, and Jandro L Abot. 2000. "Fabrication, testing and analysis of composite sandwich beams." *Composites Science and Technology* 60 (12-13):2455-2463.

Davalos, Julio F, Pizhong Qiao, X Frank Xu, Justin Robinson, and Karl E Barth. 2001. "Modeling and characterization of fiber-reinforced plastic honeycomb sandwich panels for highway bridge applications." *Composite structures* 52 (3-4):441-452.

Donga, Amarnath. 2011. "Application of sandwich beam in Automobile front bumper for frontal crash analysis." Wichita State University.

El Mahi, A, M Khawar Farooq, S Sahraoui, and A Bezazi. 2004. "Modelling the flexural behaviour of sandwich composite materials under cyclic fatigue." *Materials & design* 25 (3):199-208.

Essassi, Khawla, Jean-luc Rebiere, Abderrahim El Mahi, Mohamed Amine Ben Souf, Anas Bouguecha, and Mohamed Haddar. 2020. "Experimental and analytical investigation of the bending behaviour of 3D-printed bio-based sandwich structures composites with auxetic core under cyclic fatigue tests." *Composites Part A: Applied Science and Manufacturing* 131:105775.

Feng, Yixiong, Hao Qiu, Yicong Gao, Hao Zheng, and Jianrong Tan. 2020. "Creative design for sandwich structures: A review." *International Journal of Advanced Robotic Systems* 17 (3):1729881420921327.

Freeman, Brian, Eric Schwingler, Mohammad Mahinfalah, and Ken Kellogg. 2005. "The effect of low-velocity impact on the fatigue life of Sandwich composites." *Composite structures* 70 (3):374-381.

Grünewald, Jonas, Patricia Parlevliet, and Volker Altstädt. 2017. "Manufacturing of thermoplastic composite sandwich structures: A review of literature." *Journal of Thermoplastic Composite Materials* 30 (4):437-464.

Guedes, Rui Miranda. 2019. *Creep and fatigue in polymer matrix composites*: Woodhead Publishing.

Harris, Bryan. 2003. *Fatigue in composites: science and technology of the fatigue response of fibre-reinforced plastics*: Woodhead Publishing.

International, ASTM. 2016. *Standard test method for core shear properties of sandwich constructions by beam flexure*: ASTM International.

Jen, Yi-Ming, and Li-Yen Chang. 2009. "Effect of thickness of face sheet on the bending fatigue strength of aluminum honeycomb sandwich beams." *Engineering Failure Analysis* 16 (4):1282-1293.

Jen, Yi-Ming, Chih-Wei Ko, and Hong-Bin Lin. 2009. "Effect of the amount of adhesive on the bending fatigue strength of adhesively bonded aluminum honeycomb sandwich beams." *International Journal of Fatigue* 31 (3):455-462.

Jen, Yi-Ming, Fu-Lung Teng, and Ta-Cheng Teng. 2014. "Two-stage cumulative bending fatigue behavior for the adhesively bonded aluminum honeycomb sandwich panels." *Materials & Design (1980-2015)* 54:805-813.

Khan, Tayyab, Volkan Acar, M Raci Aydin, Burak Hülagü, Hamit Akbulut, and M Özgür Seydibeyoğlu. 2020. "A review on recent advances in sandwich structures based on polyurethane foam cores." *Polymer Composites* 41 (6):2355-2400.

Kulkarni, Nitin, Hassan Mahfuz, Shaik Jeelani, and Leif A Carlsson. 2003. "Fatigue crack growth and life prediction of foam core sandwich composites under flexural loading." *Composite Structures* 59 (4):499-505.

Kulkarni, Nitin, Hassan Mahfuz, Shaik Jeelani, and Leif A Carlsson. 2004. "Fatigue failure mechanism and crack growth in foam core sandwich composites under flexural loading." *Journal of reinforced plastics and composites* 23 (1):83-94.

Lee, Stuart M. 1992. *Handbook of composite reinforcements*: John Wiley & Sons.

Li, Xiang, Gangyan Li, and Chun H Wang. 2012. "Optimisation of composite sandwich structures subjected to combined torsion and bending stiffness requirements." *Applied Composite Materials* 19 (3-4):689-704.

Ma, Mingze, Weixing Yao, Wen Jiang, Wei Jin, Yan Chen, and Piao Li. 2020. "Fatigue Behavior of Composite Sandwich Panels Under Three Point Bending Load." *Polymer Testing* 91:106795.

Mallick, Pankar K. 2007. *Fiber-reinforced composites: materials, manufacturing, and design*: CRC press.

Manalo, AC, T Aravinthan, and W Karunasena. 2010. "Flexural behaviour of glue-laminated fibre composite sandwich beams." *Composite Structures* 92 (11):2703-2711.

Manalo, AC, T Aravinthan, and W Karunasena. 2013. "Mechanical properties characterization of the skin and core of a novel composite sandwich structure." *Journal of composite Materials* 47 (14):1785-1800.

Manca, Marcello, Amilcar Quispitupa, Christian Berggreen, and Leif A Carlsson. 2012. "Face/core debond fatigue crack growth characterization using the sandwich mixed mode bending specimen." *Composites Part A: Applied Science and Manufacturing* 43 (11):2120-2127.

Masuelli, Martin Alberto. 2013. "Introduction of fibre-reinforced polymers− polymers and composites: concepts, properties and processes." In *Fiber reinforced polymers-the technology applied for concrete repair*. IntechOpen.

Mathieson, Hale, and Amir Fam. 2014. "High cycle fatigue under reversed bending of sandwich panels with GFRP skins and polyurethane foam core." *Composite Structures* 113:31-39.

Maurya, Manisha, Jatin Sadarang, I Panigrahi, and Dipti Dash. 2021. "Detection of delamination in carbon fibre reinforced composite using vibration analysis and artificial neural network." *Materials Today: Proceedings*.

Miracle, DB. 2005. "Metal matrix composites–from science to technological significance." *Composites science and technology* 65 (15-16):2526-2540.

Njuguna, James. 2016. *Lightweight composite structures in transport: design, manufacturing, analysis and performance*: Woodhead publishing.

Palomba, Giulia, Vincenzo Crupi, and Gabriella Epasto. 2019. "Collapse modes of aluminium honeycomb sandwich structures under fatigue bending loading." *Thin-Walled Structures* 145:106363.

Pehlivan, Levent, and Cengiz Baykasoğlu. 2019. "An experimental study on the compressive response of CFRP honeycombs with various cell configurations." *Composites Part B: Engineering* 162:653-661.

Rajak, Dipen Kumar, Durgesh D Pagar, Ravinder Kumar, and Catalin I Pruncu. 2019. "Recent progress of reinforcement materials: A comprehensive overview of composite materials." *Journal of Materials Research and Technology* 8 (6):6354-6374.

Rajak, Dipen Kumar, Durgesh D Pagar, Pradeep L Menezes, and Emanoil Linul. 2019. "Fiber-reinforced polymer composites: Manufacturing, properties, and applications." *Polymers* 11 (10):1667.

Rajaneesh, A, Y Zhao, GB Chai, and I Sridhar. 2018. "Flexural fatigue life prediction of CFRP-Nomex honeycomb sandwich beams." *Composite Structures* 192:225-231.

Ravishankar, B, Sanjay K Nayak, and M Abdul Kader. 2019. "Hybrid composites for automotive applications–A review." *Journal of Reinforced Plastics and Composites* 38 (18):835-845.

Reifsnider, Kenneth L. 2012. *Fatigue of composite materials*: Elsevier.

Sayyad, Atteshamuddin S, and Yuwaraj M Ghugal. 2017. "Bending, buckling and free vibration of laminated composite and sandwich beams: A critical review of literature." *Composite Structures* 171:486-504.

Shi, Huiyuan, Weiqing Liu, and Hai Fang. 2018. "Damage characteristics analysis of GFRP-Balsa sandwich beams under Four-point fatigue bending." *Composites Part A: Applied Science and Manufacturing* 109:564-577.

Shi, Shan-shan, Zhi Sun, Xiao-zhi Hu, and Hao-ran Chen. 2014. "Carbon-fiber and aluminum-honeycomb sandwich composites with and without Kevlar-fiber interfacial toughening." *Composites Part A: Applied Science and Manufacturing* 67:102-110.

Singh, Jashanpreet, Mandeep Kumar, Satish Kumar, and SK Mohapatra. 2017. "Properties of glass-fiber hybrid composites: a review." *Polymer-Plastics Technology and Engineering* 56 (5):455-469.

Standard, ASTM. 2013. "Standard test method for shear properties of sandwich core materials." *ASTM Int*:1-7.

Strong, A Brent. 2008. *Fundamentals of composites manufacturing: materials, methods and applications*: Society of Manufacturing Engineers.

Sun, Guangyong, Xintao Huo, Dongdong Chen, and Qing Li. 2017. "Experimental and numerical study on honeycomb sandwich panels under bending and in-panel compression." *Materials & Design* 133:154-168.

Upreti, Shubham, Vishal K Singh, Susheel K Kamal, Arpit Jain, and Anurag Dixit. 2020. "Modelling and analysis of honeycomb sandwich structure using finite element method." *Materials Today: Proceedings* 25:620-625.

Vinson, JackR. 2018. *The behavior of sandwich structures of isotropic and composite materials*: Routledge.

Wahl, Laurent, Stefan Maas, Danièle Waldmann, Arno Zürbes, and Patrick Frères. 2014. "Fatigue in the core of aluminum honeycomb panels: Lifetime prediction compared with fatigue tests." *International journal of damage mechanics* 23 (5):661-683.

Wang, S, X Shui, X Fu, and DDL Chung. 1998. "Early fatigue damage in carbon-fibre composites observed by electrical resistance measurement." *Journal of materials science* 33 (15):3875-3884.

Wu, Xiaorong, Hongjun Yu, Licheng Guo, Li Zhang, Xinyang Sun, and Zilong Chai. 2019. "Experimental and numerical investigation of static and fatigue behaviors of composites honeycomb sandwich structure." *Composite Structures* 213:165-172.

Zenkert, Dan, and Magnus Burman. 2011. "Failure mode shifts during constant amplitude fatigue loading of GFRP/foam core sandwich beams." *International Journal of Fatigue* 33 (2):217-222.

VITA

Mehmet Deniz GÜNEŞ

EDUCATION

- ***Ph.D.*** in English, 2021, Mechanical Engineering, İzmir Institute of Technology.

- ***M.Sc.*** in English, 2014, Material Science and Engineering, İzmir Institute of Technology.

- ***B.Sc.*** in Turkish, 2010, Metallurgical and Materials Engineering, Dokuz Eylül University.

SELECTED CONFERENCES AND PUBLICATIONS

N. Öztoprak, **M. D. Güneş**, M. Tanoğlu, E. Aktaş, O. Ö. Eğilmez, Ç. Şenocak, G. Kulaç, *Developing Polymer Composite-Based Leaf Spring Systems for Automotive Industry*, Science and Engineering of Composite Materials, (2018), 25(6), 1167–1176

M. D. Güneş, M. Tanoğlu, *Effect of The Amount of Adhesive on Fatigue Behavior of Aluminum Honeycomb Cored Carbon Fiber Reinforced Epoxy Composite Based Sandwich Structures*, 4th International Porous and Powder Materials Symposium and Exhibition (PPM 2019), 9-11 October 2019, Muğla, Turkey

M. D. Güneş, M. Z. Okur, S. Kangal, M. Tanoğlu, *Development of Aluminum Honeycomb Cored Carbon Fiber Reinforced Epoxy Composite Based Sandwich Structures and Characterization of Their Fatigue Life,* 5th International Polymeric Composites Symposium and Workshops (IPC 2017), 2-4 November 2017, Izmir, Turkey

M. D. Güneş, S. Şen, H. A. Deveci, G. Tanoğlu, M. Tanoğlu, *Optimization and Characterization of Fatigue Behavior of Glass Fiber Reinforced Polymer Matrix Composites,* 4th International Symposium on Composite Materials (KOMPEGE 2018), 6-8 September 2018, Izmir, Turkey

O. Ç. Güneş, S. Yıldız, **M. D. Güneş**, F. Şenel, M. Tanoğlu, *Personel Koruyucu Uygulamaları için Sıvı Zırh Teknolojisinin Geliştirilmesi*, 9th Defense Technologies Congress (SAVTEK 2018), June 2018, Ankara, Turkey

AWARDS

10. UTİB Ar-Ge Proje Pazarı (8-9 March 2018)

1st Prize on PhD. thesis category
Development and Fatigue Characterization of Carbon Fiber Polymer Composites and Sandwich Structures